Università degli Studi di Messina

Dipartimento di

Scienze Chimiche, Biologiche, Farmaceutiche ed Ambientali

Dottorato di Ricerca in "Scienze Chimiche"

Doctor of Philosophy in "Chemistry"

INNOVATIVE MULTIDIMENSIONAL CHROMATOGRAPHIC APPROACHES FOR THE ISOLATION, IDENTIFICATION AND GENUINENESS ASSESSMENT OF FOOD CONSTITUENTS

Tesi di Dottorato di / Ph.D. Thesis of:

Antonino Schepis

Tutor / Supervisor:

Chiar.mo Prof. Danilo Sciarrone

Coordinatore / Coordinator:

Chiar.mo Prof. Sebastiano Campagna

XXXI Ciclo 2015-2018

Table of contents:

Abstract

The first part of the Ph.D. course was devoted to the development and validation of a fast gas chromatographic (GC) method for the analysis of pesticides in food samples. Two reduced-scale quick, easy, cheap, effective, rugged, and safe (QuEChERS) procedures, combined with fast gas chromatography-triple quadrupole mass spectrometry (GC-QqQ MS), were developed and then validated for the determination of 35 pesticides in different vegetable products. Another project concerned the development of an MDGC-MS/IRMS prototype. Isotope Ratio Mass Spectrometry (IRMS) is commonly recognized to be able to provide information about the geographical, chemical, and biological origins of substances. Even if GC-C-IRMS can provide isotopic analysis of complex mixtures, the reduced chromatographic performance could generates coeluted GC peaks leading to an unreliable isotopic ratio measurement. To overcome this issue, an MDGC-MS/IRMS prototype was developed during the three years, characterized by an improved resolution capability thanks to the heart-cut approach and simultaneous qMS and IRMS detection. Based on the isotopic ratio of a target compound, an application was developed dealing with the investigation of several natural italian white truffles together with the genuineness evaluation of commercial products flavoured with truffles. Another project concerned the isolation and characterization of high amounts of pure molecules, by means of a multidimensional prep-GC instrument. Conventional preparative GC systems present different limitations when highly pure compounds have to be collected at milligrams level. With the intention to improve the productivity of the preparative approach, a tridimensional GC system has been successfully developed, exploiting wide-bore columns operated in heart-cut mode, allowing the collection of high amounts of highly pure components in a reasonable working time.

Chapter I

1 Theory of Gas Chromatography

Gas chromatography (GC) is a physical separation technique used extensively in scientific investigations, petroleum technology, environmental pollution control, and modern biology and medicine. Its primary role is the separation of different chemical compounds that are introduced into the system as a mixture and to determine quantitatively their relative quantitative. When combined with other analytical techniques, GC can also provide qualitative information on the separated substances. The method is limited to volatile and semi-volatile (low-molecular-weight) compounds. The principle of separation is a relative affinity of the components to the stationary phase (a solid or a liquid), while the mobile phase (a gas) migrates them through the system. GC is a dynamic separation method, where the separation of components occurs in a heterogeneous phase system.

1.1 Gas chromatographic separation

Separating chemical substances from each other has been extremely important to various branches of science and technology for many years. Simple separation procedures such as distillation, crystallization, precipitation, and solvent extraction have been used by humankind from time immemorial. More refined forms of separation, such as chromatography and electrophoresis, have been among the major causes of scientific revolution during the history. In this concern gas chromatography is one of the several chromatographic methods. The scientific principles of chromatography were discovered by a russian botanist M. S. Tswett (1872–1919) but hardly developed into useful chemical separation procedures until the 1930s. The name *chromatography* was originated by Tswett who primarily investigated plant pigments (*chromatos* is the Greek name for color)[1]. However, any method that utilizes a distribution of the molecules to be separated between the mobile phase (a gas or a liquid) and the stationary phase (a solid or a liquid that is immiscible with the mobile phase) now qualifies as chromatography. The physical state of the mobile phase determines whether we deal with gas or liquid chromatography. Variation in the type of stationary phase is important as well: if a solid

is used as the stationary phase, the molecules under separation interact with the phase by adsorption forces; if a liquid is used in the same capacity, the molecules under separation interact according their solubilities. According to this type of interaction, we distinguish between adsorption chromatography and partition chromatography. This classification is further showed in Table 1.

Tswett's original work concerned liquid adsorption chromatography, while the first experiments on liquid partition chromatography were described in the early 1940s by A. J. P. Martin and his co-workers in Great Britain[2].

Several investigations concerning to the use of gas as the mobile phase in gas/adsorption systems were reported in Austria, Czechoslovakia, Russia, and Sweden during the 1940s. However, the development of gas–liquid chromatography, reported in 1952 by A. T. James and A. J. P. Martin, is widely considered the beginning of GC as a powerful analytical method[3].

Table 1. Separations methods in chromatography

Mobile Phase (MB)	Stationary Phase (SP)	Type of chromatography	Separation method
Liquid	Solid	Liquid-Solid	Adsorption
Liquid	Liquid (immiscible)	Liquid-Liquid	Solubility (partition)
Gas	Solid	Gas Solid	Adsorption
Gas	Liquid	Gas liquid	Solubility (partition)

The essential parts of the gas chromatographic system are showed in Figure 1. At the heart of the system is the separation column, at which the crucial physicochemical process of the separation occurs. The separation column contains the stationary phase, while the mobile phase (the carrier gas) is flowing through this column from a pressurized gas cylinder (source of the mobile phase). The rate of mobile-phase delivery is controlled by a pressure and/or flow-regulating unit. An exclusive separation mode for the analytical GC is elution chromatography, in which the sample (a mixture of chemicals to be separated) is introduced at once, as a sharp concentration impulse (band), into the mobile-phase stream.

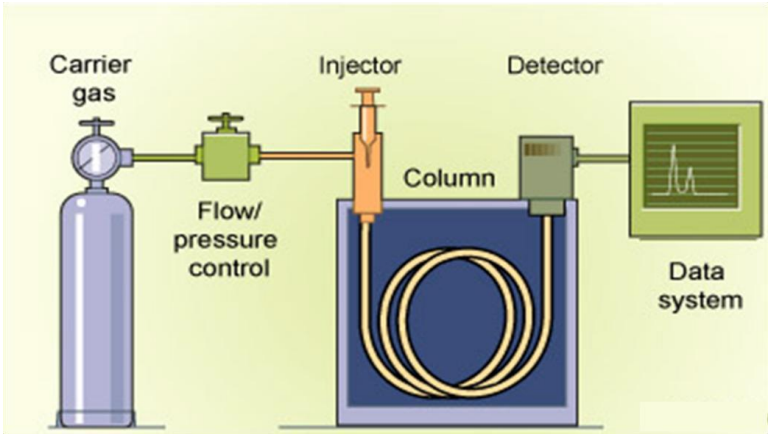

Figure 1. The main components of a gas chromatograph.

The introduction of the sample is performed through a unit called injector. The whole sample is transferred from that part to the chromatographic column, where continuous redistributions between the mobile phase and the stationary phase occur. Due to their different affinities for the stationary phase, the individual components eventually form their own concentration bands, which reach the column's end at different times. A detector is situated at the column's end to identify and quantify the single components eluting from the column. The detector, together with auxiliary electronic and recording devices, generates the chromatogram of which an example is shown in Figure 2. Such a chromatogram is, basically, a plot of the sample concentration (y axis) versus time (x axis). It represents the individual component bands, separated by the chromatographic column and modified by a variety of physical processes into a peak shape.

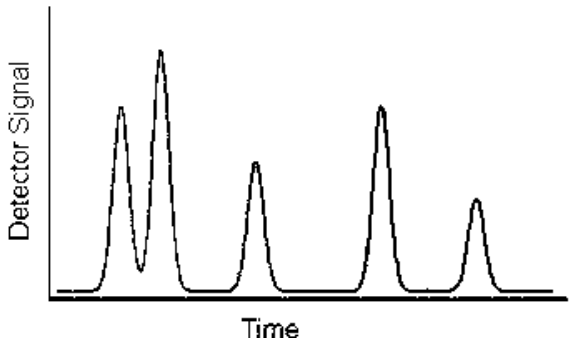

Figure 2. GC chromatogram example

The position of a peak on the time scale of the total chromatogram bears some qualitative information, since each chromatographic peak represents at least one chemical substance. The areas under the peaks are, however, related to the amounts of individual substances separated in time and space.

A typical gas chromatograph has three independently controlled thermal zones: the injector zone that ensures rapid volatilization of the introduced sample; the column temperature that is controlled to optimize the actual separation process; and the detector zone that have to be at temperatures where the individual sample components are measured in the vapor phase.

As shown in Figure 2, different sample components appear at the column's end at different times. The retention time t_R is the time elapsed between injection and the maximum of a chromatographic peak. It is defined as

$$t_R = t_0(1 + k), (1)$$

where t_0 is the retention time of a mixture component that has no interaction with the stationary phase, and *k* is the capacity factor. The capacity factor is further defined as

$$k = K \frac{V_S}{V_M}, (2)$$

where *K* is the solute's distribution coefficient (concerning to a distribution between the stationary and the mobile phases), V_S is the volume of the stationary phase, and V_M is the volume of the mobile phase in a chromatographic column. The distribution coefficient $K = C_S/C_M$ (where C_S is the solute concentration in the stationary phase and C_M is the solute concentration in the mobile phase) is a thermodynamic quantity that depends on temperature. The molecular interactions between the phases and the solutes under separation are strongly temperature-dependent. If, for example, a solid adsorbent (column material) is brought into contact with a permanent (inorganic) gas and a defined concentration of organic (solute) molecules in the gas phase at a certain temperature, some solute molecules become adsorbed on the solid, and others remain in the permanent

gas. When the system temperature increases, less solute molecules are adsorbed, and more of them join the permanent gas; the distribution (adsorption) coefficient, as defined above, changes correspondingly. Likewise, if the stationary phase happens to be a liquid, the solute's solubility in it decreases with increasing temperature, according to Henry's law, resulting in a decrease of the distribution (partition) coefficient. According to Eqs. (1) and (2), the retention time in GC depends on several variables: (a) the chemical nature of the column phase and its temperature, as reflected by the distribution coefficient; (b) the ratio of the phase volumes in the column V_S/V_M; and (c) the value of t_0. In the practice of chromatography, these variables are used to maximize the component separation and the speed of analysis. Unlike some other chromatographic processes, the physical interactions between the mobile phase and solute molecules in GC are, for all practical purposes, negligible. Thus, the carrier gas serves only as means of molecular (solute) transport from the beginning to the end of a chromatographic column. The component separation is then primarily due to the interaction of solute molecules with those of the stationary phase. Since a variety of column materials are available, various molecular interactions can be used to enhance the component separation. Moreover, these interactions are temperature-dependent. For the mixture component with no affinity for the stationary phase, the retention time t_0 serves merely as the marker of gas linear velocity μ (in cm/s) and is actually defined as:

$$t_0 = \frac{L}{\mu}, \quad (3)$$

where L is the column length. The gas velocity is, in turn, related to the volumetric flow rate F since

$$\mu = \frac{F}{s}, \quad (4)$$

where s is the column cross-sectional area. The gas-flow rate is mainly regulated by the inlet pressure value; the higher the inlet pressure the greater the gas-flow rate (and linear

velocity) becomes, and consequently, the shorter t_0 is. Correspondingly, fast GC separations are performed at high gas-inlet pressures. The so-called retention volume V_R is a product of the retention time and volumetric gas-flow rate:

$$V_R = t_R F, (5)$$

Since the retention times are somewhat indicative of the solute's nature, a means of their comparison must be available. Within a given chemical laboratory, the relative retention times (the values relative to an arbitrarily chosen chromatographic peak) are frequently used:

$$\alpha_{2,1} = \frac{t_{R2}}{t_{R1}} = \frac{V_{R2}}{V_{R1}} = \frac{K_2}{K_1}, (6)$$

This equation is also a straightforward consequence of Eqs. (1) and (2). Because the relative retention represents the ratio of distribution coefficients for two different solutes, it is frequently utilized (for the solutes of selected chemical structures) as a means to judge selectivity of the solute–column interactions.

For interlaboratory comparisons, the retention index appears to provide the best method for documenting the GC properties of any compound. The retention index system compares retention of a given solute (on a logarithmic scale) with the retention characteristics of a set of standard solutes that usually are a homologous series of compounds:

$$I = 100_z + 100 \frac{\log t_{R(x)} - \log t_{R(z)}}{\log t_{R(z+1)} - \log t_{R(z)}}, (7)$$

The subscript *z* represents the number of carbon atoms within a homologous series, while *x* relates to the unknown. For example, a series of *n*-alkanes can be used in this direction; each member of a homologous series (differing in a single methylene group) is assigned

an incremental value of 100 (e.g., 100 for methane, 200 for ethane, and 300 for propane, etc.) and if a given solute happens to elute from the column exactly half-way between ethane and propane, its retention index value is 250. Retention indices are relatively independent of the many variables of a chromatographic process.

The success of GC as a separation method is primarily dependent on maximizing the differences in retention times of the individual mixture components. An additional variable of such a separation process is the width of the corresponding chromatographic peak. Whereas the retention times are primarily dependent on the thermodynamic properties of the separation column, the peak width is largely a function of the efficiency of the solute mass transport from one phase to the other and of the kinetics of sorption and desorption processes. Figure 3 is important to understanding the relative importance of both types of processes. In Figure 3a a situation where two sample components are eluted too closely together is showed, so that the resolution of their respective solute zones is incomplete; Figure 3b represents a situation where the two components are resolved from each other through choosing a (chemically) different stationary phase that retains the second component more strongly than the first one; finally, Figure 3c shows the same component retention but much narrower chromatographic peaks, thus represents the most "efficient" handling of the two components. This efficiency, represented by narrow chromatographic zones, can actually be attained in GC practice by a proper design in physical dimensions of a chromatographic column.

The width of a chromatographic peak is determined by various column processes such as diffusion of solute molecules, their dispersion in flow streamlines of the carrier gas, and the speeds by which these molecules are transferred from one phase to another. An arbitrary, but the most widely used, criterion of the column efficiency is the number of theoretical plates, *N*. Figure 4 demonstrates its determination from a chromatographic peak.

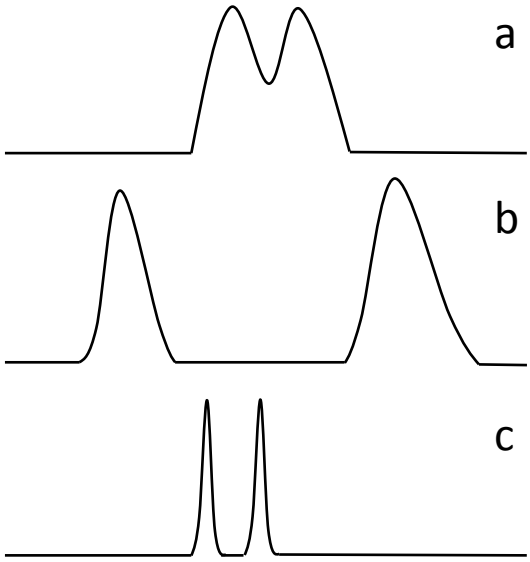

Figure 3. Component resolution based on the selectivity and efficiency of the separation process: (a) two not resolved components, (b) resolution based on the column selectivity, and (c) resolution based on the column kinetic efficiency.

This number is simply calculated from the measured retention distance t_R (in length units) and the peak width at the peak half-height $W_{1/2}$:

$$N = 5.54 \left(\frac{t_R}{w_{1/2}}\right)^2, (8)$$

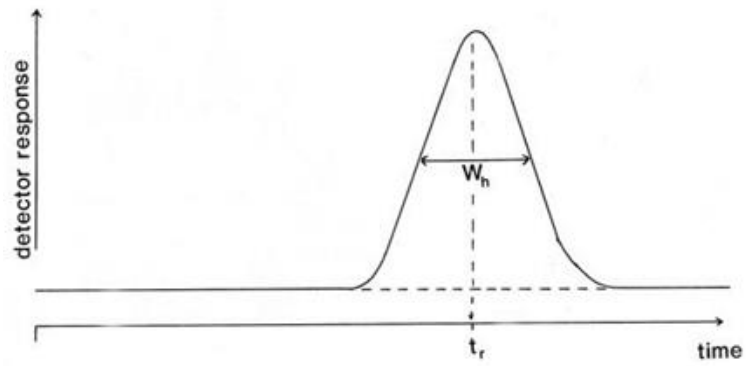

Figure 4. Determination of the number of theoretical plates of a chromatographic column.

The length of a chromatographic column L is viewed as divided into imaginary volume units (plates) in which a complete equilibrium of the solute between the two phases is

attained. Obviously, for a given value of t_R, narrower peaks provide greater numbers of theoretical plates than broader peaks.

Equation (8), is used to determine the number of theoretical plates, relates to a perfectly symmetrical peak (Gaussian distribution). While good GC practice results in peaks that are nearly Gaussian, departures from peak symmetry occasionally occur. In Figure 5, (a) is usually caused by a slow desorption process and undesirable interactions of the solute molecules with the column material, and (b) is associated with the phenomenon of column overloading (if the amount of solute is too large, exceeding saturation of the stationary phase, a fraction of the solute molecules is eluted with a shorter retention time than the average).

When feasible, GC should be carried out at the solute concentrations that give a linear distribution between the two phases.

The length element of a chromatographic column occupied by a theoretical plate is the plate height (*H*):

$$H = \frac{L}{N}, (9)$$

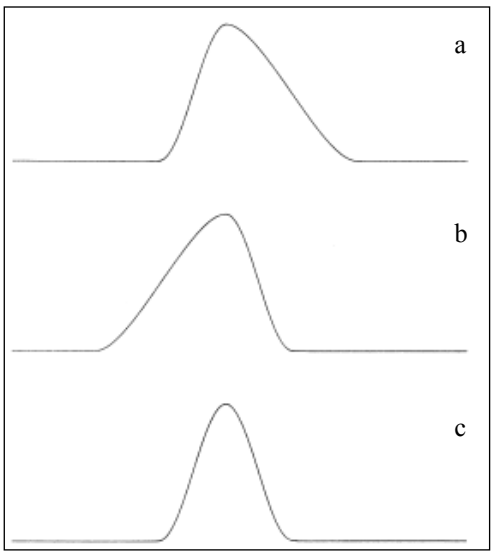

Figure 5. Departures from peak symmetry: (a) slow desorption process and (b) column overloading. (c) Gaussian distribution.

The column efficiency *N* can be dependent on a number of variables. Most importantly, the plate height is shown to be a function of the linear gas velocity μ according to the van Deemter equation:

$$H = A + \frac{B}{u} + Cu, (10)$$

where the constant *A* describes the chromatographic band dispersion caused by the gas-flow irregularities in the column. The *B*-term represents the peak dispersion due to the diffusion processes occurring longitudinally inside the column, and the C-term is due to a flow-dependent lack of the instantaneous equilibrium of solute molecules between the gas and the stationary phase. The mass transfer between the two phases occurs due to a radial diffusion of the solute molecules. Equation (10) is represented graphically by a hyperbolic plot, the van Deemter curve, in Figure 6. The curve shows the existence of an optimum velocity at which a given column exhibits its highest number of theoretical plates. Shapes of the van Deemter curves are further dependent on a number of variables: solute diffusion rates in both phases, column dimensions and various geometrical constants, the phase ratio, and retention times. Highly effective GC separations often depend on thorough understanding and optimization of such variables[4].

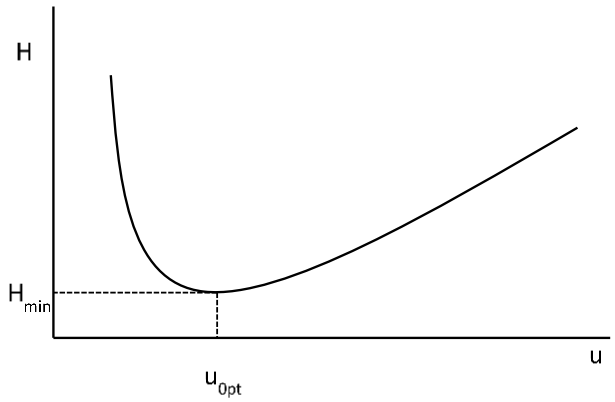

Figure 6. Relationship of the plate height and linear gas velocity (van Deemter curve).

Since open tubular or capillary columns were introduced in GC, the absence of any packing material inside the column modified the van Deemter equation because their rate equation does not have the *A*-term. This conclusion was pointed out by Golay[5], who also proposed a new term to deal with the diffusion process in the gas phase of open tubular columns. His equation had two *C*-terms, one for the mass transfer in the stationary phase, C_S (similar to van Deemter), and one for mass transfer in the mobile phase, C_M. Thus the Golay equation is:

$$H = \frac{B}{u} + (C_S + C_M)u, (11)$$

The *B*-term of equation (11) accounts for the well-known molecular diffusion. The equation governing molecular diffusion is:

$$B = 2D_G, (12)$$

where D_G is the diffusion coefficient for the solute in the carrier gas. The equation tells us that a small value for the diffusion coefficient is desirable so that diffusion is minimized, yielding a small value for *B* and for *H*. In general a low diffusion coefficient can be achieved by using carrier gas with larger molecular weights like nitrogen or argon. In the Golay equation (eq. 11), this term is divided by the linear velocity, so a large velocity or flow rate will also minimize the contribution of the *B*-term to the overall peak broadening. That is, a high velocity will decrease the time a solute spends in the column and thus decrease the time available for molecular diffusion. The *C*-terms in the Golay equation relate to mass transfer of the solute, either in the stationary phase or in the mobile phase[6].

Ideally, fast solute sorption and desorption will keep the solute molecules close together and keep the band broadening to a minimum.

Mass transfer in the stationary phase can be described from the Figure 7. In both parts of the figure, the upper peak represents the distribution of a solute in the mobile phase and

the lower peak the distribution in the stationary phase. A distribution constant of 2 is used in this example so the lower peak has twice the area of the upper one. At the equilibrium, the solute achieves relative distributions like those shown in part (a) but an instant later the mobile gas moves the upper curve downstream giving rise to the situation shown in (b). The solute molecules in the stationary phase are stationary; the solute molecules in the gas phase have moved ahead of those in the stationary phase thus broadening the overall zone of molecules. The solute molecules which have moved ahead must now partition into the stationary phase and vice versa for those that are in the stationary phase as shown by the arrows. The faster they can make this transfer, the less will be the band broadening.

The C_S-term in the Golay equation is:

$$C_S = \frac{2\ K\ d_f^2}{3(1+K)^2\ D_S}, (13)$$

where d_f is the average film thickness of the liquid stationary phase and D_S is the diffusion coefficient of the solute in the stationary phase. To minimize the contribution of this term, the film thickness should be small and the diffusion coefficient large. Rapid diffusion through thin films allows the solute molecules to stay closer together. Thin film can be achieved by coating small amounts of liquid on the capillary walls, but diffusion coefficients cannot usually controlled except by selecting low viscosity stationary liquids. Minimization of the C_S-term results when mass transfer into and out of the stationary liquid is as fast as possible. The other part of the C_S-term is the ratio $K/(1+K)^2$. Large values of K result from high solubilities in the stationary phase. This ratio is minimized at large values of K, but very little decrease occurs beyond a K-value of about 20. Since large values of retention factor result in long analysis times, little advantage is gained by K-values larger than 20.

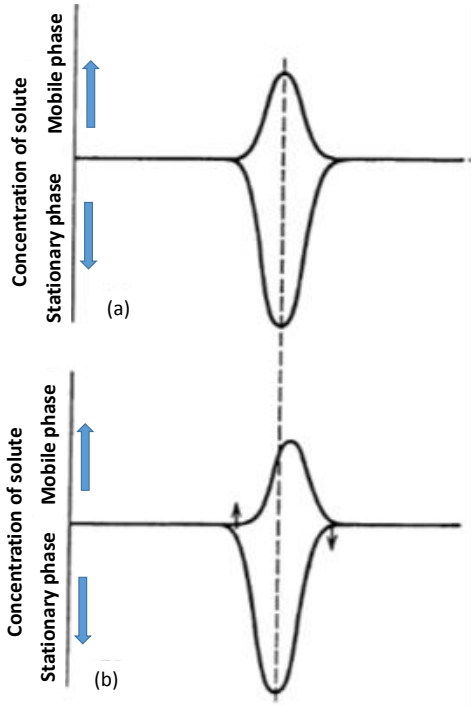

Figure 7. Band broadening due to the mass transfer. ($K_c = 2$).

Mass transfer in the mobile phase is shown in the Figure 8 which shows the profile of a solute zone as a consequence of non-turbulent flow through a tube. Inadequate mixing in the gas phase can result in band broadening because the solute molecules in the centre of the column move ahead of those at the wall. Small diameter columns minimize this broadening because the mass transfer distances are relatively small.

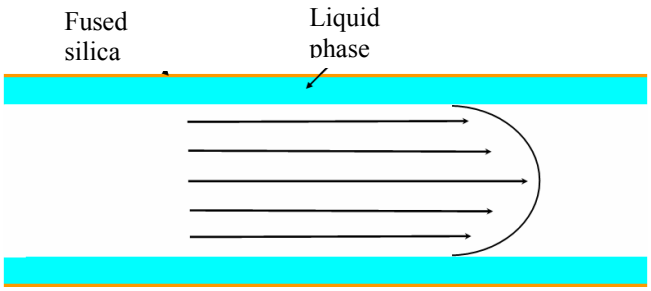

Figure 8. Illustration of mass transfer in the mobile phase.

Golay's equation for the C_M term is:

$$C_M = \frac{(1 + 6k + 11k^2) r_C^2}{24\,(1 + k)^2\, D_G}, (14)$$

where r_c is the radius of the column.

The relative importance of the two C-terms in the rate equation depends primarily on the film thickness and the column radius.

We can say that for thin films (< 0.2 µm), the C-term is controlled by mass transfer in the mobile phase; for thick films (2-5 µm), it is controlled by mass transfer in the stationary phase; and for the intermediate films (0.2 to 2 µm) both factors need to be considered. For the larger wide bore columns the importance of mass transfer in the mobile phase in considerably greater.

Finally, another consideration can be made on the C-terms that are multiplied by the linear velocity in equation 11: they are minimized at low velocities and so there's much time for the molecules to diffuse in and out of the liquid phase and to diffuse across the column in the mobile gas phase[6].

1.2 Mass Spectrometry in GC (GC/MS)

Mass spectrometry (MS) may be defined as the study of systems causing the formation of gaseous ions, with or without fragmentation, which are then characterized by their mass to charge ratios (*m/z*) and relative abundances[23]. The analyte may be ionized thermally, by electric field or by impacting energetic electrons, ions or photons.

During the last decades there has been a remarkable growth in popularity of mass spectrometers (MS) as a tool for both, routine analytical experiments, as well as, advanced investigations. This is due to a number of features including relatively low cost, simplicity of design and extremely fast data acquisition rates. Although sample is destroyed by the mass spectrometer the technique is very sensitive and only trace amounts of material are used in the analysis. In addition, the potential of combined gas chromatography/mass spectrometry (GC/MS) for determining volatile compounds,

contained in very complex flavour and fragrance samples, is well-known. The subsequent introduction of powerful data acquisition and processing systems, including automated library search techniques, ensured that the information content of the large quantities of data generated by GC/MS instruments was fully exploited. These early successes were the foundation of an increasingly diverse range of applications, utilizing many different mass spectrometric techniques. It is expected that a mass spectrometer has the ability to form, separate and detect ions. To fulfill these requirements three fundamental units are required; an ion source, a mass analyzer and a detector[24].

The components of the mass spectrometer are contained in a housing usually kept at moderately high vacuum (10^{-3} to 10^{-6} torr), which ensures that once the ions formed in the ion source begin to move towards the detector, they will not collide with other molecules. The collision of ions would result in further fragmentation or deflection from their desired path. Furthermore, the vacuum also protects metal and oxide surfaces of the ion source, analyzer, and detector from corrosion by air and water vapour, which could compromise the spectrometer's ability to form, separate and detect ions. In brief, the sample has to be introduced into the ionization source of the instrument; volatile compounds are most commonly ionized by electron ionization (EI) sources.

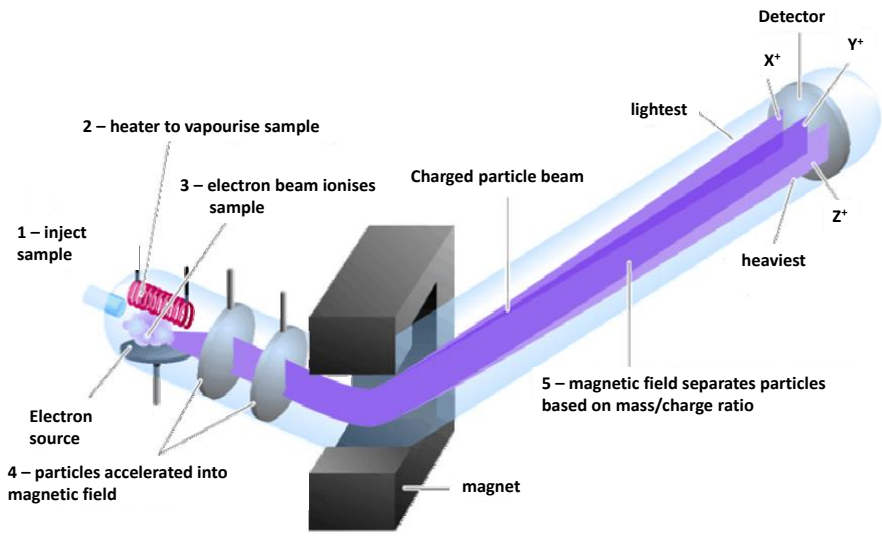

Figure 9. Scheme of a mass spectrometry system.

In an electron impact source a high energy beam of electrons is used to displace an electron from the organic molecule forming a radical cation ($M^{+\bullet}$), the molecular ion. The ionization normally supply considerable energy to this first-formed ion, so that it is almost immediately fragmented. The product ions formed may themselves fragment to produce a characteristic fragmentation pattern, creating a cascade of ion forming reactions before leaving the ion source[25] (see Figure 10).

The collection of ions is then focused into a beam and accelerated into the magnetic field and deflected along circular paths according to the masses of the ions. By adjusting the magnetic field, the ions can be focused on the detector. The individual ion current intensities at each mass are sequentially recorded, generating a mass spectrum. The latter is an histogram of the relative abundance of the ions generated by ionization of the sample and their subsequent separation, based on their *m/z*. The mass spectrum is a fingerprint of the molecule conveying information about its molecular weight, and the relative abundance that generates during the fragmentation process.

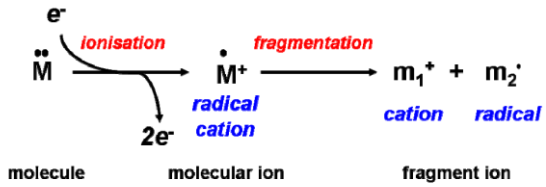

Figure 10. Cascade of ion forming reactions

An MS generates an enormous amount of data, especially when allied to separation techniques such as GC. The raw data is stored in the form of a three-dimensional array with time, *m/z*, and intensity as independent axes[26], while as aforementioned, the mass spectrum itself is a two-dimensional representation of signal intensity versus *m/z*. The raw data are generated by repetitively scanning the mass analyzer over a particular mass range during the separation procedure and storing the intensity data for each scan separately. Alternatively, the mass analyzer is set to switch between a few selected ions, and only these ion intensities are stored during the chromatographic separation in selected ion monitoring[27].

In general mass spectrometers are classified on the basis of their mass analyser; quadrupole mass spectrometer (qMS), tandem MS (MS/MS) and Time of Flight (TOF). The first will be briefly presented in the following subsection.

1.2.1 Quadrupole Mass Spectrometry

A type of mass analyzer commonly used in the flavour and fragrance research field is the quadrupole mass spectrometer (or quadrupole mass filter). This analyser, besides being more compact, inexpensive, and easy to operate, is capable of transmitting only the ion of choice by filtering sample ions according to their *m/z.*

The mass analyzer comprises four parallel hyperbolic or cylindrical metal rods arranged in a square array (Figure 11); each pair of opposing rods is held at the same potential which is composed of a direct current (DC) and an alternating current (AC) component. If the applied voltage is composed of a DC voltage (*U*) on which an oscillating radio-frequency (RF) voltage ($Vcos(\omega t)$), is applied between one pair of rods, and the other, the field within the analyzer is created. A direct current voltage is then superimposed on the RF voltage (*V*) and the ions introduced into the quadrupole field undergo complex trajectories. Only ions of a certain *m/z* will be transmitted to the detector for a given ratio of voltages, while all other ions will oscillate with greater amplitudes, causing them to become unstable and neutralized through collision with one of the rods. This allows selection of a particular ion, or scanning by varying the voltages[27].

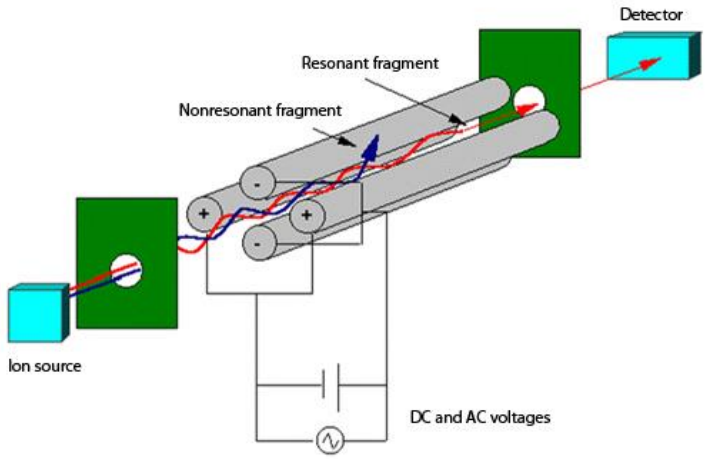

Figure 11. Schematic representation of a quadrupole mass analyzer.

The mass range is scanned by varying the DC and RF fields whilst keeping the voltage ratio and oscillator frequency constant. This produces a low resolution spectrum. In general when the amplitude of *U* equals zero a wide band of *m/z* values will be transmitted, and as the value of *U*/*V* increases, resolution is enhanced so that at the stability limit only a single value of *m/z* corresponds to the trajectory, resulting in the transmission and collection of a single ion. In this manner qMS acts as a mass filter, and can be referred hereafter as a quadrupole mass filter.

Standard quadrupole analyzers have rods of 15 to 25 cm length and 10 to 20 mm in diameter. The RF is in the order of 1 to 4 MHz, and the DC and RF voltages are in the range of 10^2 to 10^3 V; ions of about 10 eV kinetic energy undergo approximately 100 oscillations during their passage[28].

A mass spectrum may be generated by scanning values of *U* and *V* with a fixed *U*/*V* ratio and constant drive frequency, or by scanning the frequency and holding *U* and *V* constant[27]. The transmitted ions of certain *m/z* are then linearly dependent on the voltage applied to the quadrupoles, producing an *m/z* scale that is linear with time. The voltages applied to the rods are usually chosen to give equal peak widths over the entire mass range and unit resolution throughout the mass spectrum. The latter is then evaluated to

determine the original structure of the analytes and compared with reference libraries for positive identification, providing an unparalleled qualitative ability.

1.2.2 Triple quadrupole mass spectrometric detection

At present, the triple quadrupole[26] is the most widely used tandem mass spectrometer. It is a linear assembly of three quadrupoles. Only the first and the third quadrupoles are mass analysers, being operated with the combination of both r.f. and d.c. potentials necessary for mass selection. The second quadrupole, the central one, has a fixed r.f. voltage only. Thus, ions of every mass can pass this quadrupole, which is used as a collision cell with ion focusing properties. A positive ion will travel towards the negative rod but, owing to the frequency of the applied signal, the polarity of the positive rods quickly changes to positive and vice versa. This change in polarity can be compared to a saddle on which a ball has been placed. The ball will roll down the slope, but if the saddle is quickly rotated by 90°, the rolling ball will face a hill, and will roll back to the center of the saddle. If there are several balls and the trajectories change owing to collisions between them, they will be driven back to the centre by the effect of the rapidly rotating saddle. This is analogous to what happens to the ions in the central quadrupole. Even if they undergo collisions with a neutral gas in the cell, the effect of the r.f. potential will bring them back to the centre of the device. This means that loss of ions by scattering after collision is avoided. An offset voltage between the source and this quadrupole collision cell can be adjusted, to allow the collision energy to be varied between zero and several hundred volts. This is low compared with magnetic instruments, where the usual values are fixed somewhere in the range 2-10 KeV. However, a relatively large number of collisions are usually allowed to occur in a triple quadrupole collision cell, so that the conversion of the main beam of parent ions into product ions is normally much greater than the corresponding value for a sector tandem mass spectrometer. Important advantages of triple quadrupole instruments are relatively lower cost and ease of use. Once both quadrupole mass analysers have been calibrated switching between different scan modes and mass ranges can be done instantaneously,

and with unit mass resolution in both analysers for all types of MS/MS experiments. The three main scan modes available using tandem mass spectrometers, are product ion, precursor ion and neutral loss scans. The two mass spectrometers may, a priori, be of any kind. The most common type is that in which the analysers are quadrupole mass spectrometers and the collision cell includes a focusing quadrupole, hence the name triple quadrupole[26]. Other frequently used types consist of either a magnetic and a quadrupole mass spectrometer or two magnetic mass spectrometers. Magnetic instruments consisting of one magnetic and one electric sector can also be used to perform MS/MS experiments, but they have limited capabilities. The most common tandem mass spectrometric experiment is the product ion scan. In this experiment, ions of a given m/z value are selected with the first mass spectrometer. The selected ions are passed into the collision cell, typically filled with helium, argon or xenon. The ions are activated by collision, and therefore are induced to fragment. The product ions are then analysed with the second mass spectrometer, which is set to scan over an appropriate mass range. A product ion spectrum, formerly known as a daughter ion spectrum, is obtained. Such a spectrum allows one to record fragments arising from the molecular ion of a specific compound present as a component in a mixture and generate fragmentation data that can be used to provide information on the structure of the selected ion when necessary. If a reactive gas is introduced into the collision cell of a tandem-in-space mass spectrometer (or into an ion trapping instrument), ion-molecule reactions can be observed[29]. In multiple analyser mass spectrometers, the time allowed for reaction will be short and can be varied over only a limited range. Moreover, it is difficult to achieve the very low collision energies which promote exothermic ion-molecule reactions. Nor will equilibrium be achieved, except with very special dedicated instruments. Nevertheless, product ion spectra arising from ion-molecule reactions can be recorded, and increasing use is being made of these spectra as an alternative to CID in characterizing ions. Instruments based on the coupling of two mass spectrometers allow so-called precursor ion scans, also known as parent scans, to be recorded. In this scan mode, the second mass spectrometer is set to pass only ions with a particular, selected m/z value. The first mass

spectrometer is scanned over a chosen mass range, with a collision gas present in the instrument. Ions which pass through the first mass spectrometer will be detected if, and only if, after fragmentation (or more generally, reaction) in the collision cell it produces the pre-selected product ion. This product ion is the only ion that the second mass analyser can transmit to the detector. For example, if the second analyser is set on m/z 77 ($[C_6 H_5]^+$), the precursor ion scan will provide a record of compounds containing the phenyl group. Adventitious formation of m/z 77 by other ions or non-routine fragmentation by phenyl-containing ions which do not yield m/z 77 as a product, can of course interfere with this determination. Note that the experiment is selective for ions containing particular functional groups, and that it yields the masses of all the ions which satisfy this criterion. In many experiments, this information corresponds to the molecular masses of compounds containing the functional group in question. As in the case of the precursor ion scan, this scan mode cannot be performed with time-based tandem mass spectrometers. It is a form of functional group-selective scan but is more complex in practice than the precursor ion scan, since it requires that both analysers are now scanned together, but with a constant m/z difference between the two spectrometers. This scan allows the selective recognition of all ions which, by fragmentation, lead to the loss of a given neutral fragment. Triple-quadrupole MS systems are exploited for the selective, sensitive analysis of target solutes (i.e. pesticides), often in the multiple-reaction monitoring (MRM) mode. The employment of the MRM approach, compared to SIM analyses, enables enhanced S/N values[30]. Furthermore, the MRM approach is so selective that less attention can be devoted to the sample-preparation and chromatography steps. For this reason, the following question is justified: ‘‘Is there a need for a GC×GC step, prior to the QqQ MS process?’’ Considering MRM analysis, the answer can only be negative. In this respect, the first ever GC×GC-QqQ-MS experiment was described by Poliak *et al*. in 2008[29]. Modulation was performed by using a ‘‘pneumatic’’ device, with flows of 20 mL/min generated in the 2D. MS ionization was achieved using supersonic molecular beam (SMB) EI, an approach defined as ‘‘cold EI’’, due to the capability to generate intense molecular ions. Furthermore, the high outlet flow was handled well by

the SMB interface, with the authors reporting no sensitivity reduction. Recently, Tranchida *et al*. evaluated a novel fast MS/MS instrument, under the extreme flow conditions generated by flow-modulated GC×GC, in the analysis of mandarin essential-oil compounds. The flow exiting the modulator was ~30 mL/min, greatly exceeding the maximum MS limit (10 mL/min), so the authors were obliged to divert a considerable part (≈70%) of the flow to waste, inevitably causing an decrease in sensitivity. The MS/MS system was capable of operating under high-speed conditions in both full-scan (maximum scan speed: 20,000 amu/s) and MRM modes. Furthermore, the MS instrument could generate simultaneous full-scan/MRM data, also in a very rapid manner. A GC×GC-MS/MS method was developed for simultaneous:

•full-scan qualitative analysis of untargeted mandarin essential oil compounds;

•MRM quantitative analysis of targeted compounds, namely three preservatives (o-phenylphenol, butylated hydroxytoluene, and butylated hydroxyanisole).

The degree of sensitivity, reached through the MRM analysis, widely exceeded current-day regulation limits for the preservatives. The untargeted/pre-targeted nature of the experiment was a novelty for MS/MS instrumentation, making sense (more for the untargeted part) of the GC×GC combination.

1.2.3 Isotope-Ratio Mass Spectrometer

The isotope-ratio mass spectrometer (IRMS) allows the precise measurement of mixtures of naturally occurring isotopes. Most instruments used for precise determination of isotope ratios are of the magnetic sector type. This type of analyzer is superior to the quadrupole type in this field of research for two reasons. First, it can be set up for multiple-collector analysis, and second, it gives high-quality 'peak shapes'. Both of these considerations are important for isotope-ratio analysis at very high precision and accuracy. The sector-type instrument designed by Alfred Nier was such an advance in mass spectrometer design that this type of instrument is often called the 'Nier type'. In the most general terms the instrument operates by ionizing the sample of interest,

accelerating it over a potential in the kilo-volt range, and separating the resulting stream of ions according to their mass-to-charge ratio (m/z). Beams with lighter ions bend at a smaller radius than beams with heavier ions. The current of each ion beam is then measured using a 'Faraday cup' or multiplier detector.

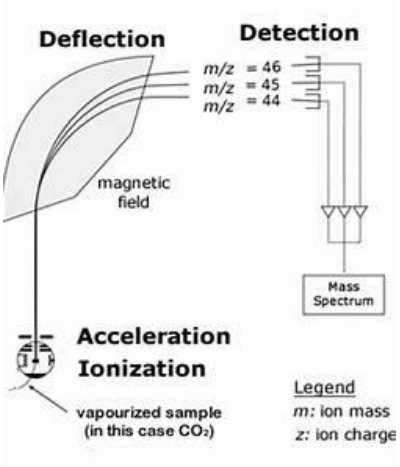

Figure 12. Schematic of an isotope-ratio mass spectrometer for measuring CO_2

Many radiogenic isotope measurements are made by ionization of a solid source, whereas stable isotope measurements of light elements (e.g. H, C, O) are usually made in an instrument with a gas source. In a "multicollector" instrument, the ion collector typically has an array of Faraday cups, which allows the simultaneous detection of multiple isotopes.

References:

1. M. Tswett, *Ber. Dtsch. Botan. Ges.* 24 (1906), 316.
2. A. J. P. Martin and R. L. M. Synge, *Biochem. J.* 35 (1941), 1358.
3. A. T. James, A. J. P. Martin, *Biochem. J.* 50 (1952), 679.
4. M. Novotny, Gas Chromatography in: *Encyclopedia of Physical Science and Technology (Third Edition)*, R. A. Meyers, Academic Press, San Diego, 2001, 455-472.
5. M.J.E. Golay, in: *Gas Chromatography*, V.J. Coates, H.J. Noebels, I.S. Fagerson (Editors), Academic Press, New York, USA, 1958.
6. H. M. McNair and J. M. Miller, *Basic Gas Chromatography*, Wiley & Sons, New York, (1998).
7. B. M. Mitzner, M.H. Jacobs, *Chemist-Analyst* 48 (1959), 104.

8. M. J. D. Low, S.K. Freeman, *Anal. Chem.* 39 (1967), 194.
9. L. V. Azzaraga, *Appl. Spectrosc.* 34 (1980), 224.
10. G. N. Giss, C. L. Wilkins, *Appl. Spectrosc.* 38 (1984), 17.
11. D. E. Henry, A. Giorgetti, A. M. Haefner, P. R. Griffiths, *Anal. Chem.* 59 (1987), 2356.
12. R. Fuoco, K. H. Shafer, P. R. Griffiths, *Anal. Chem.* 58(1986), 3249.
13. A. M. Haefner, K. L. Norton, P. R. Griffiths, S. Bourne, R. Curbelo, *Anal. Chem.* 60 (1988), 2441.
14. S. Bourne, *Vibr. Spectrosc.* 19 (1999), 47.
15. G. T. Reedy, S. Bourne, P. T. Cunningham, *Anal. Chem.* 51 (1979), 1535.
16. G. T. Reedy, D. G. Ettinger, J.F. Schneider, S. Bourne, *Anal. Chem. 57* (1985), 1602.
17. P. Jackson, G. Dent, D. Carter, D. Schofield, J. Chalmers, T. Visser, M. J. Vredenbregt, *J. High Resol. Chrom.* 16 (1993), 515.
18. K. L. Norton, P. R. Griffiths, *J. Chromatogr. A* 703 (1995), 383.
19. S. Compton, P. Stout, *LC-GC* 8 (1990), 920.
20. I. Ojanpera, R. Hyppola, E. Vuori, *Forensic Sci. Int.* 80 (1996), 201.
21. Th. Hankemeier, E. Hooijschuur, R. J. J. Vreuls, U. A. Th. Brinkman, T. Visser, *J. High Resol. Chromatogr.* 21 (1998), 341.
22. J. Auger, S. Rousset, E. Thibout, B. Jaillais, *J. Chromatogr. A* 819 (1998), 45.
23. J. F. J. Todd. *Int. J. Mass Spectrom. Ion Process.* 142 (1995), 209.
24. R. M. Smith in: *Understanding Mass Spectra: a basic approach*. Wiley & Sons, New York, 2004.
25. F. W. McLafferty, F. Tureček in: *Interpretation of Mass Spectra*. University Science Books, Mill Valley, 1993.
26. R. A. Yost and C. G. Enke, *J. Am. Chem. SOC.* 100 (1978), 2274.
27. D. D. Fetterolf and R. A. Yost, *Int. J. Mass Spectrom*. Ion Processes 62 (1984), 33.
28. J.H. Gross, *Hyphenated methods, Mass Spectrometry*, Springer-Verlag, Berlin, Heidelberg, (2004), 475.
29. M. Poliak, A.B. Fialkov, A. Amirav, *J. Chromatogr. A* 1210 (2008), 108.
30. P.Q. Tranchida, F.A. Franchina, M. Zoccali, S. Panto, D. Sciarrone, P. Dugo, L. Mondello, *J. Chromatogr. A* 1278 (2013), 153.

Chapter II

2 Miniaturization of the QuEChERS Method in the Fast Gas Chromatography-Tandem Mass Spectrometry Analysis of Pesticide Residues in Vegetables

2.1 Introduction

Pesticides are extensively used in agriculture to increase crop yield, but with concerns about the presence of residues in foods and in the environment. As a consequence, many countries have passed laws regulating the presence of residues in or on a food[1] (González-Rodríguez *et al*. 2011). Maximum residual concentrations are defined as maximum residue levels (MRLs) in Europe and Japan [Regulation (EC) No 396 2005; The Japan Food Chemical Research Foundation 2005][2,3] and as tolerances in the USA (Administrator of the Environmental Protection Agency 2014)[4].

The use of green (or greener) and rapid sample preparation methods is currently a major issue in the analytical chemistry field, with the obvious reason being the reduction of costs in terms of reagents, solvents, and time[5] (De La Guardia and Armenta 2011). Miniaturization is a popular way to reach such a goal: smaller sample amounts are easy to handle (and store) in the lab and lead to a decreased necessity of solvents and reagents.

In recent decades, a series of well-accepted miniaturized extraction and pre-concentration techniques have been developed, such as single-drop microextraction (SDME)[6] (Andraščíková *et al*. 2015), stir-bar sorptive extraction (SBSE) (Camino-Sánchez *et al*. 2014)[7], dispersive liquid liquid microextraction (DLLME) (Andraščíková *et al*. 2015)[6], miniaturized solid-phase extraction (SPE) (Wen *et al*. 2014)[8], etc. On the other hand, the use of miniaturized approaches is much more limited in the case of solid samples, a factor probably due to a more demanding extraction process (viz., matrix structure disruption, efficient solvent penetration, satisfactory recovery of target compounds). Even so, miniaturized versions of existing extraction technologies have been applied, such as matrix solid-phase dispersion (MSPD) (Wen *et al*. 2014) [8], pressurized liquid extraction (PLE) (Ramos 2012)[9], ultrasound-assisted extraction (USE) (Ramos 2012)[9],

and quick, easy, cheap, effective, rugged and safe (QuEChERS) (Andraščíková *et al*. 2015, Ramos 2012)[6,9].

The QuEChERS approach appeared for the first time in 2003 and was developed by Anastassiades *et al*. (2003)[10]. The method proposed by Anastassiades *et al*. was based on salting out extraction with an organic solvent, followed by dispersive solid-phase extraction (d-SPE). The original method was applied to the analysis of target analytes in a wide variety of matrices, in particular for pesticides in foods (Anastassiades *et al*. 2003; Bruzzoniti *et al*. 2014; Martínez-Domínguez *et al*. 2014; Sapozhnikova and Lehotay 2015a)[10-13]. Adjustments have been made to the original QuEChERS approach, leading to two official methods: one based on the use of a citrate buffer [European Committee for Standardization (CEN) Standard Method EN 15662] (CEN 2008)[14] and the other on the use of an acetate buffer (AOAC Official Method 2007.01) (Lehotay 2007)[15], with the latter possessing a greater buffering capacity.

The main purpose of the use of a buffer is to extend the applicability of the approach to specific pesticides, which undergo ionization and/or degradation during extraction, depending on the pH of the matrix. In both cases, the pH is adjusted to about 5, which is a compromise to extract pesticides sensitive to either acidic or basic conditions. Other noteworthy changes have concerned the d-SPE cleanup step, involving the use of different amounts or new combinations of adsorbent materials and solvents, with the objective to attain cleaner extracts (Mastovska *et al*. 2010; Wilkowska and Biziuk 2011; Berlioz-Barbier *et al*. 2014)[16-18].

Apart from the use of miniaturized sample preparation methods, there is also a tendency to reduce gas chromatography (GC) separation times (Sapozhnikova and Lehotay 2015b)[19]. In this respect, the use of short microbore columns enables a drastic reduction of GC analyses times with little or no loss in terms of resolution; the well-known reduced sample capacity of reduced-ID columns is, for the main part, counterbalanced by the generation of narrower peaks (due to less band broadening) (Donato *et al*. 2007)[20].

Within the aforementioned analytical context, the main scope of the present research was to evaluate a reduced-scale QuEChERS approach, followed by fast GC analysis, for the

extraction and separation of target pesticides in vegetable products (tomatoes, zucchini, red peppers, and lettuce). More specifically, two different QuEChERS methods were applied in relation to the matrix type. Highly sensitive tandem mass spectrometry (MS/MS) was used for qualitative and quantitative purposes (Tranchida *et al*. 2013a, b, c)[21-23]. The results attained were compared to those derived through the (QuEChERS) official CEN Standard Method EN 15662[14]. A series of GC-amenable pesticides, with a wide MRL range, were selected from the Regulation (EC) No 396 (2005) of The European Parliament (European Parliament 2005)[2]. The miniaturization of the QuEChERS approach has already been proposed by Berlioz-Barbier *et al*. for the analysis of 35 emerging pollutants in benthic invertebrates and by De Armond *et al*. for the analysis of methomyl and aldicarb in blood and brain tissue (Berlioz-Barbier *et al*. 2014; De Armond *et al*. 2015)[18,24]. Both works reported the use of a liquid chromatography separation step, prior to MS analysis. The aim of this study was to evaluate a miniaturized version of QuEChERS, followed by fast GC combined with triple-quadrupole (QqQ) MS, by using four representative vegetables.

2.2 Experimental

The phytosanitary compounds listed in Table 1 were kindly provided by Supelco/Sigma-Aldrich Bellefonte, USA), with purity higher than 98%. All the solvents used were HPLC grade. Acetonitrile (ACN), ethyl acetate (EtOAc), formic acid (FA), and n-hexane (n-hex) were obtained from Supelco/Sigma-Aldrich. Stock solutions of the phytosanitary compounds (from 548 to 1260 mg L^{-1}) were prepared in EtOAc and stored in dark vials at −20 °C, between optimization and validation experiments.

Stock solutions were used for 2 weeks, for the purposes of method optimization and validation. Stock solutions of triphenylphosphate (TPP) and anthracene (An), used as internal standard (ISTD) and quality control (QC) standard, were prepared in EtOAc and stored in dark vials at −20 °C at concentrations of 2000 and 1000 μg L^{-1}, respectively (CEN 2008). Calibration standard solutions were prepared in EtOAc (solvent calibration) and in blank vegetable extracts (matrix matched calibration). Blank samples of zucchini,

red pepper, lettuce, and tomato (for use in validation experiments and to prepare matrix matched standards) were previously extracted with the official QuEChERS method and subjected to analysis by fast GC coupled to QqQ MS to confirm the absence of target pesticides; concentration ranges for each kind of matrix are reported in Table 1. Samples were homogenized with an Ultra-Turrax T 25 digital homogenizer (Janke & Kunkel GmbH & Co., IKA Labortechnik, Wilmington, NC, USA).

A standard mixture of pesticides at the 10,000 μg L^{-1} level, in EtOAc with 0.05% FA, was used for high (≈100 μg kg^{-1}) and medium (≈50 μg kg^{-1}) spiking levels; a mixture at the 1000 μg L^{-1} level was used for the low (≈10 μg kg^{-1}) spiking level. The three solutions were used to measure recovery.

For sample preparation, commercial QuEChERS (Supel™ QuE Citrate) containing 4 g $MgSO_4$, 1 g NaCl, 0.5 g NaCitrate dibasic sesquihydrate, and 1 g NaCitrate tribasic dehydrate was used. For d-SPE cleanup, pre-weighed mixtures containing 150 mg of primary and secondary amine (PSA) and 900 mg of $MgSO_4$ (Supel™QuE PSA), or 150 mg of primary and secondary amine, plus 45 mg of graphitized non-porous carbon (ENVI-Carb) and 900 mg of $MgSO_4$ (Supel™ QuE PSA/ENVI-Carb) were used. These materials were provided by Supelco/Sigma-Aldrich.

Table 1. List of pesticides, quantifier and qualifier ion transitions [along with collision energies (eV)], calibration (µg kg^{-1}) concentration ranges, EU MRLs values (µg kg^{-1}), repeatability (%CV) at the ≈ 50 µg kg^{-1} calibration level, LoDs and LoQs (µg kg^{-1}), % matrix effect, quantifier and qualifier % ion ratios (plus repeatability) and, R^2 for zucchini (Table 1A) and red pepper(Table 1B). [a] without considering the highest concentration level.

					Zucchini							
N°	Pesticide	Quantifier	Qualifier	Calibration	EU MRL	%CV	LoD	LoQ	%ME	Ion ratio	%CV	R^2
1	Propachlor	176>57 (8)	176>120 (12)	12.8-6400	20	3.8	0.4	1.5	7.4	77	2.3	0.998
2	Desmedipham	181>109 (14)	181>122 (12)	11-5480	50	2.3	0.5	1.6	**65.9**	59	5.0	0.997
3	Dimethipin	118>58 (6)	118>90 (4)	10.7-5350	50	2.3	1.7	5.6	**-66.7**	32	12.8	0.995
4	Cyromazine	151>109 (20)	165>56 (30)	11-5500	2000	2.0	1.8	6.0	**-35.0**	8	11.2	0.999
5	Heptachlor	271>236 (20)	272>117 (32)	11-5490	10	2.2	0.9	2.9	**-63.0**	6	10.5	0.998
6	Prosulfocarb	128>43 (20)	91>65 (20)	12.6-6300	10	1.7	0.6	2.1	-15.7	71	6.7	0.999
7	Metolachlor	238>162 (12)	238>133 (26)	11.1-5570	50	1.2	0.5	1.6	**-26.0**	40	4.2	0.999
8	Butralin	266>220 (15)	266>190 (15)	11.2-5600	10	3.1	1.7	5.6	-10.2	98	0.5	0.997
9	Beflubutamid	176>91 (20)	91>65 (20)	10.4-5180	20	4.2	1.6	5.5	1.8	97	2.1	0.999
10	Oxyfluorfen	361>300 (14)	361>317 (6)	10.7-5350	50	7.7	1.5	4.9	11.2	83	2.2	0.999
11	Carboxin	235>143 (12)	235>87 (24)	11.3-5670	100	5.7	2.0	6.7	**-24.9**	26	2.0	0.999
12	Chlorfenapyr	247>227 (16)	247>200 (24)	11.4-5690	10	5.0	0.3	1.1	-12.5	50	5.1	0.999
13	Cyproconazole isomer I	222>125 (24)	222>82 (12)	5.6-2800	50	7.4	0.5	1.7	14.3	54	2.5	0.998[a]
14	Cyproconazole isomer II	222>125 (24)	222>82 (12)	5.6-2800	50	7.4	0.5	1.7	14.3	54	2.5	0.998[a]
15	Mepronil	269>119 (14)	269>227 (6)	10.9-5450	10	4.2	0.8	2.7	5.8	31	5.0	0.999
16	Chloridazon	221>77 (24)	221>105 (12)	11.4-5680	500	3.1	1.1	3.6	3.7	27	1.9	0.999
17	Spiromesifen	272>254 (10)	71>43 (10)	11.4-5680	300	7.2	1.0	3.4	**-20.8**	48	14.0	0.997[a]
18	Captafol	79>77 (14)	79>51 (20)	11.7-5830	20	2.7	0.6	2.1	**52.5**	51	8.0	0.998
19	Dimoxystrobin	116>89 (20)	205>116 (10)	10.3-5150	10	4.1	1.3	4.4	13.8	47	8.6	0.998
20	Bromuconazole isomer I	295>173 (14)	294>145 (28)	5.6-2790	50	5.7	0.6	1.9	18.6	15	11.6	0.999
21	Fenamidone	268>180 (16)	268>77 (28)	11-5500	200	2.5	1.1	2.8	-7.0	68	0.8	0.998
22	Bromuconazole isomer II	295>173 (14)	294>145 (28)	5.6-2790	50	3.1	0.4	1.4	-6.9	15	11.6	0.996
23	Flurtamone	120>42 (20)	157>137 (15)	11.4-5710	20	1.2	0.3	0.8	**39.8**	22	3.4	0.999
24	Ioxynil octanoate	127>57 (10)	127>43 (20)	11.2-5620	10	3.2	0.3	0.9	-10.8	19	8.2	0.999
25	Prochloraz	180>138 (12)	180>69 (20)	10.9-5460	50	4.6	0.5	1.5	16.3	64	2.1	0.997
26	Cyfluthrin isomer I	226>206 (14)	226>199 (6)	4.3-2170	100	1.0	0.8	2.7	-12.8	48	5.3	0.997
27	Cyfluthrin isomer II	226>206 (14)	226>199 (6)	8.1-4030	100	6.2	0.5	1.7	**-33.3**	48	5.2	0.999
28	Boscalid	342>140 (14)	342>112 (28)	10.4-5200	3000	3.1	1.3	4.2	15.9	22	10.4	0.999
29	Fenvalerate isomer I	419>225 (6)	419>167 (12)	9-4512	20	4.5	0.8	2.5	-15.2	66	1.1	0.999
30	Fenvalerate isomer II	419>225 (6)	419>167 (12)	2.3-1128	20	3.5	0.1	0.3	-10.6	67	2.6	0.998
31	Difenoconazole isomer I	323>265 (14)	323>202 (28)	5.8-2900	300	7.3	0.3	1.1	**42.0**	16	7.9	0.999
32	Difenoconazole isomer II	323>265 (14)	323>202 (28)	5.8-2900	300	5.1	0.2	0.7	**22.8**	16	6.6	0.999
33	Dimethomorph isomer I	301>165 (14)	301>139 (14)	5-2495	500	4.2	0.4	1.3	12.6	22	2.5	0.999
34	Dimethomorph isomer II	301>165 (14)	301>139 (14)	5-2495	500	9.8	0.5	1.8	**22.3**	22	2.5	0.999
35	Fluoxastrobin	188>144 (15)	186>116 (25)	11.4-5690	50	9.4	2.6	8.6	**41.9**	16	10.9	0.999

				Red Pepper								
N°	Pesticide	Quantifier	Qualifier	Calibration	EU MRL	%CV	LoD	LoQ	%ME	Ion ratio	%CV	R^2
1	Propachlor	176>57 (8)	176>120 (12)	12.8-6400	20	5.0	4.3	14.2	-14.9	75	1.6	0.999
2	Desmedipham	181>109 (14)	181>122 (12)	11-5480	50	3.9	0.4	1.4	**38.6**	59	1.8	0.998[a]
3	Dimethipin	118>58 (6)	118>90 (4)	10.7-5350	50	5.1	2.0	6.8	-3.7	30	4.7	0.999[a]
4	Cyromazine	151>109 (20)	165>56 (30)	11-5500	1500	3.7	1.8	5.9	-7.6	7	7.0	0.999
5	Heptachlor	271>236 (20)	272>117 (32)	11-5490	10	4.7	1.1	3.6	3.4	6	9.1	0.999
6	Prosulfocarb	128>43 (20)	91>65 (20)	12.6-6300	10	3.7	2.8	9.2	**-26.5**	77	3.6	0.993[a]
7	Metolachlor	238>162 (12)	238>133 (26)	11.1-5570	50	7.2	2.2	7.4	**-22.5**	39	1.4	0.999
8	Butralin	266>220 (15)	266>190 (15)	11.2-5600	10	3.0	1.3	4.2	-12.5	99	0.5	0.997[a]
9	Beflubutamid	176>91 (20)	91>65 (20)	10.4-5180	20	10.4	2.2	7.3	-13.5	98	0.8	0.999
10	Oxyfluorfen	361>300 (14)	361>317 (6)	10.7-5350	50	2.4	1.2	3.9	-8.8	88	1.1	0.998
11	Carboxin	235>143 (12)	235>87 (24)	11.3-5670	100	10.5	1.2	4.1	11.3	26	5.4	0.999
12	Chlorfenapyr	247>227 (16)	247>200 (24)	11.4-5690	10	2.8	2.9	9.4	-10.0	51	6.7	0.992
13	Cyproconazole isomer I	222>125 (24)	222>82 (12)	5.6-2800	50	5.3	1.1	3.8	19.9	56	1.5	0.998[a]
14	Cyproconazole isomer II	222>125 (24)	222>82 (12)	5.6-2800	50	5.3	1.1	3.8	19.9	56	1.5	0.998[a]
15	Mepronil	269>119 (14)	269>227 (6)	10.9-5450	10	3.3	1.2	3.9	5.6	32	2.4	0.999
16	Chloridazon	221>77 (24)	221>105 (12)	11.4-5680	500	4.2	1.1	3.6	16.7	26	4.9	0.999
17	Spiromesifen	272>254 (10)	71>43 (10)	11.4-5680	500	3.1	2.6	8.5	-12.6	47	2.2	0.999
18	Captafol	79>77 (14)	79>51 (20)	11.7-5830	20	9.6	1.1	3.7	11.9	50	2.1	0.997
19	Dimoxystrobin	116>89 (20)	205>116 (10)	10.3-5150	10	5.0	1.4	4.7	-15.7	46	1.2	0.999
20	Bromuconazole isomer I	295>173 (14)	294>145 (28)	5.6-2790	50	4.9	1.0	3.3	-9.8	15	9.0	0.997
21	Fenamidone	268>180 (16)	268>77 (28)	11-5500	20	2.9	1.4	4.8	**-33.3**	69	1.5	0.999
22	Bromuconazole isomer II	295>173 (14)	294>145 (28)	5.6-2790	50	4.4	0.7	2.4	-6.1	15	5.6	0.999
23	Flurtamone	120>42 (20)	157>137 (15)	11.4-5710	20	4.0	1.2	4.1	6.3	22	5.0	0.999
24	Ioxynil octanoate	127>57 (10)	127>43 (20)	11.2-5620	10	7.7	1.6	5.3	-14.3	18	4.8	0.999
25	Prochloraz	180>138 (12)	180>69 (20)	10.9-5460	50	4.8	1.1	3.6	10.0	63	1.9	0.999
26	Cyfluthrin isomer I	226>206 (14)	226>199 (6)	4.3-2170	300	6.1	0.9	2.8	-1.8	49	2.2	0.999[a]
27	Cyfluthrin isomer II	226>206 (14)	226>199 (6)	8.1-4030	300	4.7	0.9	3.2	-14.7	49	3.4	0.999
28	Boscalid	342>140 (14)	342>112 (28)	10.4-5200	3000	5.4	2.7	9.0	2.5	22	5.7	0.999
29	Fenvalerate isomer I	419>225 (6)	419>167 (12)	9-4512	20	6.1	0.5	1.7	19.0	66	3.2	0.999
30	Fenvalerate isomer II	419>225 (6)	419>167 (12)	2.3-1128	20	3.4	0.2	0.6	9.6	66	2.9	0.998
31	Difenoconazole isomer I	323>265 (14)	323>202 (28)	5.8-2900	500	3.2	1.8	6.1	16.4	15	2.7	0.998[a]
32	Difenoconazole isomer II	323>265 (14)	323>202 (28)	5.8-2900	500	5.2	1.3	4.4	**23.8**	15	4.2	0.999
33	Dimethomorph isomer I	301>165 (14)	301>139 (14)	5-2495	1000	4.0	0.7	2.2	5.2	21	1.9	0.999
34	Dimethomorph isomer II	301>165 (14)	301>139 (14)	5-2495	1000	4.6	0.8	2.7	**24.8**	21	1.9	0.999
35	Fluoxastrobin	188>144 (15)	186>116 (25)	11.4-5690	50	3.8	1.5	5.0	19.4	18	8.7	0.999

2.3 Samples and Sample Preparation

Five samples for each type of vegetable, namely zucchini, red pepper, lettuce, and tomato, were purchased from retailers located in Messina (Italy). Sample preparation with the official method was based on the citrate buffer QuEChERS approach, with ACN extraction (CEN 2008). Briefly, 10 g of homogenized sample were placed into a 50-mL centrifuge tube; the matrices were spiked with adequate concentrations of standards, according to the spiking level (namely ≈10, ≈50, and ≈100 μg kg^{-1}), the ISTD, and the QC one. After 15 min, 10 mL of ACN were added and the tube was shaken vigorously by using an IKA MS 3 basic shaker (Werke GmbH & Co. KG—Staufen, Germany) for 30 s. After, 4 g $MgSO_4$, 1 g NaCl, 0.5 g NaCitrate dibasic sesquihydrate, and 1 g NaCitrate tribasic dehydrate were added, and the tube was shaken vigorously for 60 s. The tube was centrifuged for 5 min at 1512 rcf. Six milliliters of the acetonitrile layer were transferred into two different centrifuge tubes containing Supel™ QuE PSA for the zucchini and Supel™ QuE PSA/ENVI-Carb for the red peppers. The centrifuge tubes were shaken vigorously for 30 s and then centrifuged for 5 min at 1512 rcf. Then, 2 mL of the vegetable extract were concentrated ten times under a gentle stream of nitrogen (to a final amount of extract per volume of 10 g mL^{-1}) and subjected to fast GC-QqQ MS analysis. The official method was used for the analysis of zucchini and red pepper samples, and the results were used for the purpose of method comparison. With regard to the reduced-scale method, the approach was based on the same citrate buffer QuEChERS method, with ACN extraction, as described above (CEN 2008). Briefly, 3 g of homogenized sample were placed into a 12 mL centrifuge tube; adequate concentrations of standards (according to the spiking level), ISTD and the QC one, were added. For the preparation of sample blanks, 3 g of sample were spiked with internal and quality control standards only. After 15 min, 3 mL of ACN were added and the tube was shaken vigorously for 30 s. After, 1.3 g $MgSO_4$, 0.33 g NaCl, 0.16 g NaCitrate dibasic sesquihydrate, and 0.33 g NaCitrate tribasic dehydrate were added, and the tube was shaken vigorously for 60 s. The tube was centrifuged for 5 min at 1512 rcf. One and a half milliliters of the acetonitrile layer were transferred into two different centrifuge

tubes containing Supel™ QuE PSA for the tomatoes and zucchini (50 mg PSA and 300 mg $MgSO_4$) and Supel™ QuE PSA/ENVI-Carb for the red peppers and lettuce (50 mg PSA, 15 mg ENVI-Carb, and 300 mg $MgSO_4$).

The centrifuge tubes were shaken vigorously for 30 s and then centrifuged for 5 min at 1512 rcf. Then, 1 mL of the vegetable extract was concentrated ten times under a gentle stream of nitrogen (to a final amount of extract per volume of 10 g mL^{-1}) and subjected to fast GC-QqQ MS analysis.

2.4 Fast GC-QqQ MS Analyses

All fast GC-QqQ MS applications were carried out on a Shimadzu GC2010 instrument and a TQ8040 triple quadrupole mass spectrometer (Shimadzu, Kyoto, Japan). Automatic injection was performed by using an AOC-20i auto injector, equipped with a 10-μL syringe (injection volume range 0.1–8 μL). Data were acquired by using the GCMS solution software ver. 4.0 (Shimadzu), while the MS database used was the Pesticides GC/MS Library ver. 1.0 (Shimadzu) for initial pesticide screening.

The column employed was an SLB-5ms [(silphenylene polymer, practically equivalent in polarity to poly(5% diphenyl/95% methylsiloxane)], with the following dimensions: 15 m × 0.10 mm ID × 0.10 μm *df* (Supelco, Bellefonte, USA). GC temperature program: 50 °C–350 °C at 20 °C min^{-1}. He head pressure (constant linear velocity mode 50 cm s^{-1}) was 565.5 kPa. Injection temperature, mode, and volume: 280 °C, splitless (4 min, then split 1:20), and 0.2 μL. QqQ MS conditions: electron ionization (70 eV); full scan conditions: scan speed 10,000 amu s^{-1}; mass range 40–360 m/z. Interface and ion source temperatures: 220 and 220 °C. Ar (200 kPa) was employed as collision gas. For multiple reaction monitoring (MRM) transitions and collision energies (CEs), see Table 1.

2.5 Method validation

The developed method was in-house validated following the SANTE/11945/2015 guidelines (SANTE 2015)[25]. First, the reduced-scale approach was evaluated through a comparison with the official method, in terms of recovery and precision, as reported in

van Zoonen *et al*. (1999)[26]. Recovery experiments, performed on zucchini and red pepper, were carried out at three different spiking levels (≈10, ≈50, and ≈100 μg kg^{-1}), for both methods, and also considering both d-SPE procedures. Both the t test (to evaluate if the average results differ significantly) and the F test (to evaluate the difference between the standard deviations) were performed to compare the methods. The solvent calibration solutions (≈10, ≈50, ≈100, and ≈1000 μg L^{-1}) were also used to evaluate the matrix effect (ME) for each analyte in all four samples. ME values were calculated as the difference between the slope of the matrix-matched (MM) calibration curve and the solvent-only (SO) calibration curve, divided by the slope of the solvent-only calibration curve; the derived value was then expressed as a percentage: %ME = [(MM calibration curve slope − SO calibration curve slope)/SO calibration curve slope] × 100. Intra-day precision was evaluated at the 50 μg kg^{-1} level (approximately), by performing eight replicates, and expressed as %CV. Limits of detection (LoD) and quantification (LoQ) were calculated by multiplying the standard deviation of the analyte area, relative to the sample blank fortified at the lowest concentration level (n = 4), three and ten times, respectively, and then by dividing the result by the slope of the calibration curve. Matrix-matched linearity was tested at six levels in the 10–5000 μg kg^{-1} range (at the ≈10, ≈50, ≈100, ≈500, ≈1000, and ≈5000 μg kg^{-1} levels), performing four replicates at each level. Calibration curves were then constructed using the least squares method to estimate the regression line; the linearity and the goodness of the curve used were confirmed using Mandel's fitting tests. The significance of the intercept was established running a *t* test. All the statistical tests were carried out at the 5% significance level. For absolute quantification purposes, matrix-matched calibration was used.

2.6 Results and discussion

2.6.1 Fast GC-QqQ MS Optimization

The fast GC method developed was characterized by a total run time of 15 min. The GC oven required 2 min to cool down from 350 to 50 °C, giving a total analysis time of 17

min. The column employed was a low-polarity high-resolution one, capable of generating circa 150,000 theoretical plates if used under ideal conditions. A constant He linear velocity of 50 cm s^{-1} was applied. The temperature program gradient, namely 20 °C min^{-1}, was derived on the basis of a 10 °C/void time value, advised and reported in the literature (Blumberg and Klee 1998)[27].

A standard solution containing all the target analytes was injected (concentration range 1128–6400 μg L^{-1}) in the full scan mode to determine the retention times and the most significant ions of the target compounds. A time-consuming series of experiments was performed to determine the precursor and the product ions and the relative ion ratios, along with optimum CE values (Table 1). MRM transitions were all defined at a CE value of 20 eV; for CE optimization, the 5–40 eV range was evaluated at intervals of 5 eV. As recommended by SANTE guidelines (SANTE 2015), each targeted compound was characterized by four parameters: retention time, two MRM transitions, and the ratio between the product ions.

Fast GC-QqQ MS traces, relative to the analysis of a spiked zucchini at the ≈10 μg kg^{-1} level, are shown in Figure 1. The average percent of ion ratios (qualifier/quantifier), along with the related standard deviation (SD) values, are listed in Table 1 (zucchini and red pepper).

The overall chromatographic separation can be considered more than sufficient, allowing an accurate quantification of all analytes. Just in one case, namely for the cyproconazole isomers, the separation obtained did not allow the quantification of the single isomers, and for such a reason, they were quantified as sum of isomers. The isomers could have probably been resolved by tuning the oven temperature program. However, due to the fact that the European MRL considers the sum of isomers, the oven temperature program was not modified. The MRL values of all target analytes are reported in Table 1, for each kind of sample. In 25 cases, the MRLs are the same for all the samples, while in other cases, the values are very different, up to two orders of magnitude. The higher MRL values are those reported for boscalid and dimethomorph isomers: 30,000 and 15,000 μg kg^{-1} in lettuce, respectively.

2.6.2 Method Optimization

The main object of the present research was the evaluation of a reduced-scale method. The entire extraction process was performed using circa one third of the sample (3 g instead of 10 g, paying attention to properly homogenize the sample prior to extraction), extraction solvent (3 mL instead of 10 mL), and sorbent material (2.1 g instead of 6.5 g for the extraction step, 0.35 g instead of 1.05 g for the Supel™ QuE PSA step, and 0.36 g instead of 1.09 g for the Supel™QuE PSA/ENVI-Carb stage) compared to the official method, thus saving a considerable amount of solvents, sorbent material, and sample. It was highly important to reach sufficient sensitivity for European regulation requirements (European Parliament 2005), and thus a concentration step at the end of the cleanup process was found necessary; specifically, the sample solution was concentrated by a factor of 10 under a gentle stream of nitrogen (the use of the ISTD and the QC one allows to control this process carefully). In fact, as previously mentioned, one of the main disadvantages relative to the use of microbore columns is the lower sample capacity compared to conventional ID ones; such a drawback is, in part, counterbalanced by reduced band broadening. To evaluate the possible loss of volatiles during the concentration process, a comparison was made between a pesticide solution at the 100 μg L^{-1} level, concentrated 10 times, and one at the 1000 μg L^{-1} concentration level. A t test was performed between the areas of the two solutions, showing that there were no significant losses of volatile compounds ($p > 0.05$). After the concentration process, the recovery of the reduced-scale QuEChERS extraction procedure was subjected to evaluation through a comparison with the official CEN Standard Method EN 15662. Specifically, recoveries were measured for both d-SPE cleanup steps (PSA and PSA/ENVI-Carb) by using spiked matrices, namely red pepper and zucchini. Such experiments were performed at the ≈10, ≈50, and ≈100 μg kg^{-1} concentration levels ($n = 4$), with the presence of the internal standard (TPP). The t test and F test were performed at each concentration level to evaluate significant differences ($p < 0.05$) in the average and SD results, respectively. Considering the 35 pesticides evaluated at three concentration levels, a total of 105 comparisons of the average recoveries were

performed running the t test. Of these, 39 and 60 were significantly different ($p < 0.05$) between the official and the reduced-scale method using the PSA and the PSA/ENVI-Carb cleanup processes, respectively. While, comparing the SD values running the F test, 30 and 9 results were significantly different ($p < 0.05$) between the official and the reduced-scale method using the PSA and the PSA/ENVI-Carb cleanup processes, respectively. The most critical pesticide, using the PSA cleanup step, resulted to be cyfluthrin isomer 1 (26) with significantly lower results, at all three concentration levels, when applying the scaled-down method. Considering the PSA/ENVI-Carb cleanup step, significantly higher ($p < 0.05$) recoveries were obtained using the scaled down method for the following pesticides: cyproconazole isomer II (14), mepronil (15), bromuconazole isomer II (22), boscalid (28), difenoconazole isomer II (32), and dimethomorph isomer I (33) and II (34). Spiromesifen (17) showed significantly higher recoveries using the scaled-down method, except for the lowest level (L1). With regard to the official method, recovery was in the range 70–122% (on average 93%), with %CV values in the range 1–18% (on average 7%), for the PSA cleanup process (zucchini); for the PSA/ENVI-Carb (red pepper) cleanup step, recovery was in the range 71–116% (on average 90%), with %CV values in the 2–13% range (on average 5%). With regard to the reduced scale method, recovery was in the 67–124% range (on average 94%), with %CV values in the range 1–16% (on average 4%), for the PSA cleanup process; for the PSA/ENVI-Carb cleanup step, recovery was in the 70–126% range (on average 97%), with %CV values in the range 2–13% (on average 5%). Only in a single case that the recovery value for the official PSA method exceeded 120%, namely for fenvalerate isomer II (30) at the 50 μg kg^{-1} concentration level; however, an average value of 117% considering the three spiking levels was observed. With regard to the reduced-scale method, using the PSA cleanup process, recoveries were always satisfactory apart from desmedipham (2) (slightly higher than 120%) at the 50 and 100 μg kg^{-1} concentration levels (an average value of 122% was calculated for the three spiking levels), for spiromesifen (17) (slightly lower than 70%) at the 100 μg kg^{-1} level (an average value of 73% was calculated for the three spiking levels), for captafol (18) at all concentration levels (an average value of

122% was calculated), for flurtamone (23) (slightly higher than 120%) at the 50 μg kg^{-1} level (an average value of 121% was calculated for the three spiking levels), for fenvalerate isomer II (30) (slightly higher than 120%) at the 50 μg kg^{-1} level (an average value of 104% was calculated for the three spiking levels), and difenoconazole isomer I (31) (slightly higher than 120%) at the 10 and 100 μg kg^{-1} levels (an average value of 115% was calculated for the three spiking levels). Comparison of the recoveries of targeted compounds in spiked zucchini samples at ≈10 (expressed as L1), ≈50 (expressed as L2), and ≈100 (expressed as L3) μg kg^{-1} levels are reported in Figure 2 (the first columns refer to the official method). Significant differences ($p < 0.05$) obtained running the t test and F test are highlighted in Figure 2 with the symbols * and §, respectively. With regard to the reduced-scale method, using the PSA/ENVI-Carb cleanup step, recoveries were always satisfactory apart from metolachlor (7) (slightly higher than 120%) at the 10 μg kg^{-1} level (an average value of 91% was calculated for the three spiking levels) and chloridazon (16) (slightly higher than 120%) at the 100 μg kg^{-1} level (an average value of 112% was calculated for the three spiking levels). Comparison of the recoveries of targeted compounds in spiked red pepper samples at ≈10, ≈50, and ≈100 μg kg^{-1} levels are reported in Figure 3. Significant differences ($p < 0.05$) obtained running the t test and F test are highlighted in Figure 3 with the symbols * and §, respectively.

In general, all recovery values can be considered as acceptable, namely within the 60–140% range, on the basis of indications of the European Commission (European Parliament 2005). The results obtained using the reduced-scale methods appear to be in general agreement with the official methods; for such a reason, validation of both PSA and PSA/ENVICarb reduced-scale methods was performed.

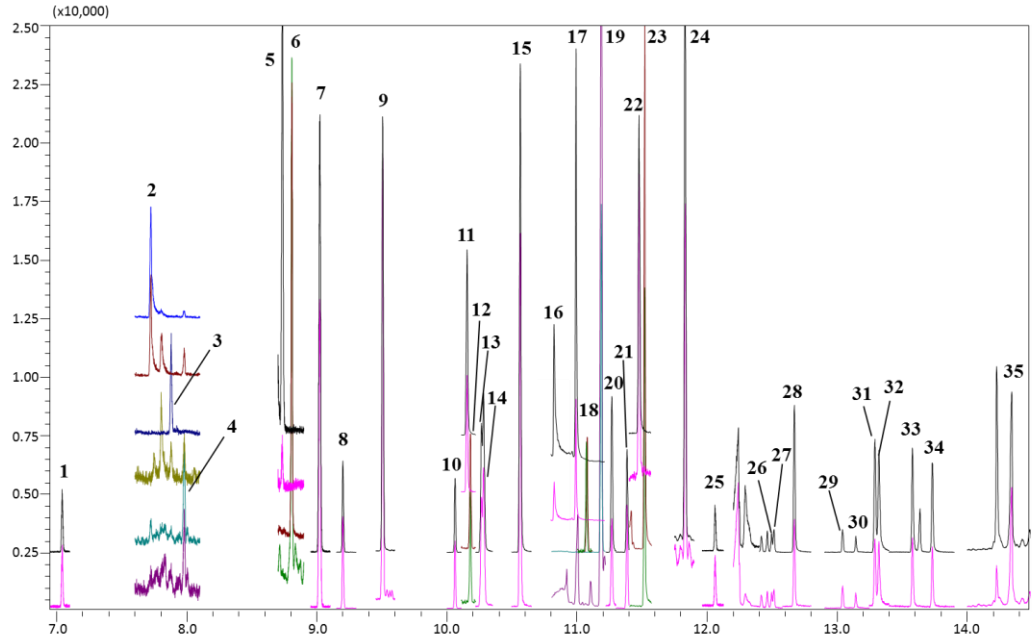

Figure. 1 Fast GC-QqQ MS chromatograms relative to the analysis of a spiked zucchini sample at the ≈10 μg kg^{-1} level. For peak assignment, refer to Table 1.

2.6.3 Method Validation

The parameters considered for method validation were as follows: ME, LoQ and LoD, linearity, recovery, and repeatability. The performances of the proposed method are reported in Table 1 for zucchini and red pepper. The extent of MEs was calculated for each sample, since specific co-extracted compounds may cause either ion suppression or the opposite effect, leading to inaccurate results. Obviously, MEs are dependent on the nature of the matrix and the efficiency of the sample preparation step. MEs calculated for all analytes are reported in Table 1 for two of the four types of samples, with values exceeding 20% highlighted in bold (in total 28). The results indicated that the degree of signal suppression/enhancement varied with the type of matrix and compound. For the zucchini, %ME values ranged from −67% for dimethipin (3) to 66% for desmedipham (2), with an average value, considering absolute values, of 23%; for the red peppers, %ME values ranged from −33% for fenamidone (21) to 39% for desmedipham (2), with an average value of 14%; for lettuce, %ME values ranged from −56% for dimethipin (3)

to 38% for cyfluthrin isomer I (26), with an average value of 16%; and finally, for the tomatoes, %ME values ranged from −33% for chlorfenapyr (12) to 47% for prosulfocarb (6), with an average value of 13%. %ME values of the analytes were variable within the same sample, but, in several cases, in good agreement for the same pesticides among the different samples. For instance, the %ME values for cyproconazole isomer I (12) were 14, 20, 20, and 18%; −7, −6, −5, and −2% for bromuconazole isomer II (22); and 38, 24, 20, and 27%for difenoconazole isomer II (32) in zucchini, red pepper, lettuce, and tomato, respectively. The results confirm the importance of using matrix-matched calibration for the purpose of quantification. LoDs ranged from 0.1 to 2.6 μg kg^{-1} for zucchini, from 0.2 to 4.3 μg kg−1 for red pepper, from 0.1 to 3.3 μg kg^{-1} for lettuce, and from 0.2 to 3.2 μg kg^{-1} for tomatoes; the LoQ values ranged from 0.3 to 8.6 μg kg^{-1} for zucchini, from 0.6 to 14.2 μg kg^{-1} for red pepper, from 0.4 to 11.0 μg kg^{-1} for lettuce, and from 0.6 to 10.8 μg kg^{-1} for tomatoes. The obtained values were always below European legislation residue limits (European Parliament 2005).

Linearity was measured using matrix-matched solutions for each sample and evaluated with the Mandel's fitting test (Fcalc < Ftab) in the 10–5000 μg kg^{-1} range for most compounds. In some cases (15), the upper limit of linearity was ≈1000 μg kg^{-1} (see Table 1). Calibration curves were characterized by regression coefficients (R2) ranging from 0.995 to 0.999 for zucchini, from 0.992 to 0.999 for red peppers, from 0.995 to 0.999 for lettuce, and from 0.991 to 0.999 for tomatoes. Repeatability was calculated at the ≈50 μg kg^{-1} level by analyzing the spiked matrices, eight times consecutively. The %CV values ranged from 1 to 10% for zucchini, from 2 to 11% for red peppers, from 1 to 13% for lettuce, and from 1 to 13% for tomatoes.

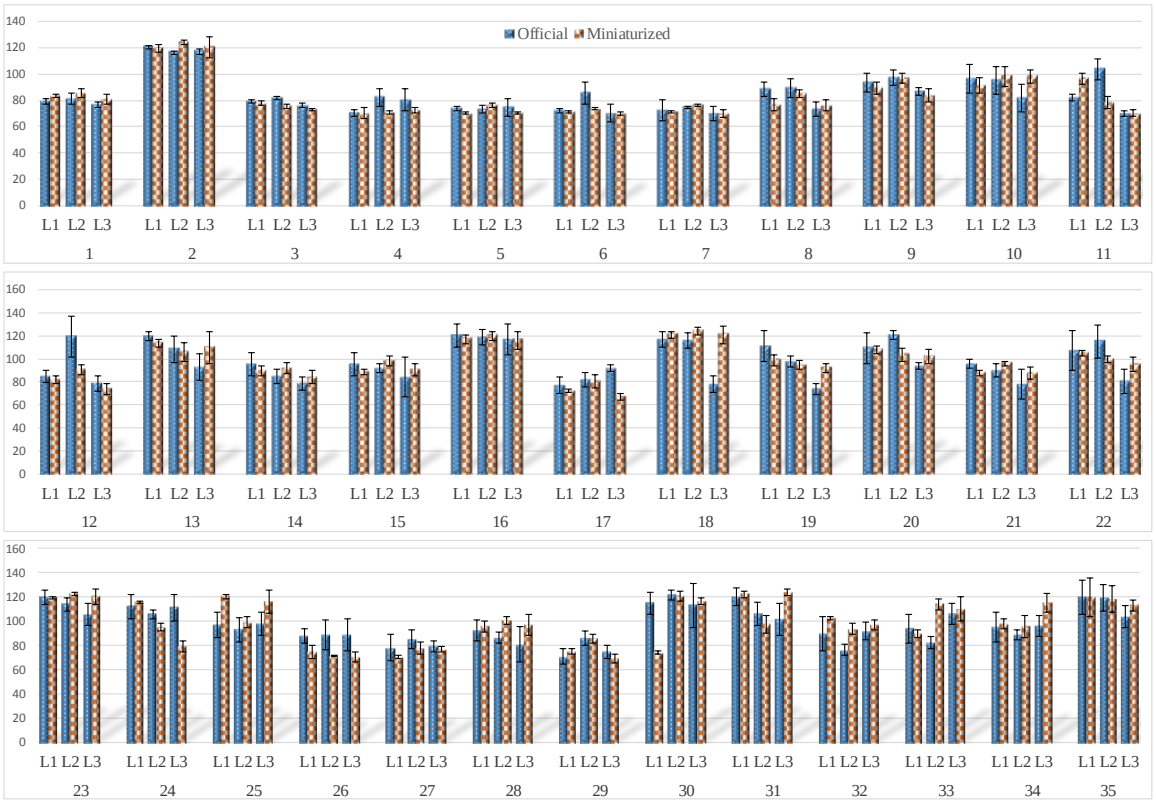

Figure 2. Comparison of the recoveries of the 35 targeted compounds in spiked zucchini samples at the ≈10 (expressed as L1), ≈50 (expressed as L2), and ≈100 (expressed as L3) μg kg^{-1} levels. The first column refers to the official method, while the second column refers to the reduced-scale one. For pesticide assignment, refer to Table 1. The symbols asterisk and section sign highlight significant differences ($p < 0.05$) obtained running the t test and F test, respectively.

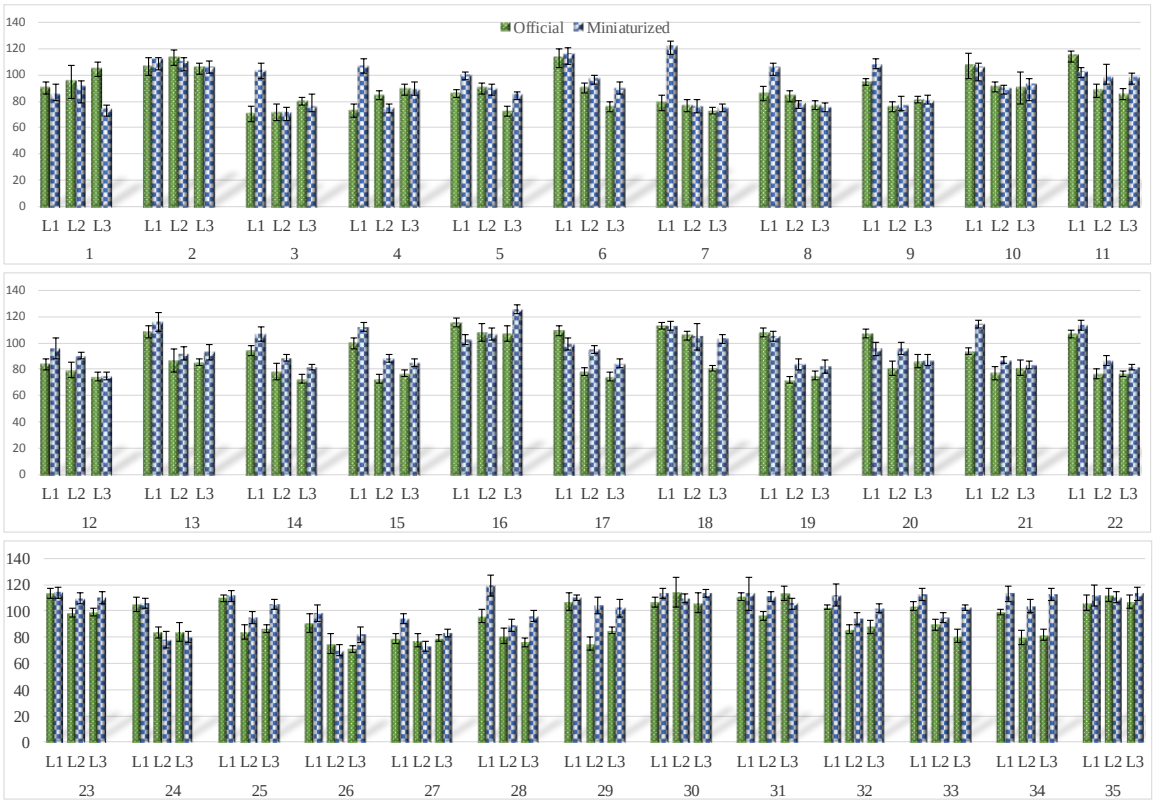

Figure 3. Comparison of the recoveries of the 35 targeted compounds in spiked red pepper samples at the ≈10 (as L1), ≈50 (as L2), and ≈100 (as L3) μg kg^{-1} levels. The symbols asterisk and section sign highlight significant differences ($p < 0.05$) obtained running the t test and F test, respectively.

2.6.4 Real-World Samples

The validated reduced-scale fast GC-QqQ MS method was used for the analysis of 35 phytosanitary compounds in 20 samples, five for each type of vegetable (zucchini, red pepper, lettuce and tomato), purchased from local retailers. Three replicates for each sample were performed. Of the 20 samples tested, none presented a contamination level higher than that allowed by current legislation (European Parliament 2005). In all, eight different pesticides were determined in eight different samples, with none detected in the tomato samples. The most frequently found pesticide was boscalid (also at the highest concentrations), it being determined in six samples in concentrations ranging from 3.5 to 757.7 μg kg^{-1}, with an average value of 109.9 μg kg^{-1}. The highest concentration level was found in a sample of lettuce, even though it was well below the European MRL of

3000 μg kg^{-1} (European Parliament 2005). The sample with the highest number of pesticides detected was a zucchini sample, with a total of 10 different pesticides detected.

2.7 Conclusions

The multi-residue method proposed proved to be suitable for the analysis of 35 pesticides in four different vegetables and, at the same time, being more environmentally-friendly and cheaper than the official QuEChERS method. The use of fast GC enabled a considerable time reduction of the preseparation step. The sample preparation process required approx. 20 min/sample, with six samples treated simultaneously.

Overall, the analysis of the six samples was performed in 2.5 h, without considering data processing.

Having demonstrated the general validity of the approach herein described, future research will be focused on an increase in the number of pesticides included in the method. Although extra-care was applied during the homogenization step to assure representativeness of the entire sample, it is noteworthy that further work is needed to verify that the 3-g samples are representative of the original 1-kg vegetable samples collected (Lehotay and Cook 2015)[28].

References:

1. R. M. González-Rodríguez, R. Rial-Otero, B. Cancho-Grande, C. Gonzalez-Barreiro, J. Simal-Gándara, *CRC Cr Rev Food Sci*, 51 (2011), 99–114.
2. Regulation (EC) No 396 (2005) The European Parliament and of the council of 23 February 2005 on maximum residue levels of pesticides in or on food and feed of plant and animal origin and amending council directive 91/414/EECText with EEA relevance, off. J Eur Union L70:1–16.
3. The Japan Food Chemical Research Foundation (2005) The maximum residue limits of substance used as ingredient of agricultural chemical in foods. (MHW Notification, No. 370, 1959, amendment No. 499 2005).
4. Administrator of the Environmental Protection Agency (2014) Code of Federal Regulations, Protection of Environment. https://www.gpo.gov/fdsys/pkg/CFR-2014-title40-vol24/xml/CFR-2014-title40-vol24-part180.xml
5. De La Guardia M, Armenta S (2011) Green analytical chemistry. Elsevier, Oxford.

6. M. Andraščíková, E. Matisová, S. Hrouzková, *Sep Purif Rev*, 44 (2015),1–18.
7. F. J. Camino-Sánchez, R. Rodríguez-Góme, A. Zafra-Gómez, A. Santos-Fandila, J. L. Vílchez, *Talanta* 130 (2014), 388–399.
8. Y. Wen, L. Chen, J. Li, D. Liu, L. Chen, *Trac-Trend Anal Chem*, 59 (2014), 26–41.
9. L. Ramos, *J Chromatogr A*, 1221 (2012), 84–98.
10. M. Anastassiades, S. J. Lehotay, D. Štajnbaher, F. J. Schenck, *J AOAC Int*, 86 (2003), 412–431.
11. M. C. Bruzzoniti, L. Checchini, R. M. De Carlo, S. Orlandini, L. Rivoira, M. Del Bubba, *Anal Bioanal Chem*, 406 (2014), 4089–4116.
12. G. Martínez-Domínguez, P. Plaza-Bolaños, R. Romero-González, A. Garrido-Frenich, Talanta 118 (2014), 277–291.
13. Y. Sapozhnikova, S. J. Lehotay, *J Agric Food Chem*, 63 (2015a), 5163–5168.
14. European Committee for Standardization (CEN) Standard Method EN 15662 (2008) Food of plant origin. Determination of pesticide residues using GC–MS and/or LC–MS/MS following acetonitrile extraction/partitioning and clean-up by dispersive SPE. QuEChERS method, (www.cen.eu).
15. S.J. Lehotay, *J. AOAC Int*. 90 (2007), 485–520.
16. K. Mastovska, K.J. Dorweiler, S.J. Lehotay, J.S. Wegscheid, K.A. Szpylka, *J. Agr. Food Chem*, 58 (2010), 5959–5972.
17. A. Wilkowska, M. Biziuk, *Food Chem*, 125 (2011), 803–812.
18. A. Berlioz-Barbier, A. Buleté, J. Faburé, J. Garric, C. Cren-Olivé, E. Vulliet, *J. Chromatogr. A*, 1367 (2014), 16–32.
19. Y. Sapozhnikova, S. J. Lehotay, *Anal Chim Acta*, 899 (2015b), 13–22.
20. P. Donato, P.Q. Tranchida, P. Dugo, G. Dugo, L. Mondello, *J. Sep. Sci*. 30 (2007), 508-526.
21. P.Q. Tranchida, M. Zoccali, L. Schipilliti, D. Sciarrone, P. Dugo, L. Mondello, *J. Sep. Sci*, 36 (2013), 2145–2150.
22. P.Q. Tranchida, M. Zoccali, F.A. Franchina, I. Bonaccorsi, P. Dugo, L. Mondello, *J. Sep. Sci*, 36 (2013), 511–516.
23. P.Q. Tranchida, M. Zoccali, F.A. Franchina, I. Bonaccorsi, F. Cacciola, L. Mondello, *J Sep Sci,* 36 (2013), 2746–2752.
24. P.D. DeArmond, M.K. Brittain, G.E. Platoff Jr., D.T. Yeung, *Anal. Methods* 7 (2015), 321–328.

25. SANTE (2015) Guidance document on analytical quality control and validation procedures for pesticide residues analysis in food and feed. SANTE/11945/2015 30 November–1 December 2015 rev. 0.
26. P. van Zoonen, R. Hoogerbrugge, S.M. Gort, H.J. van de Wiel, H.A. van 't Klooster, *Trac-Trend. Anal. Chem*, 18 (1999), 584-893.
27. L.M. Blumberg, M.S. Klee, *Anal. Chem*, 70 (1998), 3828-3839.
28. S. J. Lehotay, J. M. Cook, *J Agric Food Chem*, 63 (2015), 4395–4404.

Chapter III

3 Multidimensional chromatographic techniques

The unraveling of naturally-occurring complex samples has been from time immemorial the driving force behind improvement and innovation in the field of separation science. Significant steps forward were made by replacing packed columns with capillary columns increasing the separation power 10-fold[1], and by coupling gas chromatography (GC) with a time-of-flight (ToF) mass spectrometry (MS)[2]. Such powerful techniques are often insufficient for full understanding of complex samples. More efficient purification/separation would be necessary for easier and more reliable data interpretation. The main way explored to increase the separation power has been the exploitation of different separation mechanisms by multidimensional chromatography, with both heart-cutting and comprehensive chromatography techniques[3]. Such an approach is an interesting alternative, especially when the existing technologies (e.g., different column technologies), pushed to their limit, are still insufficient for complex samples. The coupling of the same form of chromatography (both heart-cutting and comprehensive), such as liquid chromatography (LC-LC, LC×LC) and GC (GC-GC, GC×GC), or of two different forms of chromatography (e.g., LC-GC, LC×GC) has been investigated over the years, both offline and on-line.

3.1 Introduction to Multidimensional Gas Chromatography (MDGC)

In 1984 Giddings[4] published a fundamental and theoretical paper with the title "Two-Dimensional Separations: Concept and Promise" in which he outlines the large number of two-dimensional (2D) separations which can be realized by combining one-dimensional (1D) displacement processes. He distinguishes between sequential and simultaneous zone "displacement" and states: "Sequential displacements, as those occurring in column chromatography or in two-dimensional thin-layer chromatography, are far more adaptable because optimum conditions can be applied separately to each step. One can carry out the first displacement in one medium under one set of conditions and transfer the linear array of zones to the edge of a 2D system for the second displacement". Concerning the research work on 2D methods Giddings writes: "any 2D

technology must stand on the shoulders of 1D building blocks. Whereas the thrust of 1D research is to improve the building blocks, the thrust of 2D research will be to find powerful and ingenious ways of combining building blocks", in the terminology of Giddings 2D methods such as GC-GC make use of two selective 1D displacements. These are "selective", only, if columns with different stationary phases are combined. Modern gas chromatography using the capillary columns is a highly developed building block for 2D methods because of the extraordinary high efficiencies which lead to even higher peak capacities at the separation of multi-component mixtures with two selective chromatographic building blocks.

According to the classical terminology in column chromatography separations are commonly called two or multidimensional when separations of all or certain selected groups of sample components are repeated in two or more columns of different polarity, which are coupled in series to the column in which the first separation was performed. The continuous transfer of the eluate or the transfer of selected cuts from the first to further columns is achieved by the carrier gas flow which can also be diverted to exit ("venting") or reversed for backflush by flow switching between the columns.

By the transfer of selected cuts from one column to another column of different polarity and the related selectivity of the separation the resolution of those peak groups which are contained in such cuts is improved. This methodology has very early been recognized as effective also for GC analyses in routine laboratories by Deans[5]. The selection of cuts which are to be re-separated at different selectivity and additionally also with high efficiency has to be done according to the objective of the intended analytical application. In this way mainly partial analyses of much higher performance for the separation and determination of a single or several components in a certain peak group, can be executed which may be adequate and sufficient for the solution of the analytical problem. In the analytical practice the increase of peak capacity of separations of an entire multi-component mixture is not as important. The removal of non interesting sample matrix components from the separation in the first (or pre-) column can be

accelerated by higher carrier gas flows and at elevated temperatures or with temperature programs.

Such a fast clean-up and reconditioning procedure of the first column can proceed in parallel to the separation of the significant sample components in the second column. The entire Multidimensional Gas Chromatographic system (MDGC) becomes soon be ready for the next analysis in a series of routine measurements. The transfer of either the entire eluate or of narrow or wider cuts, taken from the eluate leaving the first separation, to another separation in the coupled next column is effected by the carrier gas (mobile phase) flow. If the second column is to be operated at lower carrier gas flow only a part of the eluate can be led into the second column. The other part has to be vented between the columns. According to a stringent theoretical definition, separations with transfer of eluate cuts from a first into a coupled second column should only be called multidimensional, if additional new and significant sets of qualitative (e.g. relative retention) as well as the related better quantitative data are achieved. Basically this can only be the case if either the polarity of the stationary phase or the temperatures for the separation systems in the coupled columns are different. Temperature programs in the columns are, of course, also suited to effect the necessary change of selectivities between the first and the second separation system. One of the major aims of optimization of chromatographic separations is the improvement of resolution of certain components groups in a sample and the related better performance of the intended analytical application. Optimization of the resolution of a group of sample components selected from the eluate of a first or preseparation can also be achieved if the separation in the second column is performed at higher efficiency or sample capacity i.e. also at higher phase ratio.

In trace analysis the resolution of two components which are present in an extreme ratio of concentrations and which appear as closely neighbored and overlapped peaks in the chromatogram can be improved by the transfer of so-called heart cuts[5].They are to be taken in a way that the ratio of component concentrations is considerably decreased. In systems of coupled columns with different stationary phases and lengths (efficiencies)

the two columns may, moreover, be operated at different flows of the mobile phase, then separations with mixed selectivities are achieved which depend on the ratio of the residence times of analyte pairs or groups in each column of different polarity[6,7]. Such mixed selectivities are avoided if the sample components which are transferred from the first column are trapped in a cold trap between the columns or in the inlet of second column before the second separation is initiated by heating the same[8,9]. In a trap before or in the second column the separated species of certain "cuts" are also cryofocussed; in such a way the selectivity of the second separation is not any more influenced by the selectivity of the first separation. Moreover, cryofocusing allows to make a second separation with an efficiency which is not influenced by the band broadening and symmetry distortion which unavoidably occurs in the first separation and in inadequately constructed coupling pieces. Considering GC-based multidimensional techniques, the first coupling was presented by Simmons and Snyder in 1958[10]. Two 50-m capillary columns were connected using a pneumatically-operated diaphragm six-port valve for the analysis of a dilute hydrocarbon gas mixture.

Up today the transfer systems developed can be classified in three groups: (I) in-line valve, (II) out-line valve and (III) valveless systems. In the first group, a valve interfaces the two columns in a direct manner; out-line valves are employed to regulate the direction of gas flow towards the column interface, while valveless systems form a third minor MDGC group. When an MDGC instrument (in- or outline valve) is in the stand-by mode, a one-dimensional analysis can be carried out; when the configuration is switched to the cutting mode, the primary-column effluent is directed towards the second column. The greater the number of transfers achieved, the higher the possibility of a mix-up of previously separated compounds. Although such an occurrence goes against a “golden” rule of multidimensional chromatography, namely that “all compounds resolved in the first dimension, must remain so in the second”, the event is acceptable if all target analytes remain separated.

3.1.1 Objectives of multidimensional GC separations

In this section are summarized the main objectives of multidimensional gas chromatography:

(1) Increased peak capacity especially for the analysis of samples which consist of an high number of components. As a reminder, high peak capacities can also be achieved in a single column system by temperature programmed column operation.

(2) High resolution for isomers and enantiomers with special (e.g. enantio-) selectivity of the second column. Highly selective columns can successfully be applied only to narrow eluate cuts which contain a limited number of components.

(3) Short analysis times by partial analyses of cuts, which were taken from the eluate of a pre-separation of very complex mixtures. They are performed in the second separation system under optimized conditions with the objectives of high resolution and also signal-to-noise ratios at detection. In preparative scale MDGC separations, columns with high content of stationary phase and the corresponding higher sample capacity are to be applied; short separation (cycle) times for selected peak groups can only be achieved, when high retention components are prevented to reach the main (second) separation which must be longer and correspondingly more efficient than the first column. Matrix components of low chromatographic volatility and the corresponding high retentions can be removed by fore- or backflushing from the short precolumn and not so favorable at elevated temperatures.

(4) Improved determination of trace components eluted closely to the peaks of solvents or major components in "heart cut" mode, by using a Deans system[5].

(5) Avoidance of high column temperatures for the elution and venting of low volatility components, which are not of interest for the analysis, using short precolumns and/or backflush operations.

3.1.2 MDGC systems and instrumentation

Before the descriptions of the commercial systems and applications, attention will be devoted to the concept of in-series twin-capillary GC, the coupled-column approach proposed by Deans and Scott[11], and recent versions of that technology. Let us consider an extremely simple sample, composed of two constituents, defined as α and β. If such a sample is analyzed on two conventional capillaries (e.g., 30 m ×0.25 mm I.D.) linked in series, with different selectivities, and under ideal conditions of temperature (with a single oven) and flow, then the possible analytical outcomes are four: (I) α and β overlap to some degree on both capillaries; (II) α and β remain entirely resolved on both columns; (III) α and β are separated on the first column but overlap to some degree on the second; (IV) α and β co-elute to some degree on the first column, and are separated on the second. In cases I and II, the employment of the second stationary phase is useless, while it is entirely negative in the third situation. On the contrary, a clear advantage is attained in the fourth situation. If the aforementioned example is extended to a medium-complexity sample (e.g., 100 compounds), then the number of possible combinations becomes exceedingly high. However, the final number of compounds that one could expect to resolve would most probably be not that much higher than that attained using a 60 m ×0.25 mm I.D. column, with a single stationary phase. One way to improve the chromatography of a coupled-column system would be to operate each stationary phase using independent temperature programs[12]. A further way of improving the separation performance of a twin-capillary system can be achieved by manipulation of the gas flows in each column, by using an additional pressure source connected to the columns connection point[11]. A series of interesting papers, based on such an approach, have been described by Sacks and co-workers[13-15]. A scheme representing a "series-coupled column ensemble with stop-flow operation" is shown in Figure 1. The system illustrated is one belonging to the out-line valve MDGC systems. The valve is connected on one side to the columns junction point, and on the other to an aluminum ballast chamber (BC). The pressure in BC is controlled by an electronic pressure controller (PC). An FID is also located between the two chromatography dimensions. If a pressure

pulse, equal to that of the injector (I), is applied to the columns connection point, then a condition of stop-flow will arise in the first column, while elution continues in the second dimension.

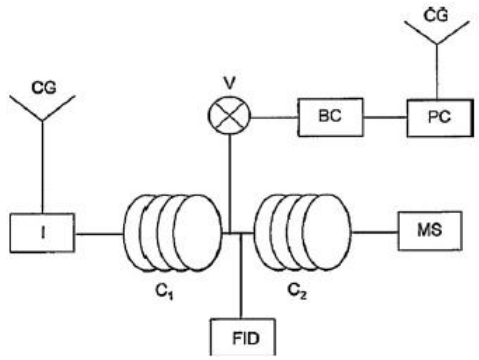

Figure 1 Scheme of a coupled column system, with stop-flow operation. Abbreviations: C1 = first dimension; C2 = second dimension; V = pneumatic valve; BC = ballast chamber; PC = pressure controller; I = injector; CG = carrier gas source.

The stop-flow MDGC instrument was employed in combination with a third separative dimension, *viz*., a time-of-flight (ToF) mass spectrometer, in the high-speed analysis of essential oil compounds[15]. Such MS systems possess the unique capacity to unravel coeluting GC peaks through spectral deconvolution. Figure 2 illustrates three chromatograms relative to the analysis of 9 compounds, using the tandem-column ToF MS system.

About 10% of the first-dimension (7 m × 0.18 mm I.D. × 0.2 µm d_f trifluoropropylmethyl polysiloxane) effluent was directed to an FID (Figure 2a); the single-column GC-FID chromatogram shows that peaks 3–4 overlap completely, while compounds 5–6 coelute partially. Observing the middle total-ion-current (TIC) chromatogram, that is an application carried out with no mid-pressure regulation, it can be easily concluded that the chromatography situation has become worse: peaks 1–2, separated on the polar column, co-elute completely on the apolar second column (7 m × 0.18 mm I.D. × 0.2 µm d_f, 5% phenyl); though peaks 3 and 5 are now entirely separated from components 4 and 6, respectively, peaks 4 and 6 now overlap completely;

compounds 7-8-9, previously resolved, are now mixed together after their passage on the second capillary.

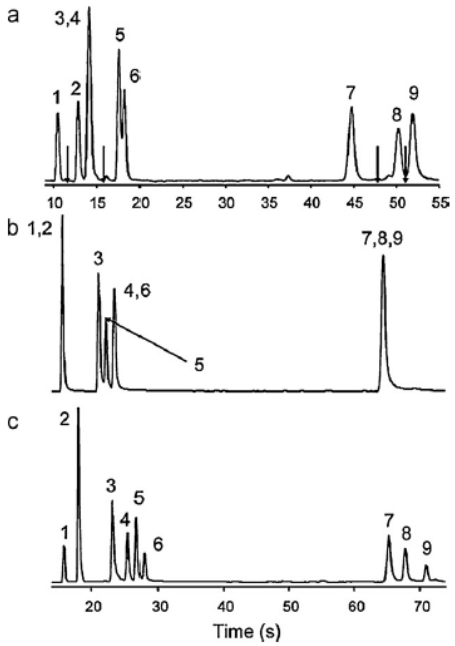

Figure 2. Chromatograms relative to the FID primary-column analysis (a), to the total ion- current MS result with no stop-flow operation (b), and to the total-ion-current MS analysis with stop-flow operation (c). Peak identification for the essential oil compounds: (1) camphene; (2) furfural; (3) eucalyptol; (4) terpinolene; (5) benzaldehyde; (6) octanal; (7) β-caryophyllene; (8) geranyl acetate; (9) eugenol.

A 4-point stop-flow experiment, carried at times indicated by the arrows in Figure 2a, enabled the chromatographic separation of all nine volatiles. The first stop-flow operation was made just after the first-dimension elution of peak 1: compound 2 was halted for 5 s in the final primary-column segment. Elution in the first dimension was interrupted a further 3 times: once to separate compounds 4 and 6, and the remaining two times to separate compounds 7-8-9. Mass spectral deconvolution was necessary for the chromatogram illustrated in Figure 2b, but was clearly not needed in the stop-flow analysis (Figure 2c). The stop-flow approach is both simple and attractive, and could be employed as an alternative MDGC method, though currently it is hard to encounter going through the literature.

An MDGC instrument, characterized by a microfluidic transfer device (Agilent Technologies), has been recently described[16]. The interface is a thermally stable, leak free, chemically inert, low dead volume, Deans switch, manufactured through capillary flow technology (CFT): through holes and flow channels are etched into stainless steel plate halves, which are folded, heated to a very high temperature (>1000 °C); then, high pressure is used to produce a diffusion-bonded metal sandwich. The internal channels, created in a similar mode to the production of integrated circuits, are deactivated with a coating layer. Leak-free connections are made by using metal ferrules. Optimum conditions for stand-by, cutting and backflushing processes are created by using electronic pressure control. The interface contains five ports: two are connected to the primary and secondary columns, while another is linked to a restrictor, with the same flow resistance as the second dimension. The latter requisite is important, because the pressure drop across the primary column must remain constant during the two operational modes. If pressure-drop differences do occur, then there will be a mismatch between the programmed chromatography-band transfers, which are set on the basis of a preliminary stand-by separation, with those which occur during an MDGC analysis. The restrictor is usually connected to a detector, to monitor the first-dimension separation. The remaining two entrances are fixed, being linked to a two-way solenoid valve. Figure 3 shows how the device achieves the bypass (stand-by) and inject (cut) states. The primary flow, which is always lower than the auxiliary flow, enters the interface through the central port.

During the standby mode, the solenoid valve directs the auxiliary flow to the top left part of the Deans switch, which is connected, *via* an internal channel, to the port linked to the secondary capillary. Once inside the interface, the additional gas flow is divided in two parts, one directed to the second column and the other crosses the internal vertical channel ending up in the restrictor. Prior entry to the restrictor, the auxiliary flow is mixed with the first-dimension flow.

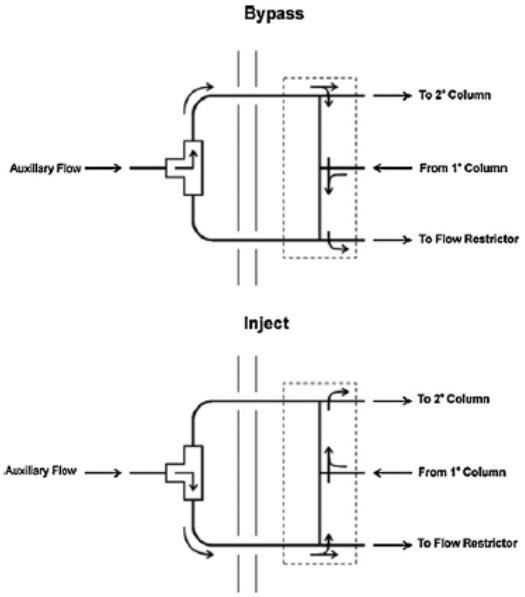

Figure 3. Scheme of the "Agilent" Deans switch in bypass (stand-by) and inject (cut) modes.

When the solenoid valve is switched to the cutting state, the auxiliary flow is directed to the bottom left part of the transfer device, which is connected, *via* an internal channel, to the port linked to the flow restrictor. Once inside the interface, the auxiliary gas flow is split between the restrictor and the second column. As in the standby mode, the additional flow is mixed with the primary-column flow.

Another commercial system is the integrated "selectable 1D/2D GC–MS" system, currently commercialized by Gerstel and characterized by an Agilent capillary flow technology interface and low thermal mass GC modules[17]. The unified system is equipped with dedicated software to deal both with GC–MS and MDGC–MS applications. The main novelty is that the same mass spectrometer is employed in both application types, namely for stand-by and cutting analysis, meaning that peaks subjected to one- and two-dimensional analysis appear in the same GC–MS chromatogram. Apart from the MS system, other detectors can be used for one- and two-dimensional GC applications. Figure 4 shows schemes of the unified instrument: an Agilent GC was equipped with a thermal desorption inlet, two independent LTM units, a CFT Deans switch and a CFT cross-union, to connect the restrictor (0.54 m × 0.10 mm I.D.), the

second (5% phenyl) column (10 m × 0.18 mm I.D. × 0.40 µm d_f), the MS transfer line, and the transfer line to other detectors.

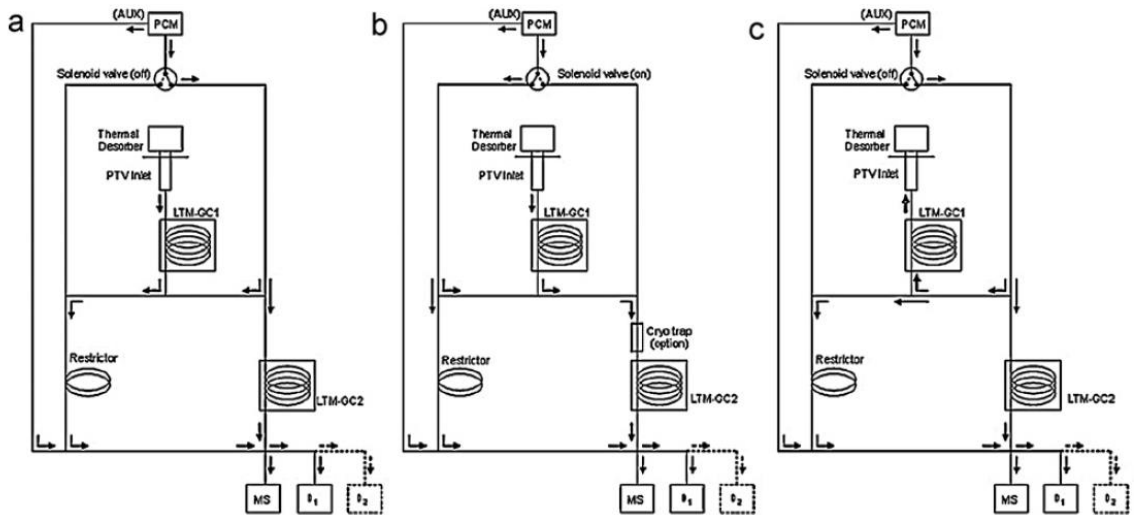

Figure 4. Schemes of the Gerstel "selectable 1D/2D GC–MS" system. The one-dimensional GC–MS configuration is reported in (a); the transfer configuration is illustrated in (b); the two-dimensional GC–MS/backflush configuration is shown in (c). Abbreviations are defined in the text.

The Agilent Deans switch connections have been described previously. Apart from the PCM (pressure control module) connection (168.4 kPa) to the transfer device, a further line of the auxiliary pressure source (21.0 kPa) supplied make-up gas to the cross-union. A stand-by GC–MS application is carried out by diverting the "wax" primary column (10 m × 0.18 mm I.D. × 0.30 µm d_f) flow towards the restrictor (Figure 4a), while a second-dimension GC–MS analysis is performed by activation of the solenoid valve (Figure 4b); if required, the transferred chromatography band can be re-concentrated at the head of the secondary column by using a cryotrap. At the end of the transfer period, the remaining part of the sample can be backflushed by reducing the head pressure to 10 kPa (initially 212.7 kPa), and the second-dimension LTM heating can begin (Figure 4c). Though the "selectable D^1/D^2 GC–MS" system is certainly interesting it also appears to be characterized by a drawback, mainly the difficulty to perform multiple heart-cuts. The latter operation could be achieved by accumulating more than one heart-cut in the cryo-trap (or even at the ambient GC temperature if not excessively volatile) or by performing

a single application for each heart-cut. The successful outcome of the first option would depend on the capability of the second column to separate all the entrapped compounds, while high time costs could characterize the second route. Gerstel also commercializes a more classical heart-cutting MDGC system (MCS: "multidimensional column switching" system), with a Deans switch, and a primary (monitor) and secondary (main) column detector.

A further effective Deans-switch MDGC system has been developed and introduced by Shimadzu Corporation. The MDGC instrument is commercialized in the double-oven configuration, and is equipped with a quadrupole mass spectrometer. The first and second dimension capillaries are linked by using a low dead-volume, thermally stable and chemically inert stainless steel interface. The latter is housed in the first oven, is characterized by very small dimensions (ca. 3 cm long), is connected to an auxiliary pressure source (2 ports) and to a stand-by detector. Furthermore, a fused-silica restrictor (R_1) is fixed inside, and crosses the interface. Figure 5 reports two schemes of the entire "Shimadzu" transfer system in the "stand-by" (Figure 5a) and "cut" positions (Figure 5b).

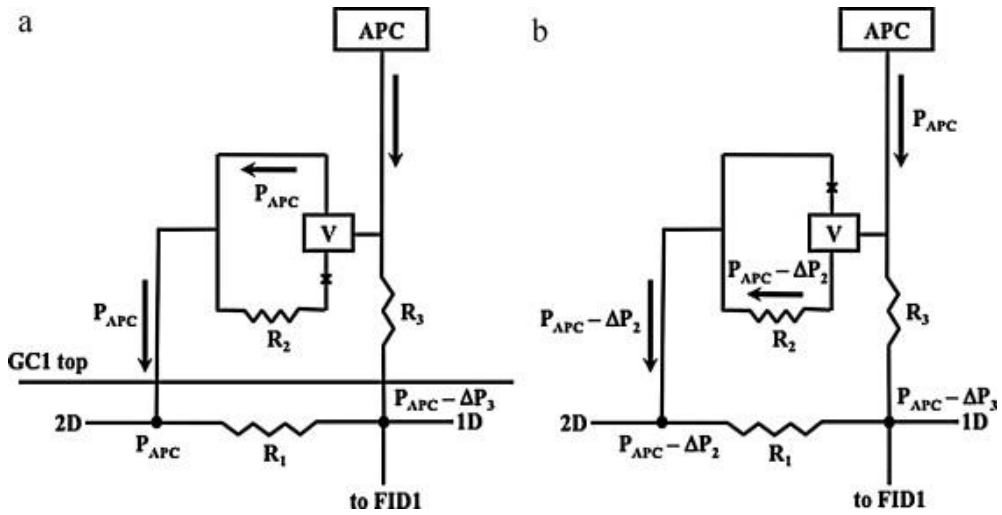

Figure 5. Scheme of the "Shimadzu" Deans switch in stand-by (a) and cut (b) configurations. The abbreviated definitions are reported in the text.

Though the five-port metallic interface is located in the first GC, defined as GC1 (Figure 5a), it is obvious that a web of external connections is necessary to create the required MDGC conditions. In both operational modes, an advanced pressure control unit (APC) supplies a gas flow at constant pressure to an external (with respect to the GC oven) fused-silica restrictor (R_3) and to a two-way solenoid valve (V). The latter is connected to two metal branches, one with another fused-silica restrictor (R_2) and one without: R_2 produces a pressure drop, slightly higher than that generated by R_3 ($\Delta P_2 > \Delta P_3$). In the stand-by mode (Figure 5a), the APC pressure is reduced on the side of the first dimension (e.g., 100 kPa – ΔP_3), while it reaches the second dimension branch, passing through the solenoid valve, unaltered. It is clear that through such a configuration, analytes eluting from the first (apolar) column are directed to FID1. Once the solenoid valve is activated, the transfer device passes to the cutting mode (Figure 5b): the pressure on the first-dimension side of the interface remains unaltered, while the pressure on the second-dimension side becomes 100 kPa – ΔP_2 (a pressure lower than 100 kPa – ΔP_3). It is clear that, under such conditions, the primary-column eluate is free to reach the second (polar) capillary. The instrument is automatically controlled by using a dedicated software that also enables the calculation of fundamental GC parameters, such as gas flows, linear velocities, and analyte recovery.

With respect to the "Agilent" system, the main differences are that: the capillary linked to the stand-by detector does not need to be characterized by the same flow resistance as that of the secondary column (meaning that if one wants to change the second column, then one does not need to replace the restrictor also); the external design of the (3-restrictor) transfer system is a little more elaborate. However, both the commercial instruments work in an effective manner.

Among a series of MDGC experiments, a 14-cut application on perfume allergens will be herein described[18]. In recent years, the relation between a series of perfumery ingredients and contact allergy has been the subject of wide scientific discussion[19]. On the basis of European legislation (7th Amendment of the Cosmetic Directive), the 26 most frequently-recognized skin allergens must be reported on the final cosmetic product if

specific concentrations are reached: 10 and 100 mg L^{-1} in leave-on and rinse-off products, respectively. Twenty-four compounds, out of the twenty-six, are amenable to GC analysis. Prior to an MDGC experiment it is of common use to inject a standard solution of target analytes to define the heart-cut windows.

In the case of solutions containing perfume allergens, it is well known that they are characterized by a short life-time due to instability. To circumvent such a problem a valid alternative was found: an alkane mixture was subjected to stand-by MDGC–MS analysis, prior to the injection of the allergen standard solution. Experimental linear retention indices (LRI) were derived for each compound on the primary (5% diphenyl) column; LRI cut windows were established by adding and subtracting 10 LRI units, with respect to the experimental value. Once an LRI cut window was established, the definition of a time window for each target analyte is straightforward. A total of fourteen cuts were extrapolated for 24 compounds, because the retention time difference between several allergens was only small. Through such an approach, the injection of an allergen solution prior to each MDGC application would not be necessary: it would be only necessary to derive the LRI values through preliminary hydrocarbon analysis. It is obvious that such an approach can be extended to any sample-type. A chromatogram relative to the first-dimension perfume analysis, after heart-cutting (the position of each cut is shown), is illustrated in Figure 6. No retention-time shifts occurred during heart-cutting. The second dimension TIC MDGC-MS result is illustrated in Figure 7. As it can be seen, 12 allergens were nicely separated from other matrix interferences. The general mass spectral purity was very good, with MS database similarities always over 90%. Each allergen was subjected to quantification; the data attained were in good agreement with the allergens reported on the perfume container.

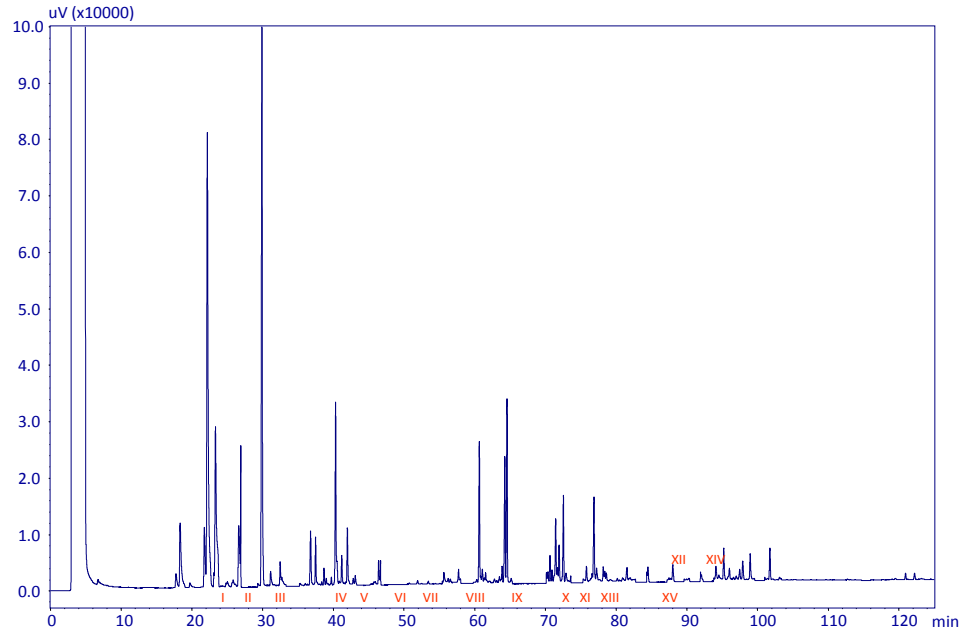

Figure 6. Chromatogram relative to a first-dimension perfume analysis, after heart-cutting and with the position of each cut indicated by a Roman number.

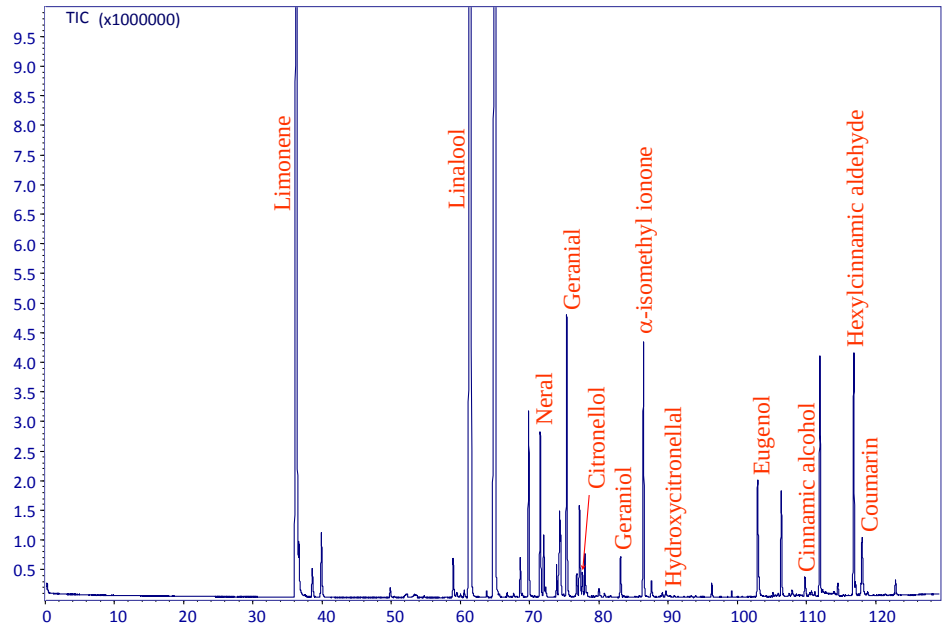

Figure 7. TIC chromatogram relative to a second-dimension perfume analysis.

3.2 On-line coupled liquid chromatography-gas chromatography

Multidimensional chromatographic techniques, such as on-line coupled liquid chromatography–gas chromatography (LC–GC), are excellent tools for the analysis of complex mixtures. The high sample capacity and wide range of separation mechanisms of LC can be used in selective clean-up, fractionation and preconcentration of the sample. For the final separation, GC offers high separation efficiency and a variety of selective detection methods. The main benefits from combining the two techniques are relative to the analysis time that is faster, less solvent is needed and the cost of analysis decreases.

The analysis and sample preparation take place in a closed and usually automated system, where the risks of sample loss and contamination are minimized and, thus, the reliability and repeatability of the analysis are improved. In addition, the negative effects of atmospheric oxygen and moisture are eliminated. One of the main benefits of LC–GC is that, because of the efficient clean up provided by LC, the whole sample fraction containing the analytes can be transferred to the GC. Since none of the sample material is wasted and the disturbing compounds are eliminated, sensitivity is high.

In contrast to conventional GC, the LC fractions transferred to the GC are typically as large as several hundred microliters. This cannot be done without special interfaces. In addition, the LC eluent must be suitable for both LC and GC analysis. At present, most liquid chromatographic analyses are made in reversed-phase mode (RP). Most LC–GC methods, however, are normal-phase (NP) LC–GC. In part, this is because the organic eluents used in NPLC are typically compatible with GC, making the coupling simpler. Another reason is that many of the samples analyzed by GC require extraction into organic solvent before analysis, and normal-phase separation is the obvious choice. If the whole range of analytical possibilities is to be exploited RPLC–GC must be used as well. The on-line LC–GC systems are understandably more complicated than single chromatographic methods. It would be unreasonable, therefore, to use LC–GC for simple analytical problems that are easily solved with traditional methods. Rather, LC–GC is appropriate for samples that are difficult or even impossible to analyze by a single conventional technique. Off-line LC–GC techniques provide a good alternative to

conventional techniques, when the sample amount is sufficient and the sensitivity required is not very high. They offer most of the benefits of on-line techniques and the instrumentation is more flexible. The sensitivity is, however, usually lower than in on-line methods because only a part of the sample is injected to the GC. Certainly, the sensitivity can be increased substantially through the use of off-line large volume injection. The on-line technique is always the best choice, however, when large series of samples have to be analysed, the amount of sample is limited as, for example, in human exposure studies, or very high sensitivity is required. Figure 8 gives guidelines for choosing a LC–GC method.

The main factors to consider in the selection are the complexity of the sample, i.e., the amount of matrix components, the characteristics of the analytes and the selectivity and sensitivity required. The analytes of interest should also be suitable for the final GC analysis, i.e., they should be sufficiently volatile and non-polar or derivatisation should be possible either before the analysis or on-line. In addition, the number of samples to be analysed is relevant. If the number is small, there is usually no need for an automated method and the time-consuming development of such a method, and conventional methods will suffice. The more complex the sample matrix is, the more efficient the sample clean-up must be and then LC–GC is suited for the task. LC–GC may also be preferable for relatively clean samples if very high sensitivity or selectivity is required for the analysis, for example, if the analytes of interest are present at trace level or group-type separation of the analytes is needed before the final analysis[20].

3.2.1 Apparatus and conditions for on-line coupled LC-GC

A typical LC–GC instrument, consists of a basic LC system, an interface valve and LC–GC interface, and a GC system with solvent vapour exit (SVE). One or two pumps are used in LC and often the separation is monitored with a UV detector.

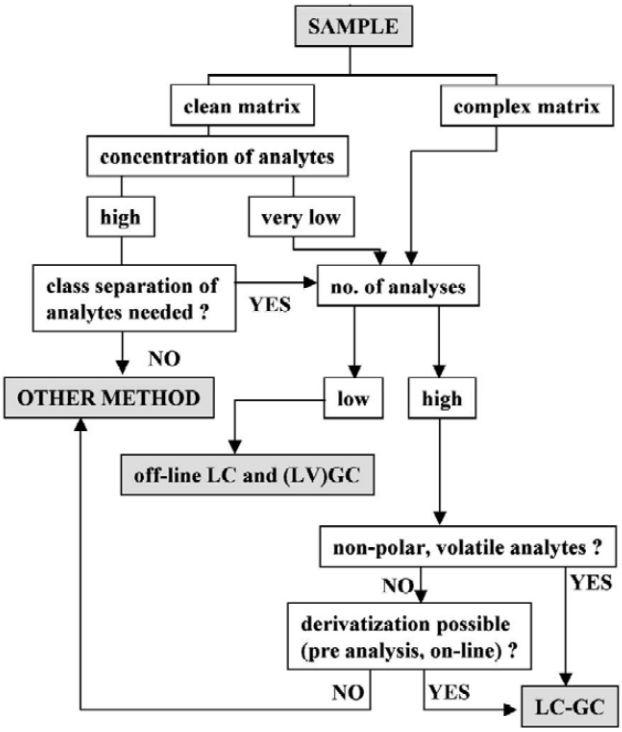

Figure 8. Guidelines for choosing an LC-GC method.

A detailed description of the instrumentation can be found in the paper published by K. Grob in 1991[21]. A number of interfaces have been developed for the LC–GC coupling, but early versions[22-25] have mostly been abandoned and only on-column[26-32], loop-type[33-39] and vaporizer interfaces[40-43] are commonly employed today. The GC part is typically a normal GC equipped with a suitable interface and a solvent vapour exit. When a vaporizer interface is used, the SVE is not always necessary. In the development of an LC–GC method, the LC method is chosen first, keeping in mind the conditions required for transfer and GC analysis. The selection of interface and evaporation techniques is largely dependent on the volatility of the analytes. In GC, the dimensions of the retention gap and conditions during the transfer must be optimized for the selected interface and evaporation techniques. The other GC conditions (i.e., column type, temperature program and detection) can then be selected quite independently.

3.2.2 LC dimension

The LC step can be a simple separation of the target compounds from the bulk of the matrix, or a selective clean-up exploiting the separation efficiency and the selectivity of the LC column for a concentration or fractionation of the sample. The main LC-separation mechanisms have been intensively explored over the years[44, 45].

Normal-phase (NP) chromatography has been employed most, since the eluents used are suitable for GC. Few applications using size-exclusion chromatography (SEC) have been published, but this technique involves high solvent volumes, which are not easily managed by the transfer device. Reversed-phase (RP) chromatography has been used less, since it requires particular effort to eliminate solvents; however there are a number of applications in this field. Generally, the column dimensions are selected taking into account that the optimum column flow has to fit the evaporation rate necessary for transfer optimization into the GC, especially when the retention-gap technique is used for LC-GC transfer. Consequently, the 2-mm I.D. column seems to be the best compromise for obtaining the optimum column flow (optimum LC flow about 0.3–0.5 mL/min) and saving the sensitivity necessary for some applications (e.g., Mineral Oil contamination). Larger column diameters can be employed but using a different approach: the optimum flow (1–2 mL/min) is applied until the elution of the fraction of interest starts, then the flow is decreased until the end of the transfer (generally to 0.1 mL/min).

Backflush is a very important step, especially when NPLC is applied. The bulk of the sample (generally polar by-product) has to be removed from the column efficiently to avoid shifting of the retention time or, what is worse, any trace of the matrix reaching the GC column. MTBE and iso-propanol are very efficient solvents for cleaning silica columns (i.e. triglycerides, TAGs), but reconditioning with hexane is not easy and is usually time consuming, since it is too weak to remove solvents of such a higher strength (ε^0) efficiently, so dichloromethane is usually preferred.

3.3 Interfaces in LC-GC

The heart of an LC-GC system is the transfer technique, extensively described in dedicated books[3, 20] and by several reviews as previously reported in *section 3.2.1*. The choice of a suitable interface depends on the volatility of the target analytes and the size of the fractions to be transferred. A brief overview of the most employed interfaces is given herein.

3.3.1 Retention-gap technique

The retention-gap interface is based on the on-column (OC) large volume injection (LVI) technique. The LC eluent is directed through a switching valve to the waste, or, during transfer, to a rather long retention gap (5–10 m) of large diameter (usually 0.53 mm I.D.) connected through a T-union to the analytical GC column and a solvent-vapor exit (SVE). Two transfer mechanisms can be employed using such an interface, namely partially or fully concurrent eluent evaporation. The main difference is the transfer temperature (below or at the solvent boiling point, respectively), which leads to optimum volatile refocusing or a faster transfer but causing loss of volatiles, respectively. In 2009, the OC interface evolved into the Y interface[46] to reduce the memory effect deriving from the previous transfer from 0.5–3% to 0.02%. Such an interface is employed by the commercial instrument supplied by Brechbühler (Switzerland). The principles of the retention-gap technique are also exploited in the instrument commercialized by Sra Instruments (Italy), but using a flow-cell autoinjector system to transfer the fraction of interest into the OC injector.

3.3.2 Programmed-temperature vaporizer (PTV) interface

In 1979 an autoinjector interface was introduced at the Pittsburgh Conference[47, 48]. The injector was modified with a flow-through a side arm syringe. The volume of the fraction was limited (0.1–3 µL) since it was injected in a split/splitless flash–vaporization

injector. The problem was faced by replacing the conventional LC column with a 1 mm microbore column, positioning a splitter between the LC and the autoinjector interface, and operating in the split mode in the GC injector. Several years later the LC fraction was significantly enlarged by using a PTV injector as interface. That approach was developed by Sandra and co-workers[42]. The LC effluent is sampled from a flow-cell by a large-volume autosampler syringe and automatically injected into a PTV injector, equipped with a liner packed with different adsorbent materials. The solvent transfer can be performed in several modes, namely PTV solvent split, PTV large volume splitless, PTV vapour overflow with or without splitting. de Koning and co-workers[49] reported some problems using the PTV interface, in particular recondensation in the split line or/and in the split valve, which causes an increase in the flow resistance in the split line, and of the pressure in the injector. Consequently, both back-flow of solvent into the carrier gas flow as well as change in the split ratio, make quantification impossible. To solve these problems the split valve is positioned as close as possible to the injector and heated. The PTV-interface is a valuable alternative to the on-column interface and presents several advantages: the packed liner retains more liquid per unit internal volume and wettability of the packing material is not required. Also the packing material is more stable than the retention gap, especially with water and non-evaporating by-products, and it prevents high boiling compounds from reaching the GC column. Considering the diffusion of the PTV injector and the flexibility of such interface in implementing different approaches, ranging from a normal split/splitless injection GC analysis to LVI and online LC–GC, it can be hypothesized that such an interface will push for the introduction of LC–GC technique in many laboratories as a routine technique. The LC–GC system exploiting the PTV syringe-type interface is commercialized by Shimadzu (Japan).

3.3.3 Dual Side-Port Syringe Interface

Another system, commonly used in combination with a PTV injector, is the dual side-port syringe interface. The latter, controlled by an autosampler, is characterized by two entrances: the lower port is used to transfer the fraction from the LC to the GC inlet via the syringe needle, while the upper port is used to direct the effluent to a waste line. The syringe is characterized by a plunger with a smaller outer diameter, with respect to the internal diameter of the barrel, and by the presence of a plug situated at the bottom of the plunger (Figure 9).

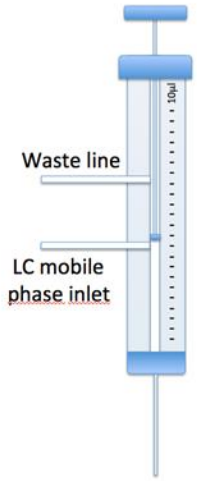

Figure 9. Dual side-port syringe

Depending on whether the standby or cut mode is selected, the LC mobile phase is allowed to flow freely inside the syringe needle, either to the GC or to the waste line depending on the plunger position. In fact, when the plug is located between the LC effluent entrance and the needle, the mobile phase is directed to the upper waste line through the barrel; on the other hand, when the plug is located between the two ports, the LC effluent is directed to the GC injector.

3.4 GC dimension

There are few restrictions for the GC column used in a LC-GC system, while particular attention has to be paid to the pre-column characteristics when the retention-gap technique is used. The pre-column has to be wettable by the solvent to form a film of liquid on the wall of the pre-column. It has to be inert, and the retention power has to be below that of the separation column (to guarantee reconcentration of bands broadened in space), and with an internal diameter large enough to assure a sufficiently high vapor-flow rate for efficient discharge of the eluent. The type of deactivation employed on fused-silica surface to obtain the retention gap is fundamental to guaranteeing the required characteristics for a specific application. The length of the pre-column depends on the transfer method employed (mainly partially or fully concurrent eluent evaporation), the volume of liquid transferred, the type of solvent, the temperature of the pre-column, and the flow rate of the carrier gas. However, as a general rule, using an uncoated open tubular pre-column of 0.32 mm I.D. the flooded zone has a length of 12–30 cm per mL of liquid introduced. Generally, the length of the retention gap varies between about 1 m to 30 m for fully and partially concurrent eluent evaporation, respectively.

References:

1. M. J. E. Golay in: *Gas Chromatography*, V.J. Coates, H.J. Noebels, I.S. Fagerson (Editors), Academic Press, New York, USA, 1958.
2. R. S. Gohlke, *Anal Chem*, 31 (1959), 535.
3. L. Mondello, A. C. Lewis, K.D. Bartle (Editors), *Multidimensional chromatography*, Wiley & Sons, Chichester, England, 2002.
4. J. C. Giddings, *Anal Chem*, 56 (1984), 1258A.
5. D. R. Deans, *Chromatographia* 1 (1968) 18.
6. D. R. Deans and I. Scott, in: *Advances in Chromatography 1973*, A. Zlatkis (Editor), University of Houston, Texas, 1973, p. 77.
7. R. E. Kaiser and R.I. Rieder, *Labor Praxis*, 12 (1985), 146.

8. G. Schomhurg and F. Weeke, in: *Gas Chromatography 1972*, S.G. Perry and E.R. Adlard (Editors), The Institute of Petroleum, United Kingdom, 1972, p. 285.
9. G. Schomburg, H. Husmann, F. Weeke, J *Chromatogr*, 112 (1975), 205.
10. M. C. Simmons, L.R. Snyder, *Anal Chem*, 30 (1958), 32.
11. D. R. Deans, I. Scott, *Anal Chem*, 45 (1973), 1137.
12. R. E. Kaiser, L. Leming, L. Blomberg, R. I. Rieder, *HRC & CC* 8 (1985) 92.
13. T. Veriotti, M. McGuigan, R. Sacks, *Anal Chem*, 73 (2001), 279.
14. T. Veriotti, R. Sacks, *Anal Chem*, 73 (2001), 3045.
15. T. Veriotti, R. Sacks, *Anal Chem*, 75 (2003), 4211.
16. B. Quimby, J. McCurry, W. Norman, *LC GC The Peak* April (2007) 7.
17. K. Sasamoto, N. Ochiai, *J Chromatogr A*, 1217 (2010), 2903.
18. L. Mondello, A. Casilli, P.Q. Tranchida, D. Sciarrone, P. Dugo, G. Dugo, *LC GC Eur*, 21 (2008), 130.
19. S. C. Rastogi, T. Menné, J. duus Johansen, *Contact Dermatitis*, 48 (2003), 130.
20. T. Hyötyläinen, M.-L. Riekkola, *J Chromatogr A*, 1000 (2003), 357.
21. K. Grob, in: *On-Line Coupled LC–GC*, Huthig, Heidelberg, Germany, 1991.
22. R. E. Majors, *J Chromatogr Sci*, 18 (1980), 571.
23. I. A. Fowlis, *J High Resol Chromatogr*, 13 (1990), 213.
24. T. V. Raglione, J. A. Troskosky, R. A. Hartwick, *J Chromatogr*, 409 (1987), 205.
25. K. Grob, D. Fröchlich, B. Schilling, H. P. Neukom, P. Nägeli, *J Chromatogr*, 295 (1984), 55.
26. F. Munari, A. Trisciani, G. Mapelli, S. Testianu, K. Grob, J. M. Colin, *J High Resolut Chromatogr*, 8 (1985), 601.
27. H. Sire´n, H. Hyvönen, M. Saarinen, S. Rovio, M.-L. Riekkola, *Chromatographia*, 34 (1992), 421.
28. L. Mondello, P. Dugo, K.D. Bartle, B. Frere, G. Dugo, *Chromatographia*, 39 (1994), 529.
29. L. Mondello, P. Dugo, G. Dugo, K. D. Bartle, *J Chromatog Sci*, 34 (1996), 174.
30. G. Jongenotter, M. A. T. Kerkhoff, H. C. M. van der Knaap, B. G. M. Vandeginste, *J High Resolut Chromatogr*, 22 (1999), 17.
31. M. Shimmo, T. Hyötyläinen, K. Hartonen, M.-L. Riekkola, *J Microcol Sep*, 13 (2001), 202.
32. M. Shimmo, H. Adler, T. Hyötyläinen, K. Hartonen, M. Kulmala, M.- L. Riekkola, *Atmos Environ*, 36 (2002), 2985.
33. K. Grob, J.-M. Stoll, *J High Resolut Chromatogr*, 9 (1986), 518.
34. F. Munari, K. Grob, *J High Resolut Chromatogr*, 11 (1988), 172.
35. J. J. Vreuls, G. J. deJong, U. A. Th. Brinkman, *Chromatographia*, 31 (1991), 113.
36. A. Artho, K. Grob, C. Mariani, *Fat Sci Techol*, 5 (1993), 176.

37. F. Lanuzza, G. Micali, G. Calabro, *J High Resolut Chromatogr*, 19 (1996), 444.
38. P. Tollbäck, H. Carlsson, C. Östman, *J High Resolut Chromatogr*, 23 (2000) 131.
39. W. Kamm, F. Dionisi, L.-B. Fay, C. Hischenhuber, H.-G. Schmarr, *J Chromatogr*, 918 (2001), 341.
40. K. Grob, *J High Resolut Chromatogr*, 13 (1990), 540.
41. K. Grob, M. Bronz, *J Microcol Sep*, 7 (1995), 421.
42. F. David, P. Huffmann, P. Sandra, *LC–GC Eur*, 9 (1999), 550.
43. S. de Koning, M. van Lieshout, H.-G. Janssen, U. A. Th. Brinkman, *J Microcol Sep*, 12 (2000), 153.
44. M. Biedermann, K. Grob, *J Chromatogr A*, 1255 (2012), 56.
45. G. Purcaro, S. Moret, L. Conte, *J Chromatogr A*, 1255 (2012), 100.
46. M. Biedermann, K. Grob, *J Chromatogr A*, 1216 (2009), 8652.
47. S. P. Cram, A. C. Brown III, E. Freitas, R. E. Majors, E. L. Johnson, Abstract of papers Pittsburgh Conference on Analytical Chemistry and Applied Spectroscopy, Ohio, 1979, Abstract 115.
48. R. E. Majors, E. L. Johnson, S. P. Cram, A. C. Brown III, E. Freitas, Abstract of papers Pittsburgh Conference on Analytical Chemistry and Applied Spectroscopy, Ohio, 1979, Abstract 116.
49. S. de Koning, H.-G. Janssen, M. van Deursen, U. A. Th. Brinkman, *J Sep Sci*, 27 (2004), 397.
50. M. Perez, J. Alario, A. Va´zquez, J. Ville´n, *J Microcol Sep*, 11 (1999), 582.
51. R. Sanchez, A. Vazquez, J.C. Andini, J. Ville´n, *J Chromatogr* A, 1029 (2004), 167.

Chapter IV

4 Isotope Ratio Mass Spectrometry

Isotope ratio mass spectrometry (IRMS) is a technique which finds increasingly widespread use in disciplines such as archaeology, medicine, geology, biology, food authenticity, and forensic science. The fastest growth is arguably in forensic applications, where the ability to differentiate substances by their geographical origins provides information that is difficult or unattainable by any other technique. Disciplines which stand to benefit from IRMS are those which require the ability to accurately and precisely measure variations in the abundance of isotopic ratios of light elements such as $^{13}C/^{12}C$, $^{18}O/^{16}O$, $^{2}D/^{1}H$, $^{15}N/^{14}N$, and $^{34}S/^{32}S$. The ratios of these isotopes are always measured relative to an isotopic standard in order to eliminate any bias or systematic error in the measurements. These standards are, or can be linked to, internationally recognized standards such as Vienna Pee Dee Belemnite (VPDB) for carbon, Vienna Canyon Diablo Troilite meteorite (V-CDT) for sulfur, Vienna Standard Mean Ocean Water (VSMOW) for oxygen and hydrogen, and laboratory air for nitrogen[1]. As primary standards can become environmentally depleted, secondary standards must sometimes be used in their place. Several of these secondary standards are discussed in detail by Valkiers *et al.*[2,3]. The International Atomic Energy Agency (IAEA; Vienna, Austria) and the National Institute of Standards and Technology (NIST; Washington, DC, USA) both supply a range of natural abundance standards[4]. Isotope ratios of samples of interest are measured relative to universal standards and are reported in the delta notation, δ:

$$\text{(eq. 1)}\ \delta = 1000(R_{sample} - R_{standard})/R_{standard}$$

The value R_{sample} is the abundance ratio of the minor, heavier isotope of the element to the major, lighter isotope (e.g. $^{13}C/^{12}C$). Samples which establish the $R_{standard}$ values are usually selected because they represent a stable material which is highly enriched in the heavy (minor) isotopes. Most analyzed substances are depleted in the heavy-isotope relative to the standard and will therefore have negative delta values. Commonly used mass spectrometers such as single quadrupoles, ion traps, and time-of-flight mass spectrometers typically do not provide the sensitivity or precision required to detect the

subtle differences in naturally-occurring isotopic abundances. It should be noted that these instruments can be useful when used with *isotope dilution*[5] – a technique in which the heavier isotopes are deliberately enriched well beyond their natural levels. However, the measurement of natural isotopic abundances requires a specialized instrument such as a multi-collector magnetic sector mass spectrometer, also known as an isotope ratio mass spectrometer (IRMS). Several authors have investigated the precision and accuracy of IRMS. Continuous flow IRMS instruments have shown precisions of 0.1‰, with the lowest reported detection limits for monoaromatic compounds between 0.07 and 0.35 mg L^{-1}. In general, detection limits vary according to the analyte: for example, halogenated hydrocarbons are reported between 0.76 and 27 mg L^{-1},[6] which is significantly higher than the limits seen for monoaromatics. Although the analyte is also the most important variable in instrumental performance, certain benchmarks in accuracy and precision can be reasonably anticipated. Wong *et al.*[7] tested three commercially-available GC-IRMS instruments to determine differences in precision and accuracy. The average precision was 0.12‰ with reproducibility of 1.48‰ and accuracy of -1.11 ± 2.16%. Additional experimental variables such as the stability of the ion current[6], dead time, bit board size dependencies[8], and even the possibilities of sample vial influences[9] can all effect precision and accuracy on individual instruments. Another technique which can be used for isotope ratio measurements is known as multiple collector inductively coupled plasma mass spectrometry (MC-ICP-MS). MC-ICP-MS is a technique which has undergone extensive research to enhance the accuracy and precision of stable isotopic measurement[10-12]. Clough *et al.*[13] have demonstrated that MC-ICP-MS can be used as a high-throughput tool for the $\delta^{34}S$ measurements of bulk aqueous and solid samples, using Si as an internal standard for correction of instrumental mass bias effects in both pure solutions and in samples with high matrix content. This technique is limited, by plasma instabilities and the performance of data acquisition in sequential mode, to the identification of large variations in isotopic abundances. There are five main sections of an IRMS instrument: a sample introduction system, an electron ionization source, a magnetic sector analyzer, a Faraday-collector detector array, and a computer-controlled

data acquisition system. Several different interfaces are used to introduce samples into the IRMS, the two most common being elemental analyzers (EA-IRMS) and gas chromatographs (GC-IRMS). Figure 1 demonstrates how each of these sample introduction systems can be coupled to the same mass spectrometer. Although liquid chromatographs (LC-IRMS) have recently gained interest for some applications, there are only a limited number of publications that have shown this technique to be successful. Here, we examine the present state of research involving IRMS and explore some of the most interesting and unusual applications.

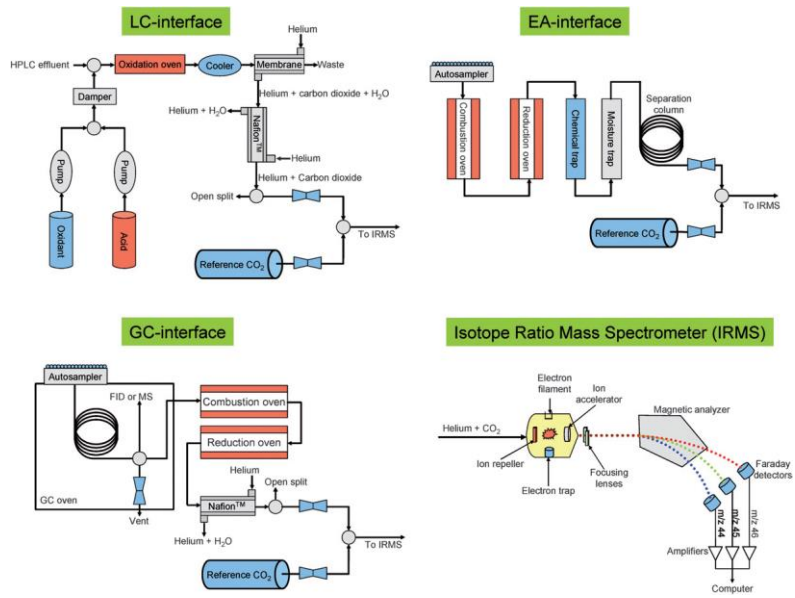

Figure 1. Scheme of the three most common sample introduction systems/interfaces for carbon isotope measurements (as CO_2) and an isotope ratio mass spectrometer. LC=liquid chromatography, EA=elemental analyzer, GC=gas chromatography.

4.1 GC-IRMS

By performing a separation prior to isotope ratio analysis, hyphenated techniques such as GC-IRMS and LC-IRMS can provide isotopic analysis of a complex mixture, thereby providing additional information and higher discriminatory power. IRMS instruments require a somewhat steady stream of a fixed gas (such as CO_2) for precise analysis. The sample first elutes from the GC column into an oxidation chamber, usually housed on the side of the GC oven. The oxidation chamber is normally a non-porous alumina tube that

contains three separate twisted wires made of copper, nickel, and platinum. The samples are combusted at elevated temperatures into a combination of gases such as CO_2, NO_x, and H_2O. For $\delta^{13}C$ measurements, the combusted sample is then carried into a reduction chamber where nitrous oxides are converted into N_2 and any excess O_2 is removed. Since CO_2 , NO_x , and H_2O will not condense at room temperature, the transfer line from the oxidation chamber to the reduction chamber does not need to be heated. The reduction chamber and subsequent valves, splitters, and pneumatic actuators, etc., are contained in a stand-alone interface system. To avoid H_2O from protonating CO_2 in the MS source – and causing deleterious isobaric interference of $^{12}CO_2H^+$ with the $^{13}CO_2^+$ peak at m/z 45 – the analyte stream is passed through a semi-permeable membrane such as Nafion^{TM}. Here, a dry helium counter-flow is used to remove the H_2O. The flow rate of the subsequent sample stream is carefully controlled to provide a stable flow rate to the IRMS ion source of approximately 0.5 mL min $^{-1}$. Deactivated fused silica capillaries are used throughout the interface systems to restrict the analyte flow to the required flow rates. The interface system also uses electronically-controlled pneumatic actuators to toggle the flow of the effluent stream between that of the analyte and that of a reference gas, such as a cylinder of CO_2.

4.2 Origins of variations in isotopic abundances

Although the average isotope ratio of each terrestrial element was fixed around the time of the earth's formation, localized variations occur based on selective enrichment/depletion of the heavier isotopes relative to the average values. For example, even though all plants use atmospheric or dissolved CO_2 as a source of carbon, various factors can influence a plant's ability to enrich or deplete ^{13}C from these common sources in a process known as fractionation. One such fractionation factor is genetic. Monocotyledonous plants (C4 plants), such as sugar cane, corn, tropical grasses, desert plants and marine plants, utilize the Hatch–Slack photosynthetic cycle[14]. These plants typically have $\delta^{13}C$ values varying from -8 to -20 ‰.[15]. Most dicotyledons plants (C3

plants), such as flowering plants, wheat, rice, rye and cotton employ the Calvin–Benson photosynthetic cycle and have $\delta^{13}C$ values varying from -22 to -35‰.[15] Crassulacean acid metabolism (CAM) plants, such as pineapple, cactus, and orchids, can utilize either the C3 or C4 metabolic systems, depending on sunlight, and therefore have $\delta^{13}C$ values ranging between -10 and -34 ‰.[15] Because animals can only incorporate carbon through the ingestion of plant or animal matter, the carbon isotope ratios in an animal will reflect the isotope ratios of the food source; i.e. 'you are what you eat'. This fact can be used to great advantage, as shown in Figure 2. For example, human European diets are richer in C3 plants (wheat, barley, and rye), whereas human North American diets are richer in C4 plants (corn, sugar cane and millet). Therefore, a person living in North America will have body matter with isotope ratios more similar to C4 plants and will have lower ^{13}C levels (i.e. less negative δ values) relative to Europeans. In addition to genetic factors, environmental factors such as temperature, rainfall, and hours of sunlight also influence fractionation. These factors can influence kinetic processes such as the diffusion of CO_2 through the stomata in plant leaves. Clear evidence for environmental sensitivity to fractionation was presented by Ehleringer *et al*. in 2000, wherein they demonstrated the ability to determine the local geographic farming regions in South America from which different cocaine plants were obtained[16]. Fractionation also occurs in common elements such as sulfur, hydrogen, oxygen and nitrogen. In the case of sulfur, fractionation occurs in an equilibrium (between reactants and products) and non-equilibrium (kinetic) mode. Kinetic effects are due to fast, incomplete, or unidirectional processes, typically resulting in a preferential enrichment of the lighter isotope in the reaction products[17]. Grassineau[18] studied fractionation of both carbon and sulfur and concluded that it is possible to limit the effects of fractionation with careful attention to detail. Hydrogen fractionation was studied by Maruoka *et al*.[19] who showed that hydrogen comparatively has the most extreme fractionation effects.

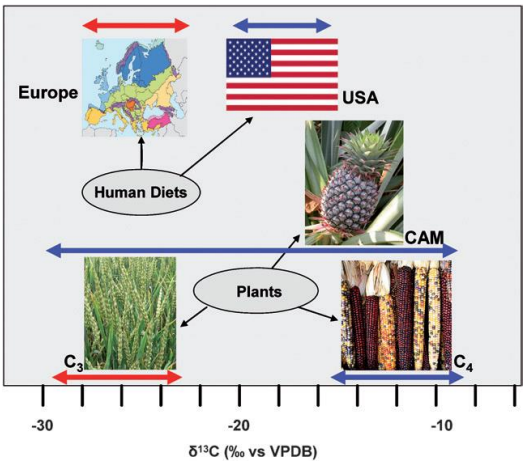

Figure 2. Examples of variations of carbon isotopic abundances of plants and human diets.

Bond strength also plays an important role in kinetic effects due to the greater strength of a deuterium–carbon bond relative to a hydrogen–carbon bond[20]. Oxygen fractionation is largely due to the combustion of the sample, with temperature a deciding factor as to whether or not the sample is completely combusted. If the sample is only partially combusted, or if the oxygen levels are depleted in the oxidation chamber, this can affect the results of the isotopic ratio. It has also been shown that oxygen fractionation can occur within a sample vial[9]. Additionally, oceanic vapors have had a large effect on the oxygen content[21]. Nitrogen fractionations in nature are due to kinetic effects: there are also two non-biological fractionation effects, dissolution in water and diffusion in water. Bacteria, in particular, display several fractionation processes: nitrification, denitrification, and nitrogen fixation[21]. General fractionation also occurs with ambient diffusion[21]. Chemical reactions and physical processes like evaporation and condensation create products that are isotopically distinct from their starting materials[22]. For example, in the hydrologic cycle, snow falling at the poles is depleted in ^{2}H (D) and ^{18}O content with respect to rainfall at the equator[22]. Fractionation effects are also observed in purely chemical reactions. As a result, any simple or complex substance will be composed of isotope ratios that provide a key in unravelling the history and origins of its precursor elements.

References:

1. Reference and intercomparison materials for stable isotopes of light elements, IAEA-TECDOC-825, International Atomic Energy Agency, Vienna, 1995, pp. 1–159.
2. S. Valkiers, M. Varlam, K. Russe, M. Berglund, P. Taylor, J. Wang, M. J. T. Milton and P. De Bievre, *Int J Mass Spectrom*, 264 (2007), 10–21.
3. S. Valkiers, M. Varlam, K. Russe, M. Berglund, P. Taylor, J. Wang, M. Milton and P. De Bievre, *Int J Mass Spectrom*, 263 (2007), 195–203.
4. S. Benson, C. Lennard, P. Maynard and C. Roux, *Forensic Sci Int*, 157 (2006), 1–22.
5. J. Meija and Z. Mester, *Anal Chim Acta*, 607 (2008), 115–125.
6. M. A. Jochmann, M. Blessing, S. B. Haderlein and T. C. Schmidt, *Rapid Commun Mass Spectrom*, 20 (2006), 3639–3648.
7. W.Wong, D. Hachey, S. Zhang and L. Clarke, *Rapid Commun Mass Spectrom*, 9 (1995), 1007–1011.
8. U. Nygren, H. Rameback, M. Berglund and D. C. Baxter, *Int J Mass Spectrom*, 257 (2006), 12–15.
9. S. Nelson, *Rapid Commun Mass Spectrom*, 14 (2000), 293–297.
10. P. Mason, J. Kosler, J. de Hoog, P. Sylvester and S. Meffan-Main, *J Anal At Spectrom*, 21 (2006), 177–186.
11. R. Santamaria-Fernandez and R. Hearn, *Rapid Commun Mass Spectrom*, 22 (2008), 401–408.
12. R. Carlson, M. Boyet and M. Schonbachler, *Geochim Cosmochim Acta*, 71 (2007), A145.
13. R. Clough, P. Evans, T. Catterick and E. Evans, *Anal Chem*, 78 (2006), 6126–6132.
14. P. Tremblay and R. Paquin, *J Agric Food Chem*, 55 (2007), 197–203.
15. M. Leuenberger and C. Huber, *Anal Chem*, 74 (2002), 4611–4617.
16. T. Platzner, Modern Isotope Ratio Mass Spectrometry, John Wiley & Sons, Inc., New York, NY, 1997.
17. J. R. Ehleringer, J. F. Casale, M. J. Lott and V. L. Ford, *Nature*, 408 (2000), 311–312.
18. J. Prietzel and B. Mayer, *Chem Geol*, 2005, 525–535.
19. N. Grassineau, *Appl Geochem*, 21 (2006), 756–765.
20. T. Maruoka, C. Koeberl, J. Matsuda and Y. Syono, *Meteorit Planet Sci*, 38 (2003), 1255–1262.
21. G. Rieley, Analyst, 119 (1994), 915–919.
22. W. Mook and J. Vries, in Environmental Isotopes in the Hydrological Cycle Principles and Applications. Volume 1: Introduction – Theory, Methods, Review, ed. W. Mook, International Atomic Energy Agency, Vienna, 2003–2004, pp. 1–271.

Chapter V

5 Multidimensional Gas Chromatography Coupled to Combustion-Isotope Ratio Mass Spectrometry/Quadrupole MS with a Low-Bleed Ionic Liquid Secondary Column for the Authentication of Truffles and Products Containing Truffle

5.1 Introduction

Truffles (*Tuber* spp.) belonging to the fungal genus Tuber are ascomycete symbiotic fungi that undergo a complex life cycle in association with plant roots. Truffles, in fact, are able to form fruiting bodies only in symbiosis with plant roots and once they establish an ectomycorrhiza they can be found every year under the same trees. The fruiting bodies produce hundreds of volatile compounds capable of attracting insects and mammals, in order to spread their ascospores[1]. Some species of truffle are among the most expensive foods available in the market, usually used as flavouring additives for their distinctive aroma or consumed raw added to certain dishes[2,3]. The most valuable species are *Tuber magnatum* Pico, better known as "Alba white truffle", *Tuber melanosporum* Vittad, the "Périgord black truffle" and *Tuber aestivum*, the "summer truffle"; the first one is routinely sold for thousands of euro per kilo. *Tuber* spp. fungi have been studied for a variety of reasons including their beneficial activities (anti-inflammatory, anti-microbial, and anti-oxidant) and their nutritional composition, but most studies have been focused on their aroma[4]. Several papers have reported the chemical constituents considered to be responsible for the typical aroma, among them, the most abundant are: bis(methylthio)methane, dimethylsulfide, hexanal, 2-methylbutanal, and 3-methylbutanal with quantitative and qualitative variations according to the truffle species and the geographical origin[5-8]. Dimethylsulfide has been identified in white, black and summer truffles, whereas 2- and 3-methylbutanal can be considered a marker of *Tuber melanosporum*, and finally bis(methylthio)methane is the key aroma compound of white truffle[4,6,9]. For such a reason, producers use it to enhance the aroma of products containing white truffle or add it to other truffle species to simulate its aroma. Torregiani *et al.* reported that neither the natural nor the artificial truffle oil samples adequately

replicated the aromas of the species of truffle examined[10]. Since bis(methylthio)methane is the main and the most characteristic contributor to the aroma of white truffle, several studies have focused on its variation during the storage of *Tuber magnatum*; the results indicated a high relative percentage of bis(methylthio)methane in fresh truffles, diminishing with time[11].

Bis(methylthio)methane can be easily added to products due to its solubility and stability, moreover it is quite cheap and its addition as a flavouring agent is permitted by the law, as reported by the Joint FAO/WHO Expert Committee on Food Additives (JECFA)[12]. Since aroma is made out of volatile organic compounds, the most used analytical techniques for its determination in foods aroma have obviously consisted of headspace (HS) extraction coupled to gas chromatography mass spectrometry (GC-MS)[13]. Several studies reported the use of HS solid phase micro extraction (HS-SPME) as a sensitive technique for the evaluation of truffle aroma and composition, also with regard to different storage conditions[3,13-15]. The headspace analysis of white truffles fresh and after storage showed significant modifications of the aroma profile, with the formation of several compounds including alcohols and acids, or changes in their quantity[16]; such variations would hamper the assessment of authenticity based on the relative abundance of the key aroma compounds. As a consequence of the increasing consumers' demand for genuine food and ingredients, in the last years there was a need for analytical approaches able to determine natural and synthetic food ingredients, in order to highlight fraudulent or unsafe practices. From the earliest stages of its development, gas chromatography coupled to combustion-isotope ratio mass spectrometry (GC-C-IRMS) has been a recognized technique for authenticity and traceability purposes, in that it allows to determine the $^{13}C/^{12}C$ ratio abundance of the key flavourings compounds used in food products[17]. GC-C-IRMS may be useful for the detection of fraudulent actions across a wide range of foods, beverages, and ingredients[18]. With regard to the determination of the carbon isotopic ratio, during a GC-C-IRMS analysis compounds eluting from the GC column are oxidized to CO_2 and transferred to Faraday cups for *m/z* 44, 45 and 46 by using a magnetic sector. Unlike what happens when using a GC hyphenated to a

quadrupole mass spectrometer (GC–qMS), where co-eluting compounds can still be identified and quantified in the selected ion monitoring (SIM) mode, excellent chromatographic resolution is mandatory for GC-C-IRMS analysis, since the isotopic ratio of the CO_2 generated from coeluted peaks cannot be treated in the same way. Baseline-to-baseline integration over an entire peak is in fact required for accurate measurement of its isotopic composition, since column fractionation would retain in a slightly different way the heavier isotopes, eluted in the first part of the peak, and the lighter ones, eluted in the tail[19]. In order to separate compounds of interest from non-target compounds, multidimensional gas chromatography (MDGC) in the heart-cut mode may be successfully applied in different analytical fields[20], including isotope ratio measurements[21-29]. The MDGC-C-IRMS approach has been used in the last decade to analyse flavor components[21,22], steroids in urine[23,24], wax compounds in tobacco leaf and smoke samples[25], selected congeners in polychlorobiphenyls (PCB) and polychloronaphthalene (PCN)[26], C_2 to C_5 hydrocarbons produced during biomass burning experiments[27], benzene, toluene, ethylbenzene, and xylenes (BTEX) in environmental samples[28] and monoaromatic hydrocarbons in complex groundwater and gas-phase samples[29]. In the present research, MDGC-C-IRMS with simultaneous quadrupole MS detection after the second dimension (^{2}D), was exploited for the δ^{13}C evaluation of bis(methylthio)methane in different natural truffles and food-aromatized samples, after extraction by HS-SPME.

5.2 Experimental Section

5.2.1 Sampling of fruiting bodies

Twenty-four samples of fruiting bodies of *Tuber magnatum* Pico were collected from different areas of Italy during the autumn 2016. For each sample, different naturally grown carpophores were harvested in their specific regional areas, and namely: 6 from Tuscany (San Miniato), 3 from Molise, 1 from Calabria (Catanzaro), 1 from Basilicata, 2 from Abruzzo (Teramo), 6 from Piedmont (Alba, Mombercelli), 5 from Umbria (Assisi).

Detailed information on the geographical origin, weight, and species of the samples are reported in Table 1, together with the name of the symbiotic plant species, if known. Three standards of bis(methylthio)methane (two synthetic and one natural flavouring substance) were kindly provided by MilliporeSigma/Supelco (Bellefonte, PA, USA) and Axxence Aromatic GmbH (Emmerich, Germany). Indiana standard (Indiana University, Bloomington, IN, USA), calibrated against an international standard [Vienna-Pee Dee Belemnite (V-PDB)] with defined $\delta^{13}C$ content, was used for multipoint calibration of the CO_2 reference gas $\delta^{13}C$ value. All samples were stored at 4 °C.

5.2.2 Commercial samples

Fourteen commercial food products aromatized with truffles were purchased from local stores (Messina, Italy), and namely: 3 olive oils, 3 sauces, 3 fresh cheeses, 1 honey, 1 cream, 1 pasta, 1 summer truffle and 1 white truffle (Table 2). Isotope ratios of the samples of interest were obtained by the following formula:

$$\text{(eq. 1)}\ \delta^{13}C_{V\text{-}PDB} = 1000\ (R_{sample} - R_{standard})/R_{standard}$$

where R represents the abundance ratio of the heavier isotope of the element against the lighter isotope ($^{13}C/^{12}C$).

5.2.3 HS-SPME conditions

Truffles were finely chopped and 0.3 g of each were put into a 20 mL crimped vial for SPME, and the extractions were carried out in the headspace mode. A 1-cm long fused silica fiber coated with a 50/30 µm layer of divinylbenzene/carboxen/ polydimethylsiloxane (MilliporeSigma/Supelco, Bellefonte, PA, USA) was chosen to extract the volatile components from the truffles. The fiber was conditioned following the manufacturer's instructions previous to its use (270 °C for 0.5 hours). Samples were conditioned for 5 min at 50 °C, under agitation (clockwise rotation at 500 rpm), and then

underwent the extraction step for 15 min at 50 °C, still under agitation as previously indicated. Analytes were then desorbed into the GC injection port for 1 min. Blanks were run between consecutive analyses. The same procedure was used for the analyses of the commercial samples (using 1 g of sample) and standard solutions (1000 ppm). Each sample was analysed in triplicate.

5.2.4 Instrumentation and operational conditions

The MDGC-C-IRMS/qMS prototype system consisted of two GC-2010 Plus gas chromatographs (defined as GC1 and GC2), connected by means of a Deans-switch (DS) transfer device, an MS-QP2010 Ultra quadrupole mass spectrometer, and an AOC-20i autosampler (Shimadzu Corporation, Kyoto, Japan). The instrument was coupled to a VisION IRMS system (Elementar Analysensysteme GmbH, Langenselbold, Germany) by means of a GC V furnace system (Elementar Analysensysteme GmbH, Langenselbold, Germany) maintained at 850 °C. GC1 was equipped with a split/splitless injector and a flame ionization detector (FID), while GC2 was connected to a rapid scanning qMS. The MDGC transfer device, located in GC1, was connected to an advanced pressure control unit (APC), which supplied the carrier gas (He). GC1: an SLB-5ms 30 m × 0.25 mm ID × 0.25 µm d_f (MilliporeSigma/Supelco, Bellefonte, PA, USA) was used as column 1 at a constant flow rate of 1 mL/min; the following inlet pressure program was applied: 185 kPa for 1 min, then to 330 kPa at 1.81 kPa/min. Injection mode (260 °C): splitless (1 min), then a 10:1 split ratio was applied. Temperature program: 40 °C (1 min) to 280 °C at 3 °C/min. FID (300 °C; H_2 flow: 40.0 mL/min; air flow rate: 400.0 mL/min; sampling rate: 80 msec) was connected to the DS switch *via* a 0.25 m × 0.18 mm ID stainless steel uncoated column. GC2: an SLB-IL60i 30 m × 0.25 mm ID × 0.2 µm d_f (MilliporeSigma/Supelco, Bellefonte, PA, USA) was used as column 2 with the same temperature program as for column 1. The following pressure program was applied by means of the APC: 140 kPa for 1 min, then to 265 kPa at 1.56 kPa/min. The effluent from the ^{2}D column was split through a zero dead-volume tee-union (Valco) to the GC V furnace and to the IRMS system *via* a 0.85 m × 0.25 mm

ID uncoated column and to the qMS *via* a 1.5 m × 0.1 mm ID uncoated column. The following settings were applied to the VisION system: acceleration voltage, 3789.907 V; trap current, 600 µA; magnet current, 3685.990 mA. MS settings were: ion source, 200 °C; interface temp., 200 °C; mass range, 40-400 *m/z*; scan speed, 1250 amu/sec. The MDGCsolution control software package (Shimadzu, Kyoto, Japan) allowed to set the analytical conditions for both the GC1 (FID) and GC2 (MS) together. The analysed compounds were identified by searching their qMS spectra against the FFNSC 3.0 mass spectral library database (Shimadzu, Kyoto, Japan). The IRMS used in the study was a bench top 5kV system with integrated monitoring gas delivery system with a high performance silicon carbide tube furnace for providing combustion/pyrolisis temperatures for the quantitative, fractionation-free conversion of organic compounds to pure gases (CO_2 and H_2O). The CO_2 produced by combustion of each component was transferred to the MS, while the resulting water was removed through a Nafion tube. The system was designed to maintain the chromatographic integrity of the separated compounds, preserving the chromatographic resolution at the IRMS. An auxiliary He line (sample line He), automatically controlled through the second channel of the APC, was used in the furnace to allow a proper control over the open split conditions for the IRMS. Since in the micro-combustion interface the open split was placed inside the furnace tube, therefore demanding that the open split is in a steady state, the APC was operated in constant flow mode. An electron-impact ionization (EI) gas source, a variable field, stigmatically focused electromagnet for beam separation and multi-channel Faraday collectors for beam detection were used. IRMS data were collected by IonOS stable isotope data processing software ver. 3.0.0.5196 (Elementar Analysensysteme GmbH, Langenselbold, Germany); the apex track integration method was exploited to automatically find the correct starting and finishing point of the peaks. A multipoint linear drift calibration was used for the correction of the IRMS data during the runs since, as discussed by Skrzypek *et al*.[30], such treatment is crucial to obtain the most accurate and precise results.

5.3 Results and Discussion

5.3.1 System configuration and optimization

In order to evaluate the quality of commercial available food products labelled with a valuable aroma, as in the case of truffle, the isotopic ratio measurement of a key component was exploited as a criterion to discriminate between genuine, fortified, or synthetic samples.

Bis(methylthio)methane is known to be one of the main components of truffle flavor and for such a reason it is commonly added as an additive in ”truffle flavoured” products. This organosulfur compound is in fact a convenient, low cost characterizing aroma for food truffle preparation, able to provide or to enhance the flavor of truffle where it is present in low amount or even absent. In this concern, the present investigation was focused on the evaluation of the $\delta^{13}C$ value of this key compound in natural fruiting bodies collected during autumn 2016 in different regions of Italy, and on commercial products bought in different local supermarkets. Twenty-four fruiting bodies were collected and analysed in a few days not to spoil the aroma profile. A first step consisted in the conventional approach used for this analysis, based on monodimensional GC after SPME extraction, with the aim to find the most suitable stationary phase for the complete separation of bis(methylthio)methane, which is mandatory to avoid isotopic ratio errors. The two most widespread phases for the analysis of the volatile fraction were investigated, namely apolar (A: equivalent to poly (5% diphenyl/95% dimethylsiloxane)) and mid polar (B: polyethylenglycol), in order to highlight possible criticisms in terms of coelution of the target compound with other sample components. Figure 1 reports as an example, coelutions occurring on both columns for two different samples.

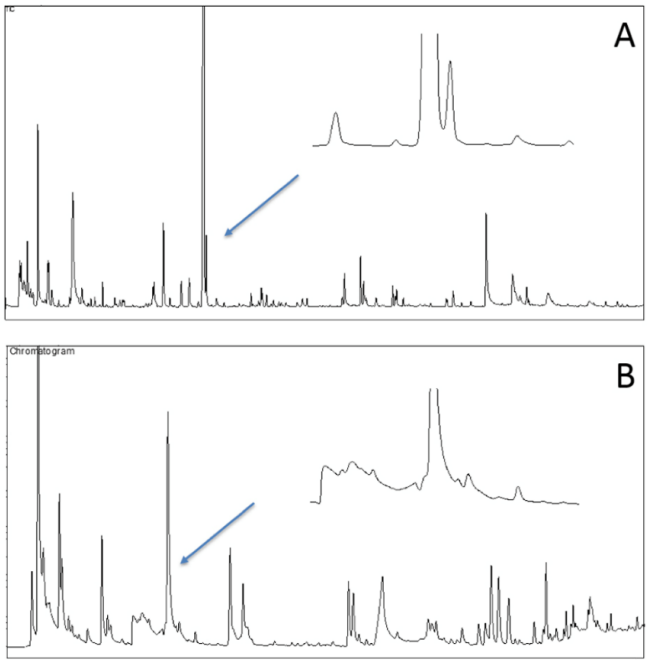

Figure 1. Coelutions of bis(methylthio)methane after monodimensional GC analysis on apolar (A) and mid polar (B) stationary phases.

The chromatograms showed a certain degree of coelutions of bis(methylthio)methane: on the 5% column (A) bis(methylthio)methane, with a linear retention index (LRI) value of 893, in fact coeluted with heptan-2-one; the latter peak was assigned by its EI spectrum (96% similarity) and LRI value of 898. On the wax phase (B), bis(methylthio)methane peak (LRI 634) coeluted with hexan-2-ol (LRI 630); however for the latter peak identification was only tentative, for two main reasons. First, LRI values on such stationary phase are not reproducible as they are on the apolar column, and furthermore hexan-2-ol and its (methyl) substituted isomers show very similar EI fragmentation patterns, preventing their unambiguous identification. Furthermore, the amount of bis(methylthio)methane decreases proportionally with the storage period, probably related to its very high volatility, therefore coelutions are more likely to occur, e.g. on a wax stationary phase, with samples that are just harvested (Figure 2A); on the other hand the separation from neighbour peaks would be easier when the concentration of bis(methylthio)methane in sample is reduced after a certain storage period (Figure 2B).

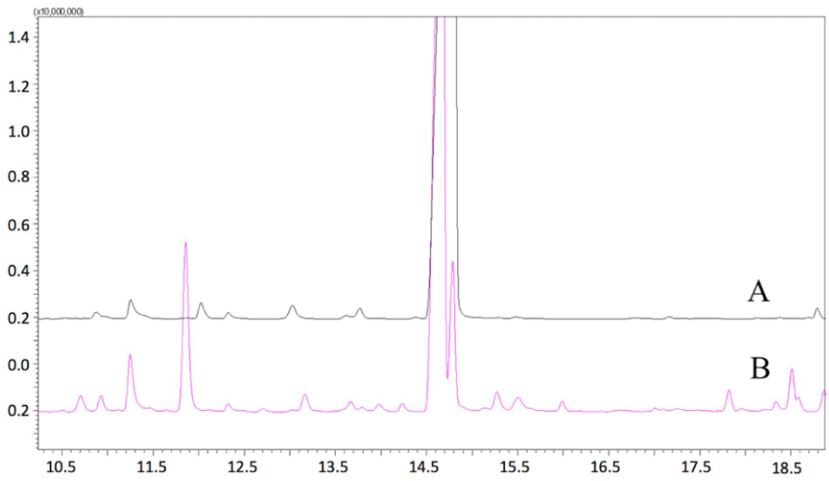

Figure 2. Comparison of the bis(methylthio)methane peak obtained on a wax column after analysis of a white truffle sample: just harvested (A) and after 2 months storage (B).

It is evident from Figures 1 and 2 that in monodimensional GC analysis, different issues can greatly affect the separation degree, possibly leading to a partial coelution of the bis(methylthio)methane peak, for which evaluation of the isotopic ratio value is likely to be undermined due to isotopic column fractionation along the chromatographic band[21].

It must be emphasised that all the organic matter is combusted to CO_2 before reaching the IRMS detector, and spectroscopic resolution of the CO_2 obtained from a chromatographic coelution is not feasible, unlike what is practical in MS, both during data monitoring (i.e. in selected ion monitoring or multiple reaction monitoring mode) and in post-run data processing (i.e. extracted ion mode). That being said, the complete resolution of a peak and its conservation avoiding extra-column band broadening due to dead volumes along the IRMS path is crucial for getting accurate results. Considering the increased complexity of commercial samples in which truffle aroma is mixed with matrix components, an MDGC was deemed as necessary to solve coelutions before the IRMS detection. The use of two-dimensional GC in heart-cut mode coupled to IRMS is not a novel concept[21], however the technology exploited in this research presents a serious step forward in its applicability. Recently, 2D systems based on a microfluidic chip have been

coupled to IRMS[23,25,28,29]. These systems have a common drawback, related to the nature of the transfer system employed, such that each cut causes a slight change in the backpressure of the first dimension (^{1}D), in this way changing the relative retention times of the next eluting components. On the contrary, the DS used in the present work was not affected by this drawback: the main feature of such a transfer device is in fact the capability to generate the same ^{1}D backpressure in both stand-by and cut conditions, allowing the transfer of substantially unlimited heart-cut fractions. Furthermore, the risk of isotopic fractionation resulting from the not quantitative transfer of peaks due to retention time shifts during consecutive heart-cuts is completely avoided. From the IRMS side, the interface (furnace) with the MDGC system has been optimized in terms of dead volumes, to accommodate the demand that a high-efficiency separation, namely a two-dimensional analysis, is realized. Another implementation of the system consists in the absence of the valve used to vent the solvent between GC and IRMS. In fact, in a standard GC-C-IRMS configuration, a heart-cut valve provides a way of removing the solvent peak from the system before it enters the micro-combustion oven; this in order to prevent exhausting the copper oxide catalyst, and provide a long-living furnace setup. Since in an MD system only the fractions of interest are transferred to a ^{2}D column, and hence to the C-IRMS, such a device useless, and therefore it was removed, to limit post-column peak broadening. An additional advantage of the MDGC-C-IRMS coupling is related to a longer duration of the copper oxide catalyst, since only a limited part of the sample is transferred to the ^{2}D column and then combustion involves a reduced amount of organic matter. The two GC columns were selected in order to guarantee the highest possible purification of the band prior to the IRMS analysis. In addition, special attention was paid in selecting the column to be used in ^{2}D, considering the foreseeable influence of column bleeding on the δ^{13}C measurement. From the GC-MS standpoint, it is well known that a reduced bleeding will positively affect identification, resulting in a better spectral matching against a database of reference spectra; on the other hand, further investigation is needed, concerning GC-C-IRMS analysis, since the influence of column bleeding on δ^{13}C measurement needs to be evaluated. As well known, the amount of

stationary phase released from the column depends on the column phase, and furthermore will be also affected by the operating temperature. Being most of the GC applications accomplished in the temperature program mode, the bleeding effect is most likely to affect the $\delta^{13}C$ measurement of those components eluted at high oven temperatures, while it may be negligible for early-eluting components, with higher volatility. Two different mid-polarity stationary phases were evaluated, and namely a polyethylene glycol column (PEG) and an ionic liquid-based SLB-IL59i, which are characterized by similar polarity but exhibit different selectivity. At a glance, a substantial advantage of the IL phase with respect to the PEG one is represented by the higher maximum operational temperature (300 °C *vs.* 280 °C). Ragonese *et al.*[31] reported a comparison of the two stationary phases, in terms of bleeding, revealing that at the column max temperature, the noise level was over one order of magnitude higher for the PEG column ($1.8\ 10^8$ pA s), with respect to the ionic liquid one ($4.9\ 10^6$ pA s). Aiming to assess the influence of the bleeding effect on the accuracy and precision of the $\delta^{13}C$ measurement, in this work some experiments were accomplished on the two stationary phases, using a standard solution. Figure 3 shows a comparison of a vanillin ex-lignin standard solution, previously determined by elemental analysis (EA) IRMS (-27.1‰), analysed with the MDGC system in triplicate with an oven temperature ramp of 5 °C/min from 50 °C in both the dimensions, using a 5% column as ^1D and: (A) the PEG or (B) the IL-based SLB-IL59i column as ^2D.

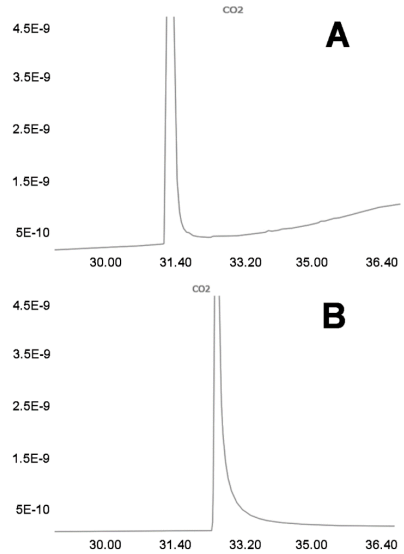

Figure 3. Analysis of standard vanillin ex-lignin for bleeding evaluation on the polyethylene glycol (A) and ionic liquid-based SLB-IL59 (B) stationary phase.

As can be appreciated, the vanillin peak eluted approximately in the same zone, even if the ionic liquid phase presented a slightly higher retention with respect to the PEG one (t_r: 1.5 min). For the IL59i column at the elution temperature of vanillin (about 220 °C), the bleeding was negligible, with an average $\delta^{13}C$ value of -27.1‰, thus in accordance with the EA-IRMS measured value and a good precision (0.22 σ). On the other hand, as predicted, a higher noise was registered for the PEG phase at the elution temperature of vanillin (about 210 °C), which affected the $\delta^{13}C$ result both in terms of accuracy (-25.7‰) and precision (1.11σ). Based on these preliminary investigations, the SLB-IL59i phase was selected as ^{2}D column in the MDGC system, coupled to a 5% column (SLB-5ms) in ^{1}D, useful for allowing the use of LRIs, to provide complementary selectivity with the lowest bleeding interference[32].

5.3.2 Analysis of genuine white truffle

The results obtained from $\delta^{13}C$ measurements (three replicates) of the 24 genuine white truffle samples are reported in Table 1. The lowest value was obtained for sample 2 from Molise (-42.6‰), while the less negative was obtained for sample 11 from Piedmont (-

33.9‰). A good precision was generally achieved employing SPME to extract the truffle flavour, with a maximum standard deviation (SD) value lower then 0.7‰, except for sample 2, where a value of 0.84‰ was calculated.

Table 1. Genuine *Tuber Magnatum* white truffle samples analysed. Symbiotic plant, geographical origin, and $\delta^{13}C$ average values of three consecutive replicates together with the measured standard deviation (SD).

ID	Symbiotic plant	Origin	avg $\delta^{13}C$ ‰ (n=3)	SD
1	*Unknown*	Molise	-36.7	0.15
2	*Unknown*	Molise	-42.6	0.84
3	*Unknown*	Molise	-39.9	0.39
4	*Unknown*	Tuscany	-41.2	0.33
5	*Populus alba*	Tuscany	-37.5	0.21
6	*Populus alba*	Tuscany	-40.1	0.58
7	*Populus alba*	Tuscany	-38.4	0.25
8	*Populus alba*	Tuscany	-37.6	0.24
9	*Populus alba*	Tuscany	-41.8	0.58
10	*Populus alba*	Piedmont	-38.3	0.21
11	*Populus alba*	Piedmont	-33.8	0.04
12	*Unknown*	Piedmont	-35.3	0.31
13	*Unknown*	Piedmont	-37.7	0.11
14	*Quercus Petraea*	Piedmont	-37.9	0.21
15	*Quercus Petraea*	Piedmont	-39.0	0.26
16	*Unknown*	Abruzzo	-40.5	0.09
17	*Unknown*	Abruzzo	-42.0	0.20
18	*Populus alba*	Umbria	-38.7	0.07
19	*Quercus cerris*	Umbria	-40.7	0.33
20	*Unknown*	Umbria	-39.1	0.14
21	*Quercus cerris*	Umbria	-38.4	0.09
22	*Juniperus communis*	Umbria	-37.8	0.61
23	*Unknown*	Basilicata	-41.5	0.60
24	*Unknown*	Calabria	-38.5	0.69

By evaluating these results in relation to the geographical origin of the samples, a slightly different variability of the $\delta^{13}C$ values can be evidenced within the different places, as reported in Figure 4.

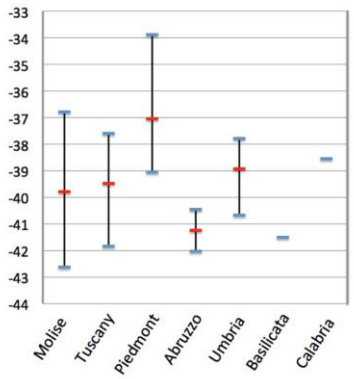

Figure 4. $\delta^{13}C$ ranges on the basis of the geographical origin for the genuine white truffle samples.

The most numerous samples were harvested in Tuscany (6) and Piedmont (6), followed by Umbria (5), Molise (3), Abruzzo (2), Basilicata (1) and Calabria (1). The samples from Molise showed the wider range (around 6) with an SD (σ) of 2.93 and an average $\delta^{13}C$ value of -39.8‰. Truffle samples from Tuscany and Umbria showed similar ranges: the 6 samples from Tuscany showed a range of around 4, with an average $\delta^{13}C$ value of -39.48‰ and 1.84σ, while the 5 samples from Umbria showed a range of around 3, with an average $\delta^{13}C$ value of -38.9‰ and 1.10σ. The two samples from Abruzzo showed an average value of -41.2‰ with 1.11σ, while samples from Piedmont showed the less negative range, with a range of around 5, an average value of -37.04‰ and 1.98σ. The other 2 samples were from Basilicata (-41.5‰) and Calabria (-38.5‰), respectively. It has to be underlined that such evaluation cannot be regarded as a statistical reference, since a limited number of samples were available; on the other hand, given the difficulty and costs related to the collection of a large number of samples for a deeper statistical evaluation, the present data represent the widest study in the field of $\delta^{13}C$ measurement of bis(methylthio)methane.

5.3.3 Analysis of commercial white truffle samples

Before the analysis of the commercial white truffle samples, three standards of bis(methylthio)methane were analysed. Two of them were of petrochemical synthetic origin, characterized by very low $\delta^{13}C$ values (-56.4‰, 0.03σ and -77.1‰, 0.34σ). The third standard presented the most positive value, viz. -28.5‰, 0.06σ, being a natural flavouring substance obtained by physical, enzymatic or microbiological processes from material of vegetable, animal or microbiological origin[33]. Subsequently, fourteen samples purchased from local stores (Messina) were analysed using the same MDGC approach (Table 2).

Table 2. Description of the commercial truffle samples analysed. The average values of five consecutive replicates together with the measured standard deviation (SD) are reported. Abbreviation: n.d. = not detected

ID	Description	Flavour	Avg $\delta^{13}C$ ‰ (*n*=5)	SD
A	Olive oil 1	White truffle	-39.6	0.19
B	Olive oil 2	White truffle	-37.4	0.27
C	Olive oil 3	Black truffle, aroma	-40.3	0.11
D	Fresh cheese 1	Summer truffle, aroma	-57.6	0.15
E	Fresh Cheese 2	Black truffle, aroma	-66.5	0.85
F	Fresh Cheese 3	Black and summer, truffle, aroma	-53.9	0.19
G	Sauce 1	White truffle	-42.1	0.35
H	Sauce 2	Summer truffle, aroma	-43.7	0.25
I	Sauce 3	Black and summer truffle, aroma	-63.7	0.09
L	Cream	White truffle, aroma	-55.0	0.12
M	Dehydrated truffle	White truffle	-37.9	0.09
N	Honey	White truffle	-39.1	0.49
O	Pasta	White truffle	-36.7	0.87
P	Summer truffle	-	n.d.	-

Eight products, namely three olive oils (A-C), two sauces (G,H), one dehydrated truffle (M), one honey (N) and one pasta (O) presented $\delta^{13}C$ values compatible with the natural white truffle range measured. Within these samples some of them, i.e. olive oil 1 (A: -39.6‰, 0.19σ) and olive oil 2 (B: -37.4‰, 0.27σ), were characterized by the presence of the so called "witness" of declared white truffle, arising from a small piece of genuine truffle added to attract the customer and to demonstrate the originality of the product . Dehydrated truffle was declared as white truffle from Alba: also in this case, the results obtained from $\delta^{13}C$ measurement (M: -37.9‰, 0.09σ) were compatible with the presence of an original white truffle, especially those within the range typical of the samples from Piedmont region (-33.9‰/-39.04‰). Sauce 1 (G: -42.1‰, 0.35σ), honey (N: -39.1‰, 0.49σ) and pasta (O: -36.7‰, 0.87σ) samples were declared to be flavoured with white truffle: the analysis confirmed what labelled on the products. A different situation was found for olive oil 3 (C: -40.3‰, 0.11σ) and sauce 2 (H: -43.7‰, 0.25σ). Both samples were declared to be added with black and summer truffle, respectively: however, both these species are characterized by the absence of bis(methylthio)methane[9], as hereby confirmed by the analysis of the summer truffle sample (P) that did not contain any bis(methylthio)methane. Addiction of an aroma was declared for samples C and H and, most probably, it was a mixture of a synthetic and a biotechnological molecule, combined to obtain a $\delta^{13}C$ value compatible with the natural white truffle flavour. The situation would be similar for the remaining samples, where no white truffle was declared among the ingredients. In detail, $\delta^{13}C$ values ranging from -53‰ to -57‰, were registered for fresh cheese 1 (D: -57.6‰, 0.15σ), fresh cheese 3 (F: -53.9‰, 0.19σ) and cream (L: -55.0‰, 0.12σ), all of them declared as flavoured with aroma and summer truffle (sample D), aroma, black and summer truffles (sample F), and aroma and white truffle (sample L). Regarding sample L, being the isotopic ratio outside the range of natural bis(methylthio)methane, it is the authors' opinion that, a low quality (probably not fresh) white truffle was used, fortified with a synthetic flavour (consistently with a reduced residue amount of bis(methylthio)methane). In this concern, in order to verify the influence of the sample aging on the $\delta^{13}C$ value, sample 15 was re-analysed after 2

months of storage. As expected, the amount of bis(methylthio)methane was reduced to about 25% (*n*=3), but no considerable variations of the $\delta^{13}C$ value was observed (-40.5‰ *vs.* -40.7‰), as reported in Figure 5.

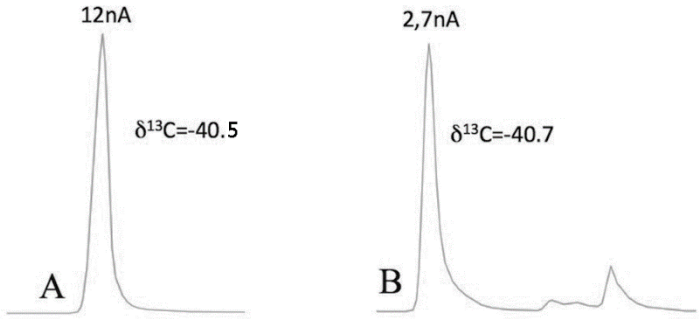

Figure 5. ^{2}D IRMS chromatograms of bis(methylthio)methane in just harvested (A) and 2-month aged truffle sample (B).

Finally, values greatly outside the natural white truffle range were measured for fresh cheese 2 (E: -66.5‰, 0.85σ) and sauce 3 (I: -63.7‰, 0.09σ), clearly flavoured with a synthetic aroma having a more negative $\delta^{13}C$ value.

5.4 Conclusions

The present work demonstrates the capability of an MDGC-C-IRMS system to overcome some of the historical problems of IRMS, associated with the combustion and measurement of impure peaks. Extra-column band broadening has been greatly reduced thanks to the optimization of the micro-combustion furnace and to the elimination of the heart-split valve, not necessary in a multidimensional configuration. The high-efficiency ^{2}D system has been applied for evaluation of the key aroma compound of white truffle, namely bis(methylthio)methane, resolving the coelution occurring with other components present in the different commercial products investigated.

References:

1. R. Splivallo, S. Ottonello, A. Mello, P. Karlovsky, *New Phytol,* 189 (2011), 688-699.
2. G. Pacioni, L. Cerretani, G. Procida, A. Cichelli, *Food Chem, 146 (*2014), 30-35.
3. R. Costa, C. Fanali, G. Pennazza, L. Tedone, L. Dugo, M. Santonico, D. Sciarrone, F. Cacciola, L. Cucchiarini, M. Dachà, L. Mondello, *LWT-Food Sci Technol,* 60 (2015), 905-913.
4. S. Wang, M. F. Marcone, *Food Res Int*, 44 (2011), 2567-2581.
5. A. Fiecchi, M. G. Kienle, A. Scala, P. Cabella, *Tetrahedron Lett,* 8 (1967), 1681-1682.
6. A. M. Gioacchini, M. Menotta, M. Guescini, R. Saltarelli, P. Ceccaroli, A. Amicucci, E. Barbieri, G. Giomaro, V. Stocchi, *Rapid Commun Mass Spectrom* 22 (2008), 3147-3153.
7. G. Mauriello, R. Marino, M. D'Auria, G. Cerone, G. L. Rana, *J. Chromatogr Sci* 42 (2004), 299-305.
8. F. Pelusio, T. Nilsson, L. Montanarella, R. Tilio, B. Larsen, S. Facchetti, J. Ø. Madsen, *J. Agric Food Chem,* 43 (1995), 2138-2143.
9. L. Culleré,V. Ferreira, B. Chevret, M. E. Venturini, A. C. Sánchez-Gimeno, D. Blanco, *Food Chem,* 122 (2010), 300–306.
10. E. Torregiani, S. Lorier, G. Sagratini, F. Maggi, S. Vittori, G. Caprioli, *Food Anal Methods*, 10(6) (2017), 1857-1869.
11. G. Pennazza, C. Fanali, M. Santonico, L. Dugo, L. Cucchiarini, M. Dachà, A. D'Amico, R. Costa, P. Dugo, L. Mondello, *Food Chem* 136 (2013), 668-674.
12. Evaluations of the Joint FAO/WHO Expert Committee on Food Additives (JECFA) http://apps.who.int/food-additives-contaminants-jecfadatabase/chemical.aspx?chemID=2952
13. M. Biniecka, S. Caroli, *TRAC-Trend Anal Chem,* 30 (2011), 1756-1770.
14. R. Costa, L. Tedone, S. De Grazia, P. Dugo, L. Mondello, *Anal Chim Acta*, 770 (2013), 1-6.
15. F. Bellesia, A. Pinetti, A. Bianchi, B. Tirillini, *Flavour Frag J, 11 (*1996), 239–243.
16. M. Piloni, L. Tat, A. Tonizzo, F. Battistutta, *Ital J Food Sci*, 17(4) (2005), 463-468.
17. F. Camin, L. Bontempo, M. Perini, E. Piasentier, *Compr Rev Food Sci Food Saf,* 15 (2016), 868-877.
18. Z. Muccio, G. P. Jackson, *Analyst* 134 (2009), 213-222.
19. M. P. Ricci, D. A. Merritt, K. H. Freeman, J. M. Hayes, *Org Geochem,* 21 (1994), 561–571.
20. P. Q. Tranchida, D. Sciarrone, P. Dugo, L. Mondello, *Anal Chim Acta, 716 (*2012), 66–75.
21. D. Juchelka, T. Beck, U. Hener, F. Dettmar, A. Mosandl, *J High Resolut Chromatogr, 21 (*1998), 145–151.
22. S. Sewenig, D. Bullinger, U. Hener, A. Mosandl, *J Agric Food Chem*, 53 (2005), 838–844.

23. A. D. Brailsford, I. Gavrilovìc, R. J. Ansell, D. A. Cowan, A. T. Kicman, *Drug Test Anal*, 4 (2012), 962–969.
24. A. Casilli, T. Piper, F. Azamor de Oliveira, M. Costa Padilha, H. M. Pereira, M. Thevis, F. R. de Aquino Neto, *Drug Test Anal*, 8 (2016), 1204–1211.
25. A. D. Brailsford, I. Gavrilovìc, R. J. Ansell, D. A. Cowan, A. T. Kicman, *Drug Test Anal*, 4 (2012), 962–969.
26. E. Dumont, B. Tienpont, N. Higashi, K. Mitsui, N. Ochiai, H. Kanda, F. David, P. Sandra, *J. Chromatogr A*, 1317 (2013), 230–238.
27. Y. Horii, K. Kannan, G. Petrick, T. Gamo, J. Falandysz, N. Yamashita, *Environ Sci Technol*, 39 (2005), 4206–4212.
28. H. Nara, F. Nakagawa, N. Yoshida, *Rapid Commun Mass Spectrom, 20 (*2006), 241–247.
29. V. Ponsin, E. T. Buscheck, D. Hunkeler, *J Chromatogr A*, 1492 (2017), 117–128.
30. G. Skrzypek, R. Sadler, *Rapid Commun Mass Spectrom*, *25 (*2011), 1625‑1630.
31. C. Ragonese, D. Sciarrone, P. Q. Tranchida, P. Dugo, G. Dugo, L. Mondello, *Anal Chem*, *83* (2011), 7947-7954.
32. C. Ragonese, D. Sciarrone, E. Grasso, P. Dugo, L. Mondello, *J Sep Sci*, 39 (2016), 537-544.
33. Regulation (EC) no 1334/2008 of the european parliament and of the council of 16 December 2008 on flavourings and certain food ingredients with flavouring properties for use in and on foods and amending Council Regulation (EEC) No 1601/91, Regulations (EC) No 2232/96 and (EC) No 110/2008 and Directive 2000/13/EC.

Chapter VI

6 Preparative Gas Chromatography

Preparative chromatography can be a very ambiguous term and its meaning will often depend on the *raison d'être* for its use. To the forensic chemist, preparative chromatography may mean the isolation of only a few microgram of material for structure elucidation by subsequent spectroscopic examination. To the biochemist, it may mean the isolation of a few milligrams of a substance required for assessing its physiological activity. In contrast, to the organic chemist, preparative chromatography will often mean the isolation of 5 or perhaps even 50 g or more of a pure intermediate for subsequent synthetic work (this can be particularly important in the separation of chiral mixtures). Thus, the amount of material that is separated does not necessarily determine whether the separation can be classed as preparative or not. It is interesting to note that the technique of chromatography, originally invented by Tswett in the latter part of the nineteenth century, was not initially developed for analytical purposes, but for the isolation of some specific pigments from plant extracts.

Preparative gas chromatography (prep-GC) is an important tool for separation and purification of components of a mixture for further uses such as structure elucidation or for recovery of bulk materials in a pure form for commercial applications. Prep-GC allows to collect single compounds, or zones of compounds isolated from a sample after GC separation. Sample collection includes preparative fraction collectors (PFC) into vials, trapping onto capillary columns or using sorbent materials attached to the end of the column. After the collection step, structure elucidation is usually the following in preparative gas chromatography; different analytical techniques as mass spectrometry (MS), Fourier Transform Infrared Spectroscopy (FTIR), Nuclear Magnetic Resonance (NMR), X-ray analysis, are used for this purpose. Implementation of prep-GC includes packed-column GC methods which allows larger sample mass to be injected into the column, capillary GC column for greater component separation, or multidimensional methods where two or more capillary columns having different stationary phases are coupled.

The most productive ways used in the past for prep-GC applications were linked to the use of a single packed column[1].

A scheme of a prep-GC system is shown in Figure 1. The method must incorporate a suitable collection or trapping device (C) which may often be operated at sub ambient temperature. It is useful to have some way to monitor the progress of the GC analysis, so a detector with a switching system is also incorporated. The switching device allows selection of the component(s) for transfer to the collection system C.

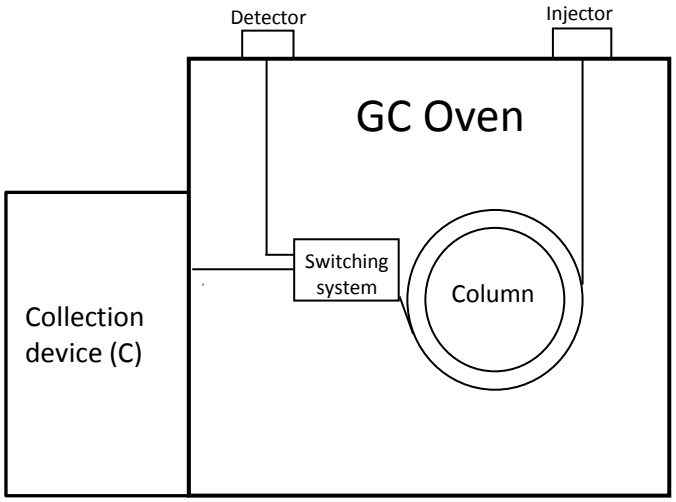

Figure 1. Scheme of a classical preparative GC system.

An alternative view of this process is shown in Figure 2. The first column (1D) effluent is cut or sampled directly into the collection device C, with as many or as few target regions (T_1–T_4) as necessary during the isolation step. The method can be repeated many times to increase the amount of material collected[2].

As aforementioned, preparative scale GC can range from the use of analytical scale methods, where sufficient material has to be collected to perform subsequent characterization methods with off-line spectroscopic or microscale methods, to the true large-scale prep-GC methods capable of producing kilograms of material per hour.

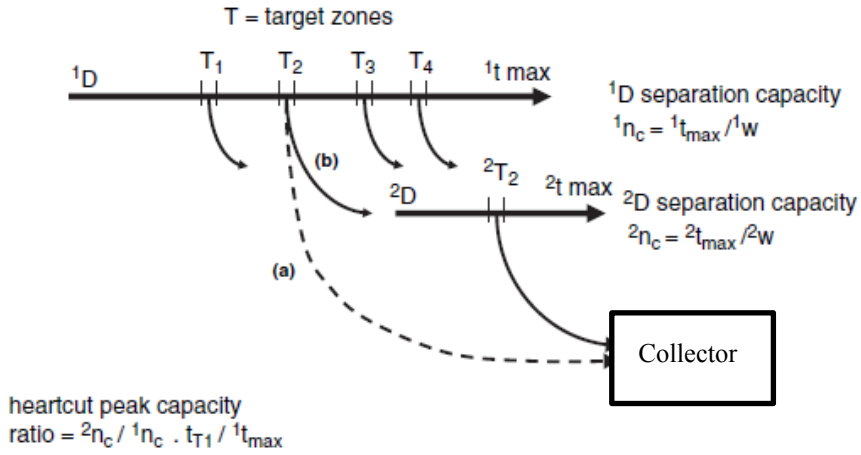

Figure 2. Transfer of selected zones T from a first column (^{1}D) to a) a collection device or b) a second column (^{2}D) and then to the collection device. The process can be repeated many times during a single GC analysis.

Packed columns allows a large volume of stationary phase to be loaded into the column, which in turn prevents column overloading. Thus, relatively large volumes of relatively high concentration samples can be injected into the column. Capillary columns can accommodate only small volumes and solute amounts to prevent overloading of the phase. Overloading leads to asymmetric peak shapes and causes reduced resolution of neighboring peaks. This is not a bad thing in itself if the peaks remain separated, but if peaks progressively merge as a result of trying to increase sample load, then the ability to isolate a pure component in the presence of a closely eluting peak diminishes.

A linear peak is defined as one that has a linear isotherm, i.e., where the relationship in Equation 15 between the distribution constant K and concentrations in the stationary (C_S) and mobile (C_M) phases is a constant:

$$(\text{eq.15})\ K = C_s/C_M, 15$$

The relationship between K and the retention factor ($k = t'_R / t_M$) and the phase ratio ($\beta = V_M/V_S$) is

$$(\text{eq.16})\ K = k\beta, 16$$

for linear chromatography. This means that the retention time under linear chromatography conditions is constant. This also means that the resolution (R_S) of neighboring peaks in packed columns is constant for even large amounts of injected solute. The width (at half height or base width, W_B) of a peak under linear chromatography conditions should also not change.

Although packed columns might be the obvious approach to implement prep-GC, many applications require a more efficient separation method. In this case the best choice is the use of a high-resolution capillary column, that can be either of megabore dimensions (0.53 mm inner diameter I.D.) or a narrower bore (0.25–0.32 mm I.D.). In most cases, logical approach is to use a smaller phase ratio (β) column (thicker film) to allow larger injected amounts than are possible with high β columns.

For the purpose of this thesis the focus is primarily on the capillary prep-GC methods, with a specific goal for the collection and identification of targeted and untargeted (as well as high and low concentrated) compounds from complex samples.

As above cited, collection of the effluent from the GC column can be achieved in many ways. Specifically, the most used technique are: (a) to direct the GC flow through a sorbent trap, with recovery by eluting the trap, (b) collection into a solvent reservoir of the eluting pure peaks, (c) use of a phase-coated capillary column so that the solute undergoes trapping in the phase according to classic chromatographic principles. Probably the more common method is to use a cryogenic or cooled region in which to collect solute. It is possible to combine a number of the above approaches, e.g., cooling down a sorbent, solvent, or phase-coated capillary trap. Roeraade[3] reported that an external phase-coated trapping capillary operated at ambient temperature is efficient at collecting solute, which should not migrate within the capillary if the K value is low enough. Nojima *et al*.[4] evaluated a selection of different capillary trapping columns, with and without phase coating, and with different phase thickness. They described a prep-GC system with a short megabore column as an efficient sample-trapping device, the Open Tubular Trap (OTT). Different trapping capillary phase thicknesses were tested, from 0.5 to 5.0 µm, and were compared with a deactivated (uncoated) capillary tube. The

effectiveness of trapping a range of ester, alcohol, and alkane compounds over an extended range of carbon numbers was evaluated. A 5.0 µm phase thickness of nonpolar DB-1 phase was able to trap compounds with retention index above 1000, whereas the thinner film-trapping capillaries could only successfully trap compounds of higher carbon number and retention index (e.g., 1100, 1200).

Prep-GC experiments with capillary columns normally require multiple injections into the GC, with the selected zone isolated from the matrix in each of these injections. It has been reported that multiple injections of up to 800 or more can be made[3] The only requirement, in this case, is the stability of the system over this extended time (without carrier gas or temperature program changes that might affect the selection of the zone to cut) and to make sure that the collection zone is viable for this time (e.g., not running out of cryogen if a coolant is used). The final result should be the high resolution of capillary GC, combined with single pure component collection.

6.1 Multidimensional preparative gas chromatography

Preparative applications in MDGC are less common than in one-dimensional chromatography, because fewer laboratories are engaged in multidimensional chromatography. MDGC experiments have not been used widely for prep-GC applications, because of the limitations in sample mass capacity. However, depending on the sample mass available, the complexity of the sample and especially potential interfering peaks in the region of the target compound(s), and the capability of increasing the dimensions of the capillary column and phase thickness while still permitting adequate resolution of the target compound, MDGC is a technology that has an obvious role to play in increasing the collection of amounts of a target compound from a GC experiment, while also permitting resolution from matrix or other components.

However, there is no obvious limitation to developing a prep-MDGC method, and the higher resolving power afforded by MDGC should make this approach beneficial if an high purity of the collected components is required. The combination of a packed column to a capillary one in MDGC-prep experiments is logical since the large capacity for

sample mass injection into the packed GC column with less chance of overloading can then allow target peaks with higher abundance to be transferred to the analytical capillary column, while still ensuring high resolution. This is especially useful for trace components. Consistent with the normal role of prep-GC, collection of a compound in capillary prep-GC is followed by subsequent spectroscopic identification for characterization purposes. This puts extra demand on the spectroscopic method in terms of sensitivity of detection and thus, the more sensitive the detection method (with capability to identify at lower concentration), the smaller the mass of component that needs to be collected in prep-GC, so the fewer the injections required. The application of prep-GC should therefore be more attractive today with the improved spectroscopic methods available. However, the most obvious application of prep-GC is in off-line hyphenation with nuclear magnetic resonance (NMR) to provide the identification that analysts seek, but recent encouraging developments in the area of online coupling of GC with NMR[15,16] may overtake the use of prep-GC for off-line NMR analysis, notwithstanding the simplicity of the prep-GC approach. In the field of prep-MDGC a lot of papers were published over the years. Eyres *et al.*[17] developed a novel prep-MDGC method to resolve an essential oil sample with geraniol as the target component (Figure 3). Geraniol was a coelution region of some six other compounds on the first column, using an essential oil mixture made up of lavender and peppermint oils to test the MDGC approach.

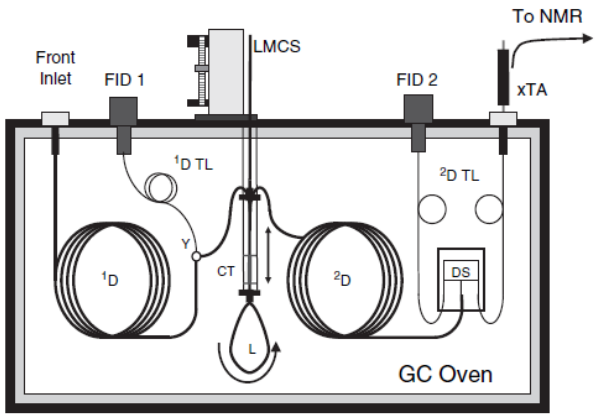

Figure 3. Design of a prep - MDGC system for the isolation of a single pure compound from a complex mixture[17].

At the end of the second column, a Deans switch was used to divert just the geraniol into an external trapping assembly. From 50 to 100 injections were made to collect sufficient geraniol for NMR analysis, using one-and two-dimensional NMR. The 800MHz NMR instrument provided an improved signal to noise ratio for the collected compound. The method was then tested to resolve dimethoxybenzene (DMB) from a similar essential oil mixture (Figure 4)[18].

The interest in DMB is that it has single NMR resonances for the aromatic (4×H) and methoxy (6×H) protons, and so should give a simple NMR trace with good sensitivity, potentially well resolved from other essential oil components. This could then be used as an internal standard. As a further demonstration, 1- and 2-methyl naphthalene were separately resolved from coeluting alkanes, cyclic alkanes, and other components in a crude oil. Since their natural abundance is of the order of 0.2–0.4%, this illustrates that the method apparently has good sensitivity for NMR analysis of the components. The two compounds have essentially the same mass spectra, but the NMR data are dissimilar.

The same group then demonstrated that multiple components could be collected by switching the Deans switch a number of times during the chromatogram, again with multiple injections. NMR was not done on this product, but it can permit a new submixture to be generated. The sample was the same as the geraniol mixture above.

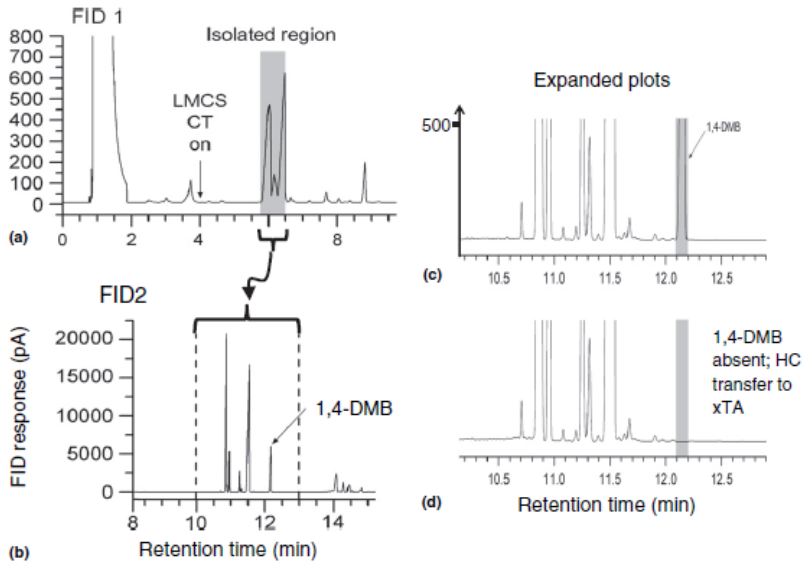

Figure 4. Example of capillary prep-GC sampling of dimethyl benzene in peppermint oil, showing the unresolved zone of peaks (a) recorded at FID 1 (see Figure 2), which are isolated and transferred to a second column for better resolution (b). The expanded trace (c) shows the isolated zone as recorded on FID2, and in (d) DMB is transferred to an external trapping assembly (xTA) for preparative collection[18].

The linearity of collection for multiple injections was reported for menthol and menthone in lavender. Collection was made using uncoated capillary tubing. The tube was eluted, both with and without adding internal standard. The correlation between the number of injections and collected analyte as recorded by GC-MS analysis was good and NMR was conducted on each component.

Werkhoff *et al.*[19] reported the use of a prep-MDGC method applied to yellow passion fruit. As a tool that supported the discovery process, this enrichment method allowed 47 sulfur-containing volatiles to be identified in yellow passion fruits, with 35 of these components shown to be present in the tropical fruit flavor for the first time. A total of 23 of these sulfur-bearing compounds had not been previously reported as constituents of food flavors, and hence were proposed as new natural components.

References:

1. R. Schmidt, M. Roeder, O. Oeckler, A. Simon, V. Schurig, *Chirality*, 12 (2000), 751
2. P. Marriott, Preparative gas chromatography as a sample preparation approach, in: *Comprehensive Sampling and Sample Preparation: Analytical Techniques for Scientists*, J. Pawliszyn (Editor), Elsevier, Amsterdam Netherlands, 2012, 971-982
3. J. Roeraade, S. Blomberg, H. D. J. Pietersma, *J Chromatogr*, 356 (1986), 271
4. S. Nojima, C. Apperson, C. Schal, *J Chem Ecol*, 34 (2008), 418
5. M. Mandalakis, Ã. Gustafsson, *J Chromatogr A*, 996 (2003), 163
6. C. M. Reddy; A. Pearson, L. Xu, A. P. McNichol, B. A. Benner, S. A. Wise, G. A. Klouda, L. A. Currie, T. I. Eglinton, *Environ Sci Technol*, 36 (2002), 1774
7. K. Günther, Nonylphenol in the Environment and Food – An Isomer Specific Issue http://www.nonylphenol.de
8. Z.-Y. Wu, Z.-D. Zeng, P. J. Marriott, *J Chromatogr A*, 1217 (2010), 7759
9. Y.-S. Kim, T. Katase, M. Makino, T. Uchiyama, Y. Fujimoto, T. Inoue, N. Yamashita, *Aust J Ecotoxicol*, 11 (2005), 137
10. C. Meinert, M. Moeder, W. Brack, *Chemosphere*, 70 (2007), 215
11. S. Nojima, D. J. Kiemle, F. X. Webster, W. L. Roelofs, *J Chem Ecol*, 30 (2004), 2153
12. S. Nojima, C. Schal, F. X. Webster, R. G. Santangelo, W. L. Roelofs, *Science*, 307 (2005), 1104
13. T. C. Tran, G. A. Logan, E. Grosjean, D. Ryan, P. J. Marriott, *Geochim Cosmochim Acta*, 74 (2010), 6468
14. P. A. Sutton, C. A. Lewis, S. J. Rowland, *Org Geochem*, 36 (2005), 963
15. M. Kühnle, D. Kreidler, K. Czesla, P. Schuler, V. Shurig, K. Albert, *Chirality*, 22 (2010), 808
16. M. D. Grynbaum, D. Kreidler, J. Rehbein, A. Purea, P. Schuler, W. Schaal, H. Czesla, A. Webb, V. Schurig, K. Albert, *Anal Chem*, 79 (2007), 2708
17. G. T. Eyres, S. Urban, P. D. Morrison, J.-P. Dufour, P. J. Marriott, *Anal Chem*, 80 (2008), 6293
18. G. T. Eyres, S. Urban, P. D. Morrison, P. J. Marriott, *J Chromatogr A*, 1215 (2008), 168
19. P. Werkhoff, M. Guntert, G. Krammer, H. Sommer, J. Kaulen, *J Agric Food Chem*, 46 (1998), 1076

Chapter VII

7 Rapid Collection and Identification of a Novel Component from *Eugenia Uniflora L.* Leaves Essential Oil by means of Three-Dimensional Preparative GC and Nuclear Magnetic Resonance /Mass Spectrometric Analysis

7.1 Introduction

Myrtaceae, the myrtle family of shrubs and trees, are flowering plants (Angiosperms). The Myrtaceae include plants of great ecological and economic importance, especially the Eucalyptus genus. This family is generally evergreen, often with persistent leaves, rich in aromatic oils. The fruits are normally capsules, nuts or berries. There are *circa* 550 Eugenia species located mostly in tropical and subtropical South America. *Eugenia Uniflora L.* (Pitanga, Brazilian Cherry), is a small tree/large bush, having medicinal, edible and other uses. The leaves, used as a substitute for tea, have antioxidant activity because they contain phenolic and flavonoids compounds, and have been used in traditional medicine against fever, to reduce infections, and for many other uses. The present research is focused on a multidimensional preparative approach, characterized by three GC dimension equipped with three different stationary phases, for the characterization of an unknown component from the distilled essential oil obtained from the leaves of *Eugenia Uniflora L.* during the summer (January, 2017) at South of Brazil (Parana State).

The identification of unknown components in complex samples requires a separation step before the isolation of target compound, thus chromatography-based preparative systems represent an effective alternative to the distillation approach. Indeed, by using a GC-Prep system is possible to reach better results in term of purity degree of the collected molecules exploiting the enhanced column efficiency and the availability of different stationary-phase selectivities.

Natural samples are usually characterized by a huge number of compounds, belonging to different chemical classes; hence, the correct structural elucidation of a single component

could be very challenging and it is strictly depending by an effective chromatography separation.

However, by using GC wide-bore columns the advantage of an increased sample capacity results in a decreasing of the peak capacity, because of the wider ID and also because of the low phase ratio (β) values (thick stationary phase films are used), causing the generation of limited theoretical plate numbers. Nevertheless, for preparative purpose, the best choice is to use columns with thick films, because sample capacity is enhanced considerably increasing the stationary phase volume.

By means of heart-cutting multidimensional gas chromatography (MDGC) is possible to increase the efficiency of the system, solving the problem of the low resolution of 0.53 ID columns, aiming to a complete separation of target compounds.

Heart-cutting MDGC is often exploited in many applications which provide for separation of complex samples, particularly when baseline separation is required [1].

MDGC systems equipped with Deans switches transfer device, have been successfully employed with preparative purpose [2-8]. In many cases, a prep-GC analysis precedes ^{1}H-nuclear magnetic resonance (NMR) experiments [2, 5, 7, 9, 10, 11]. Prep-GC fundamentals are perfectly explained in precedent researches present in literature [12].

The prep-MDGC system exploited in the present research was equipped with three Deans switch devices and has been described by Sciarrone *et al.* [13].

The instrument enabled the isolation of suitable quantities of a highly pure volatile compound, in reasonable working time. The target compound was previously incorrectly identified as α-Humulene, a monocyclic sesquiterpene usually present in the volatile fraction of *Eugenia Uniflora L.* leaves, *via* GC-quadMS. Following purification, the analyte was correctly identified by using NMR analyses.

7.2 Experimental section

7.2.1 Standard Compounds and sample

A distilled essential oil (E.O.) was obtained from the leaves of *Eugenia Uniflora L.*, during the summer (January, 2017) at Parana State (South of Brazil). The distilled E.O. was protected from light and heat and stored in refrigerator at 5 °C until used. A C_7-C_{30} *n*-alkane mix was kindly provided by Sigma-Aldrich (Bellefonte, PA, USA), and was used for the calculation of linear retention index (LRI) values. The E.O. was diluted 1:10 (*v/v*) in *n*-hexane prior to GC-FID and GC-MS analyses, while it was injected neat in the MDGC-Prep system.

7.2.2 Multidimensional GC Prep

The preparative MDGC instrument, illustrated in Figure 1, consisted of three GC 2010 plus systems (Shimadzu, Kyoto Japan), namely GC1, GC2, and GC3 connected by means of three Deans-switch transfer devices (TD), namely TD1, TD2, and TD3. Each Deans switch element in the three GC systems was connected to an advanced pressure control system (APC1, APC2, and APC3) (Shimadzu, Kyoto Japan) which supplied carrier gas (He). As such, the system configuration had been previously described elsewhere [13]. GC1 was equipped with a split/splitess injector and a flame ionization detector (FID1). Column (^{1}D) was an Equity-5 [poly (5% diphenyl/95% dimethylsiloxane)] 30 m × 0.53 mm ID × 5 μm d_f (Supelco, Bellefonte, USA), preceded by a 1-m segment of uncoated pre-column of the same ID. The carrier gas pressure was maintained constant at 141.3 kPa while 125 kPa was applied to APC1. Oven temperature program: 150 °C to 280 °C at 3 °C min^{-1}(10 min). FID1 (280 °C) was connected to TD1 *via* 1 m× 0.22 mm segment of uncoated column. The transfer line between GC1 and GC2 was maintained at 280 °C.

GC2 column (^{2}D) was a SupelcoWax 10 (100% polyethylene glycol, PEG) 30 m × 0.53 mm ID × 1.0 μm d_f (Supelco, Bellefonte USA). Oven temperature program: 150 °C (held

until the end of 1D heart-cut window) to 240 °C at 3 °C min^{-1} (10 min). APC2 pressure was constant at 105 kPa. FID2 (280 °C) was connected to TD2 *via* 0.5 m× 0.25 mm segment of uncoated column. The transfer line between GC2 and GC3 was maintained at 240 °C.

GC3 column (^{3}D) was an SLB-IL60 (custom-made ionic liquid) 30 m × 0.53 mm ID × 0.8 μm d_f (Supelco, Bellefonte, USA). Oven temperature program: 150 °C (45 min) to 240 °C at 3 °C min^{-1}(10 min). APC3 pressure was maintained constant at 35 kPa. FID3 (280 °C) was connected to TD3 *via* a 0.6 m × 0.32 mm ID segment of uncoated column.

Detector gasses (for FID1, 2 and 3) were: H_2, 50.0 mL min^{-1}; air, 400 mL min^{-1}; sampling rate, 25 Hz. Data were collected by MDGCsolution software (Shimadzu, Kyoto, Japan).

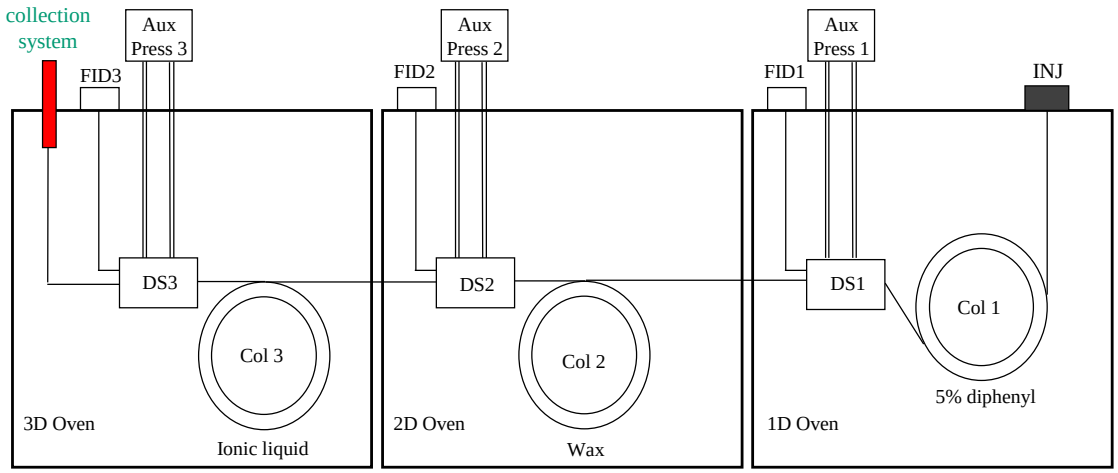

Figure 1. Scheme of the MDGC-Prep system employed.

The collection system employed, was designed and constructed in lab. It was formed of a heated (250 °C) aluminum block (11 cm height × 3 cm wide × 1.5 cm deep) located inside a modified GC injector port. The injection port enabled the introduction of a GC liner and of the collection glass tube, positioned above the liner. The main part of the collector was situated outside the block, at room temperature.

Both the liner and the collection tube were sealed and held in position through two nuts; the lower one was used to connect the column by using a ferrule for FID detection, while the upper one contained a holed rubber septum. The last 5 mm of the uncoated column protruded inside the glass tube as previously described by Sciarrone *et al.* [13].

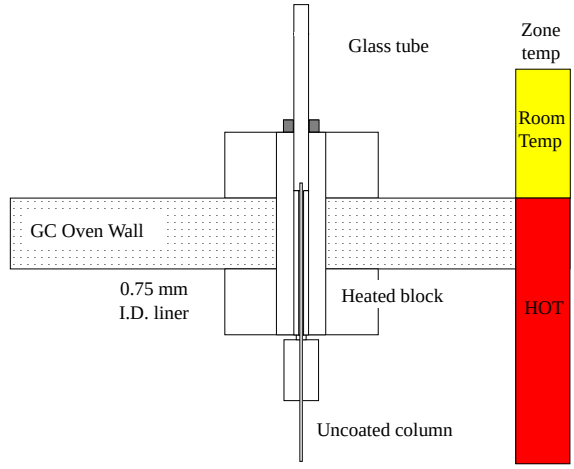

Figure 2. Scheme of the collection system developed in our lab.

After analyte isolation, the collection tube was removed and flushed (in a 2 mL vial) with 100 μL of a deuterated acetone. The volume of deuterated acetone used, was established in several experiments, in order to obtain a quantitative recovery, but at the same time was wanted the highest possible concentration of the collected compound. The solution containing the collected volatile compound was then analyzed by GC-MS for qualitative purposes before the NMR experiments.

7.2.3 GC-FID and GC-MS

A Shimadzu GC 2010 gas chromatograph equipped with an AOC-20i series autoinjector, and a GCMS-QP2010 Ultra system mass spectrometer were used to evaluate the recovery and degree of purity (Shimadzu, Kyoto, Japan). In order to verify the complete purification of the fractions collected, three different 30 m × 0.25 mm ID capillary columns were used, namely SLB-5ms (0.25 μm d_f) [silphenylene polymer, virtually

equivalent in polarity to poly (5% diphenyl/95% methylsiloxane)], Supelcowax-10 (100% polyethylene glycol) (0.25 μm d_f), and SLB-IL 60 (0.20 μm d_f) (Supelco, Bellefonte, USA) were used under the following conditions: oven temperature program, 100 °C to 280 °C at 3 °C min^{-1}; split/splitless injector (280 °C); injection mode, split 1:100 ratio; injection volume, 0.2 μL. GC-FID conditions were as follows: inlet pressure, 110 kPa; carrier gas, He; constant gas linear velocity, 30.0 cm s^{-1}. FID (310 °C) gases: H_2, 50.0 mL min^{-1}; air, 400 mL min^{-1}; make up (N_2), 40.0 mL min^{-1}; sampling rate, 10 Hz. Data were acquired by the GCsolution software ver. 2.41 (Shimadzu, Kyoto, Japan). GC-MS conditions were as follows: inlet pressure, 30.6 kPa; carrier gas, He; constant gas linear velocity, 30 cm s^{-1}; source temperature, 200 °C; interface temperature, 250 °C; mass scan range, 40-400 *m/z*; scan speed, 5 Hz. Data were acquired by GCMSsolution software ver. 2.71 and the FFNSC ver. 3.01 mass spectral database was used for library matching (Shimadzu, Kyoto, Japan).

7.2.4 Experimental Nuclear Magnetic Resonance (NMR) spectroscopy

Compound n. 30 in Fig. 8, was collected after MDGC separation and preparative collection in an almost pure form. 1H and $^{13}C\{^1H\}$ NMR spectra of compound n. 30 were recorded on an Agilent Propulse 500MHz spectrometer equipped with a one NMR probe and operating at 499.74 and 125.73 MHz frequencies respectively. 600 μL of the collected compound, dissolved in CD3COCD3, were poured in a 5 mm test-tube and was analysed after locking on the deuterium lock signal, searching for a good field homogeneity (shimming) and setting the frequency modulation (tuning). The ^1H saturation 90° pulse was calculated to be 8us at 61 dB of power level and the protonic spectrum was recorded with 2 s of acquisition time, 2 s of scan delay and 16 scans; all the other techniques were designed starting from this simple experiment.

The complete and unambiguous assignment, was confirmed by homo nuclear 2D-COSY, TOCSY and ROESY[14] and heteronuclear[15] $^{13}C\{^1H\}$-HSQC and ^{13}C-HMBC experiments. Calibration was attained using as internal standard residual proton signal of the solvent (CD_3COCD_2H quintet δ = 2.05 ppm and the ^{13}C solvent septuplets at δ = 49.0 ppm and δ

= 29.84 respectively)[16] and data were processed by vNMRj software and by the PC software package ACD/Lab, which was also exploited to validate the goodness of the structure elucidation.

7.3 Results and discussion

An essential oil from the leaves of *Eugenia Uniflora L.*, Brazilian Cherry, was subjected to GC-FID and GC-MS analysis (Figure 3), to evaluate the volatile quali/quantitative composition (Table 1).

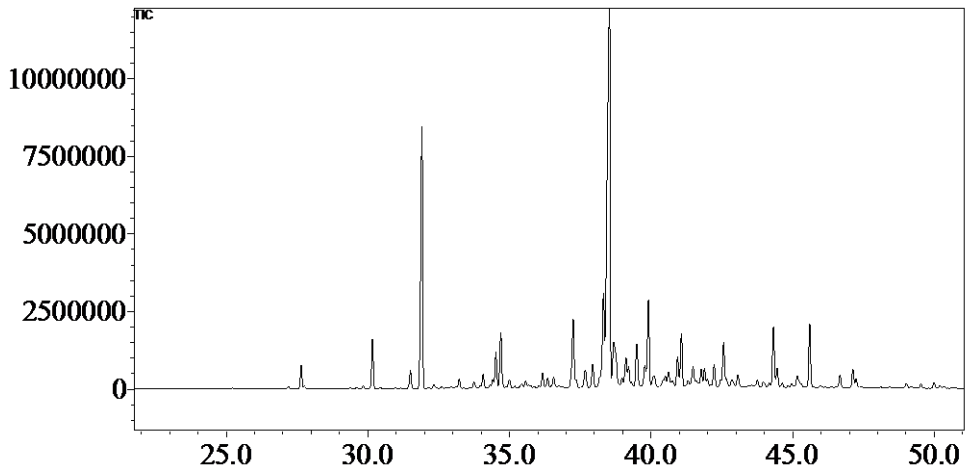

Figure 3. GC-MS Chromatogram of Eugenia Uniflora L. leaves Essential Oil.

38 components (1 unknown), identified by means of a twin-filter mass spectral library (spectral similarity ≥ 90% and linear retention index range), one component (peak 30), accounting for about 36.64 % (GC-FID data) of the entire sample, was unidentified and chosen for further investigations; those compounds are reported in Table 1.

Table 1. Compounds identified in the *Eugenia Uniflora L.* leaves Essential oil.

ID	Compounds Name	% MS Similarity	LRI exp	LRI lib	Area
1	Phellandrene <alpha->	95	1008	1007	0.03
2	Terpinene <alpha->	95	1018	1018	0.01
3	Cymene <para->	98	1025	1025	0.09
4	Terpinene <gamma->	95	1059	1058	0.03
5	Terpinolene	94	1087	1086	0.04
6	Linalool	97	1099	1101	0.10
7	Elemene <delta->	98	1337	1335	0.12
8	Isoledene	91	1374	1372	0.04
9	Elemene <beta->	92	1392	1390	2.55
10	Gurjunene <alpha->	92	1411	1406	0.04
11	Maaliene <beta->	95	1415	1415	0.02
12	Caryophyllene <(E)->	89	1424	1424	0.97
13	Elemene <gamma->	90	1433	1432	15.89
14	Maaliene <alpha->	95	1439	1438	0.04
15	Aromadendrene	94	1443	1438	0.19
16	Caryophyllene <9-epi-(E)->	98	1465	1464	0.42
17	Selina-4.11-diene	94	1477	1476	0.33
18	Amorphene <alpha->	94	1483	1482	0.11
19	Germacrene D	92	1485	1480	0.58
20	Selinene <delta->	90	1491	1489	0.09
21	Selinene <beta->	96	1493	1492	0.29
22	Bicyclogermacrene	95	1500	1497	2.35
23	Amorphene <delta->	84	1507	1506	0.24
24	Cadinene <delta->	96	1522	1518	0.16
25	Selina-4(15).7(11)-diene	95	1542	1540	0.36
26	Selina-3.7(11)-diene	97	1547	1546	0.41
27	Germacrene B	95	1562	1557	3.06
28	Spathulenol	91	1581	1576	0.99
29	Viridiflorol	93	1591	1594	3.94
30	Unknown		1595		36.64
31	Rosifoliol	96	1612	1609	1.08
32	Eudesmol <gamma->	83	1638	1632	0.53
33	Naphth-1-ol <1.2.3.4.4a.7.8.8a-octahydro -. 4-isopropyl-. 1.6-dimethyl->	88	1647	1641	0.16
34	T-Muurolol	93	1649	1645	0.24
35	Cadin-4-en-10-ol	93	1660	1659	0.98
36	Intermedeol	92	1664	1668	1.78
37	Amorpha-4.9-diene<7.14-anhydro->	81	1753	1752	2.16
38	Cedren-13-ol acetate<8->	88	1788	1790	2.17

GC-MS analyses have highlighted for the target compound a low mass spectral similarity (75%) with α-Humulene and the incompatibility of linear retention index (LRI_{data} 1473/

LRI_{exp} 1595), have confirmed the hypothesis that peak 30 could have a similar structure to α-Humulene, but it must be another molecule.

Monodimensional analyses (GC-FID and GC-MS) are not the first choices for the evaluations of complex matrices like are, in many cases, food samples. Especially when are employed wide-bore columns. Also in the analysis of *Eugenia Uniflora L.* leaves essential oil, is very challenging to obtain a good resolution for all compounds. This involves the presence of coeluted compounds, so the purity degree of the collected fraction would be often unsatisfactory. The peak capacity could be increased by reducing the injection volume. However the total analysis time to collect a certain amount is greatly affected by the sample injection volume. In fact, the higher is the injection volume, the lower is the total time required to collect a specific compound thus the highest injection volume should be always used. In this regard, the sample capacity is higher by using mega-bore columns than by using micro-bore columns. However, the low efficiency of the mega-bore columns, allows to coelutions that compromise the purity degree of the compound collected. With the intention to improve the productivity of the system, a multidimensional prep-GC instrument was used with the goal to reduce the total collection time and to improve the purity degree of the components collected. The multidimensional approach is very important in order to gain a good resolution, in particular it is necessary in order to increase the efficiency of the mega-bore columns employed when the goal is the collection of high pure compounds with a preparative system. A high amount (1.5μL) of neat E.O. were injected on the GC-1 in the direct mode. Initially, the first Deans switch was set in the stand-by configuration (with the valve of the TD1 disactivated). All the sample was analyzed by the FID1 to select the first dimension heart-cut window. The resulting first dimension chromatogram is showed in Figure 4 (relative to the stand-by, and heart-cut between 34.5 and 36.5 min applications), in both chromatograms, every peak is overloaded and the chromatography band belonging to the target compound was wide, that's easily predictable because of the high neat sample amount injected (1.5 μL) in direct mode, and the low efficiency column employed.

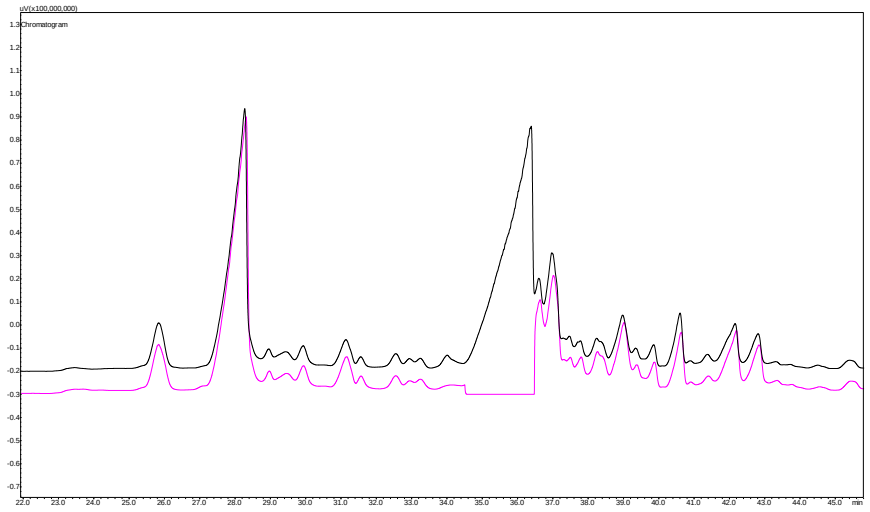

Figure 4. GC-FID chromatogram relative to the first dimension stand-by and heart-cut.

The entire peak was selected for the heart-cut in the second dimension, in order to reach a better resolution and so an higher purity grade by solving co-elutions present in the first dimension. The choice of these two orthogonal stationary phases, allowed the purification of the target constituent from several interferences, as shown in the middle chromatogram in Figure 5 obtained by using a mid-polar column (SupelcoWax 10). However, the purity degree of peak 30 was not satisfactory, so a second heart-cut was planned from 56.5 to 58.4 min.

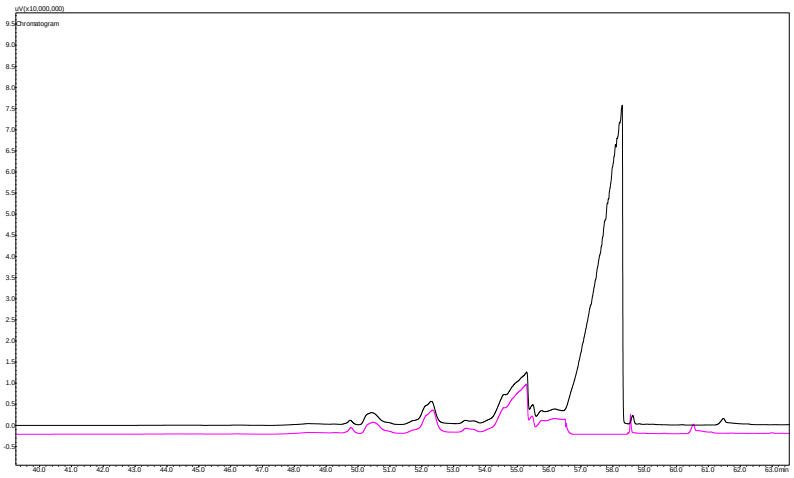

Figure 5. GC-FID chromatogram relative to the second dimension stand-by and heart-cut.

Figure 6 shows how a third separation step was necessary to reach the desired purity degree. The choice of an ionic-liquid column in the third dimension was made in order to obtain an increasing of polarity in the system (Equity5, SupelcoWax10, SLB-IL60), even if SLB-IL60 column has also the same polarity of the SupelcoWax10, the selectivity of these two columns is different.

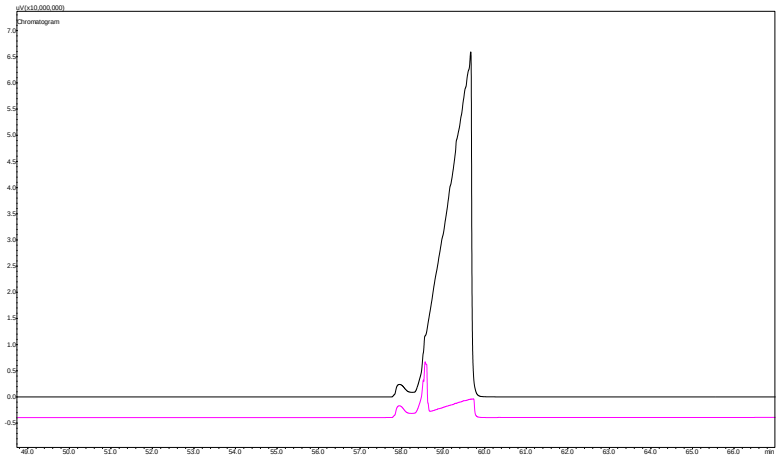

Figure 6. GC-FID chromatogram relative to the third dimension stand-by and heart-cut.

Working in constant pressure mode, with different columns dimensions, and as consequence with different backpressures in each dimension, is not possible to have ideal conditions in each dimension. In this regard, often is searched a compromise that guarantees decent efficiency in the three dimensions, despite suboptimal conditions can't be avoided. However, in this application it was very important to reach satisfactory chromatographic efficiency in the first dimension, because the retention in the first apolar column resulted to be higher than the retention of the other two columns. In this way, the efficiency in the second and third dimensions was suboptimal but reaching a good separation in the first dimension most of the impurities had been removed. By considering the results obtained it can be observed that by using three different chromatographic dimensions, the purity degree can be considerably increased. In fact, the contamination present in the fraction of interest after the first heart-cut reaches high level (*circa* 20%). Contrariwise the fraction collected after three separation steps, can be considered highly pure with an overall contamination of *circa* 2%. After analyte isolation

in the third dimension, the collection vessel was removed immediately and flushed in a vial with 100 μL of deuterated acetone, and then injected in a GC-FID system showing a purity of about 98% (Figure 7). The solution attained, after MD prep-GC applications, was subjected to NMR analysis, to elucidate the structure of the unidentified component. Blank samples were achieved by flushing again the collection tube after the key compound recovery; the solutions thus obtained were analyzed by GC-FID. In this way it was possible to get two responses: monitoring that the recovery was really quantitative and ensure that the collection tube was totally devoid in contaminations before the following analysis.

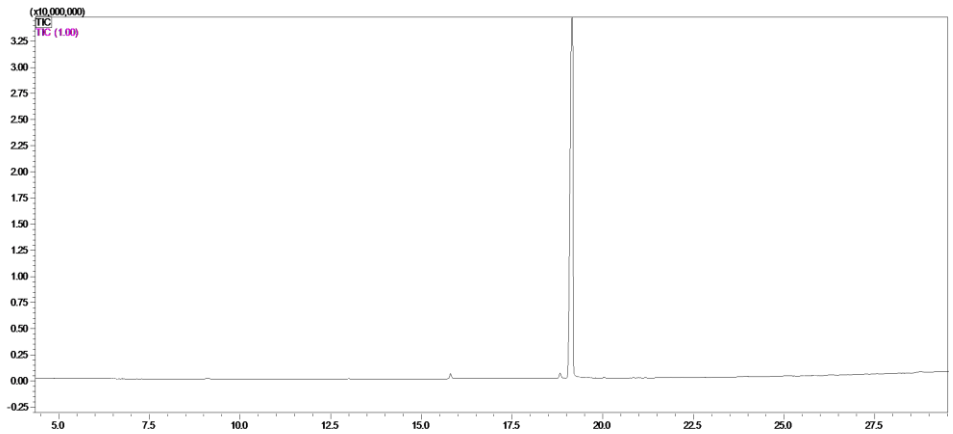

Figure 7. GC-MS chromatogram of the collected compound.

About 3.6 mg of pure analyte were collected in 9 analyses (*circa* 10 working hours); this is a great amount of pure compound considering only 10 working hours with a Prep-MDGC system, this was possible thanks to the high percent area of the compound in the *Eugenia Uniflora L.* leaves essential oil, and thanks to the optimization of the entire working system. The common strategy of structural characterization and conformational analysis by NMR is successful because of the specific NMR data crossing[17]. Briefly, after running the 1D NMR experiments able to detect the proton and ^{13}C resonances of the unknown compound, we have used the 2D HSQC-DEPT with the aim to connect 1H

resonances with their parent ^{13}C parent resonance, whereas the sign of the peaks indicates the number of attached H atoms per C atoms.

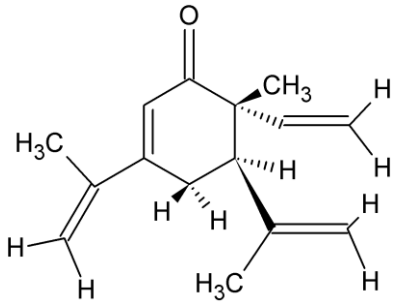

Figure 8. Structure of the characterized compound.

This analysis evidenced the presence of three vinylic terminal CH2, one methylene moiety (aliphatic CH2), three methyl groups (CH3) and two olefinic CH groups. In order to understand the specific connections through the bonds among these chemical groups the homonuclear 2D-COSY experiment provided connection between H atoms separated by less than 3 (sometimes 4) bonds, whereas, the heteronuclear 2D-HMBC was definitely crucial for the "long-range" connection among ^{13}C resonances and proton resonances coming from nuclei which are separated by 2, 3 or 4 bonds. The combination of these data often leads to the structure elucidation, however it has to be confirmed by the homonuclear 2D-NOESY data which are evidencing connections between neighbouring protons regardless the specific bonding connections. These through-the-space contacts are the best way to infer the configurational and conformational arrangement of the molecules in solution. In this case it is specifically useful to define the stereochemistry.

7.4 Conclusions

In the present research, the main compound of the *Eugenia Uniflora L.* leaves E.O. was isolated from the neat oil in a reasonable collection time with no sample preparation. The characterization of the unknown compound leads to a better knowhow of the volatile composition of the Pitanga leaves essential oil. The GC-GC-GC-prep configuration allowed the collection of pure amounts of the separated component by a lab-constructed device placed at the outlet of the 3D column. The higher sample capacity of the mega-

bore columns employed increased the productivity of the system in terms of amount of component collected/per run, allowing for 1.5 µL of the neat sample to be injected. The system can be regarded as a viable alternative to the classical fractional distillation method, for the collection of pure components that are not available commercially, and whose content in the matrix is regulated.

References:

1. D. Sciarrone, A. Schepis, M. Zoccali, P. Donato, F. Vita, D. Creti, A. Alpi, L. Mondello, *Anal Chem*, 90 (2018), 6610-6617.
2. P.G. Ruhle, J. Niere, P.D. Morrison, R. Jones, T. Caradoc-Davies, A.J. Canty, M.G. Gardiner, V-A. Tolhurst, P.J. Marriott, *Anal Chem*, 82 (2010), 4501-4509.
3. G.T. Eyres, S. Urban, P.D. Morrison, J-P. Dufour, P.J. Marriott, *Anal Chem*, 80 (2008), 6293-6299.
4. G.T. Eyres, S. Urban, P.D. Morrison, P.J. Marriott, *J Chromatogr A*, 1215 (2008), 168-176.
5. D. Sciarrone, S. Pantò, C. Ragonese, P.Q. Tranchida, P. Dugo, L. Mondello, *Anal Chem*, 84 (2012), 7092–7098.
6. D. Sciarrone, S. Pantò, A. Rotondo, L. Tedone, P.Q. Tranchida, P. Dugo, L. Mondello, *Anal Chim Acta*, 785 (2013), 119-125.
7. D. Sciarrone, S. Pantò, P.Q. Tranchida, P. Dugo, L. Mondello, *Anal Chem*, 86 (2014), 4295-4301.
8. C. Ruhle, G.T. Eyres, S. Urban, J-P. Dufour, P.D. Morrison, P.J. Marriott, *J Chromatogr A*, 1216 (2009), 5740- 5747.
9. M. Lo Presti, D. Sciarrone, M.L. Crupi, R. Costa, S. Ragusa, G. Dugo, L. Mondello, *Flavour Fragr J*, 23(4) (2008), 249-257.
10. G. Dugo, I. Bonaccorsi, D. Sciarrone, L. Schipilliti, M. Russo, V. Raymo, A. Cotroneo, P. Dugo, L. Mondello, *J Essent Oil Res*, 24 (2) (2012), 93–117.
11. J. Tong, L. Yuan, F. Guo, Z.H. Wang, L. Jin, W.S. Guo, *Nat Prod Res*, 27(1) (2013), 32-36.
12. L. Kim, B. Mitrevski, K. L. Tuck, P.J. Marriott, *J Sep Sci*, 36 (2013), 1774-1780.
13. D. Sciarrone, S. Pantò, C. Ragonese, P.Q. Tranchida, P. Dugo, L. Mondello, *Anal Chem*, 84 (2012), 7092–7098.
14. A. E. Derome, (2013). Modern NMR techniques for chemistry research. Elsevier.
15. W. Willker, D. Leibfritz, R. Kerssebaum, W. Bermel, *Magn Reson Chem*, 31(3) (1993), 287-292.
16. H. E. Gottlieb, V. Kotlyar, A. Nudelman, *J Org Chem*, 62(21) (1997), 7512-7515.
17. A. Rotondo, R. Ettari, M. Zappalà, C. De Micheli, E. Rotondo, *J Mol Struct*, 1076 (2014), 337–343.